HOLLOW MICRONEEDLES AS A CARRIER FOR ENHANCING SKIN PENETRATION OF HYDROPHILIC PERMEANTS

By

Miss Nanthida Wonglertnirant

A Thesis Submitted in Partial Fulfillment of the Requirements for the Degree
Doctor of Philosophy Program in Pharmaceutical Technology
Graduate School, Silpakorn University
Academic Year 2011

HOLLOW MICRONEEDLES AS A CARRIER FOR ENHANCING SKIN PENETRATION OF HYDROPHILIC PERMEANTS

By

Miss Nanthida Wonglertnirant

A Thesis Submitted in Partial Fulfillment of the Requirements for the Degree
Doctor of Philosophy Program in Pharmaceutical Technology
Graduate School, Silpakorn University
Academic Year 2011

การเพิ่มการซึมผ่านผิวหนังของสารซึมผ่านที่มีคุณสมบัติชอบน้ำโดยอาศัยตัวพาไมโครนีดเดิ้ลชนิดรูกลวง

โดย
นางสาวนันทิดา วงศ์เลิศนิรันดร์

วิทยานิพนธ์นี้เป็นส่วนหนึ่งของการศึกษาตามหลักสูตรปริญญาเภสัชศาสตรดุษฎีบัณฑิต
สาขาวิชาเทคโนโลยีเภสัชกรรม
บัณฑิตวิทยาลัย มหาวิทยาลัยศิลปากร
ปีการศึกษา 2554

The Graduate School, Silpakorn University has approved and accredited the Thesis title of “Hollow microneedles as a carrier for enhancing skin penetration of hydrophilic permeants” submitted by Miss Nanthida Wonglertnirant as a partial fulfillment of the requirements for the degree of Doctor of Philosophy in PHARMACEUTICAL TECHNOLOGY.

…….....

(Assistant Professor Panjai Tantatsanawong, Ph.D.)

Dean of Graduate School

...../...../.....

The Thesis Advisors

1. Associate Professor Tanasait Ngawhirunpat, Ph.D.
2. Associate Professor Praneet Opanasopit, Ph.D.

The Thesis Examination Committee

…….. Chairman

(Associate Professor Suwannee Panomsuk, Ph.D.)

...../...../.....

…….. Member

(Jittima Chatchawansaisin, Ph.D.)

...../...../.....

…….. Member

(Associate Professor Tanasait Ngawhirunpat, Ph.D.)

...../...../.....

…….. Member

(Associate Professor Praneet Opanasopit, Ph.D.)

...../...../.....

50353801 : MAJOR : PHARMACEUTICAL TECHNOLOGY
KEY WORDS : HOLLOW MICRONEEDLES / INJECTION / TRANSDERMAL DELIVERY / MACROMOLECULES
NANTHIDA WONGLERTNIRANT : HOLLOW MICRONEEDLES AS A CARRIER FOR ENHANCING SKIN PENETRATION OF HYDROPHILIC PERMEANTS. THESIS ADVISORS : ASSOC. PROF. TANASAIT NGAWHIRUNPAT, Ph.D., AND ASSOC. PROF. PRANEET OPANASOPIT, Ph.D. 114 pp.

The objective of this research was to study the parameters affecting the skin permeability of drug when employing the hollow microneedle as a delivery method. Thus, the potential of a hollow microneedle for enhancing the transdermal delivery of a large molecular hydrophilic compound was investigated. The effect of variable parameters i.e. injection volume, number of injections, concentration, and molecular size, on the *in vitro* drug release behavior was determined from skin. A hollow microneedle was prepared from a 33-gauge hypodermic needle. Fluorescein isothiocyanate (FITC)-dextrans (MW 4 kDa), FD-4, was used as a model compound, and it was favorably loaded into the lower epidermis as well as the superficial dermis of the dorsal rat skin by a hollow microneedle. Up to 20 μL (bolus injection) of FD-4 solution was successfully administered into the excised rat skin without any leakage. In all cases, more than 60% of FD-4 was released from the skin over 8 h. The release profiles of FD-4 were analyzed by the Higuchi model based on Fick's law of diffusion. It was observed that release rates of FD-4 from the skin were approximately linearly increased with the amount of FD-4 injected (R^2=0.955–0.985), and almost the same independent of the number of injections with the same total volume delivered. The release profiles from skin of the different concentrations of FD-4 solution were not significant difference. The FD-4 release rates of the first 30% release, however, were tended to decrease with the small injection volume of the higher concentration. The diffusivity of FD-4 after administration by a hollow microneedle was almost the same as its diffusivity in the viable epidermis and dermis layer and much greater than that in the stratum corneum (SC), indicating that the SC is a rate-limiting barrier for any substances to cross the skin into the body. The release profiles from drug-loaded skins were also compared by changing the molecular weight (MW, 20–40,000 Da) of the hydrophilic model compounds. The larger molecular size of compounds caused the lower release rate from skin. Moreover, the results revealed that the viable epidermis and dermis restricted the penetration of macromolecules which have MW more than 40 kDa. These studies suggest the utilization of hollow microneedle to enhance transdermal delivery of even large molecular hydrophilic compounds and provide useful information for designing an effective hollow microneedle system.

Program of Pharmaceutical Technology Graduate School, Silpakorn University
Student's signature ..... Academic Year 2011
Thesis Advisors' signature 1. ..... 2. .....

50353801 : สาขาวิชาเทคโนโลยีเภสัชกรรม
คำสำคัญ : ไมโครนีดเดิ้ลชนิดรูกลวง / การฉีด / ระบบนำส่งผ่านผิวหนัง / สารโมเลกุลใหญ่

นันทิดา วงศ์เลิศนิรันดร์ : การเพิ่มการซึมผ่านผิวหนังของสารซึมผ่านที่มีคุณสมบัติชอบน้ำโดยอาศัยตัวพาไมโครนีดเดิ้ลชนิดรูกลวง. อาจารย์ที่ปรึกษาวิทยานิพนธ์ : ภก.รศ.ดร.ธนะเศรษฐ์ ง้าวหิรัญพัฒน์ และ ภญ.รศ.ดร.ปราณีต โอปณะโสภิต. 114 หน้า.

การวิจัยนี้มีวัตถุประสงค์เพื่อศึกษาปัจจัยที่ส่งผลต่อการซึมผ่านผิวหนังของสารต้นแบบเมื่อนำส่งโดยใช้ไมโครนีดเดิ้ลชนิดรูกลวง โดยศึกษาความสามารถของไมโครนีดเดิ้ลชนิดรูกลวงในการเพิ่มการซึมผ่านผิวหนังของสารโมเลกุลใหญ่ที่มีคุณสมบัติชอบน้ำและศึกษาผลของปัจจัยต่างๆ ได้แก่ ปริมาตรที่ฉีด จำนวนครั้งของการฉีด ความเข้มข้น และขนาดโมเลกุล ต่อพฤติกรรมการปลดปล่อยยาออกจากผิวหนังด้วยวิธีภายนอกร่างกาย ไมโครนีดเดิ้ลชนิดรูกลวงที่ใช้เตรียมจากเข็มฉีดยาเบอร์ 33 สารต้นแบบที่ใช้ในการทดสอบ คือ ฟลูออเรสซีนไอโซไธโอไซยาเนตเด็กซ์แทรนส์น้ำหนักโมเลกุล 4000 ดอลตัน (FD-4) จากผลการศึกษาพบว่า การใช้ไมโครนีดเดิ้ลชนิดรูกลวงสามารถนำส่ง FD-4 เข้าสู่ผิวหนังหนูในชั้นหนังกำพร้าส่วนล่างรวมถึงส่วนบนของชั้นหนังแท้ในปริมาณที่มากสุดถึง 20 ไมโครลิตรต่อการฉีดหนึ่งครั้ง โดยไม่พบการรั่วซึมของสารทดสอบออกจากผิวหนัง FD-4 มากกว่า 60% ถูกปลดปล่อยออกจากผิวหนังภายในระยะเวลา 8 ชั่วโมง รูปแบบการปลดปล่อยของ FD-4 ถูกนำมาวิเคราะห์โดยสมการของฮิคุชิ (Higuchi model) ซึ่งเป็นไปตามกฎการแพร่ของฟิค (Fick's law of diffusion) พบว่าอัตราเร็วในการปลดปล่อยของ FD-4 ออกจากผิวหนังเพิ่มขึ้นโดยมีแนวโน้มเป็นเส้นตรง (สัมประสิทธิ์การทำนายมีค่าระหว่าง 0.955 ถึง 0.985) เมื่อเพิ่มปริมาณยาที่ฉีดเข้าสู่ผิวหนัง และให้ค่าใกล้เคียงกันโดยไม่ขึ้นกับจำนวนครั้งของการฉีดสารในปริมาตรสุทธิที่เท่ากัน ไม่พบความแตกต่างอย่างมีนัยสำคัญต่อรูปแบบการปลดปล่อยของ FD-4 ออกจากผิวหนังเมื่อใช้สารละลายที่มีความเข้มข้นต่างๆกัน อย่างไรก็ตามพบว่าการฉีดสารละลายที่มีความเข้มข้นสูงแต่ลดปริมาตรในการฉีดทำให้อัตราเร็วในการปลดปล่อยของ FD-4 ลดลง สัมประสิทธิ์การแพร่ของ FD-4 ในผิวหนังเมื่อนำส่งด้วยไมโครนีดเดิ้ลชนิดรูกลวงมีค่าใกล้เคียงกับสัมประสิทธิ์การแพร่ในชั้นหนังกำพร้าที่มีชีวิตและชั้นหนังแท้ แต่มากกว่าในชั้นสตราตัม คอร์เนียมอย่างมาก แสดงให้เห็นว่าผิวหนังชั้นสตราตัม คอร์เนียมแสดงบทบาทสำคัญในการควบคุมอัตราการดูดซึมผ่านผิวหนังของสารต่างๆที่จะเข้าสู่ร่างกาย นอกจากนี้รูปแบบการปลดปล่อยยาออกจากผิวหนังถูกเปรียบเทียบระหว่างสารต้นแบบที่มีคุณสมบัติชอบน้ำซึ่งมีมวลโมเลกุลต่างๆกัน พบว่าสารประกอบมวลโมเลกุลใหญ่จะมีอัตราในการปลดปล่อยออกจากผิวหนังช้า ชั้นหนังกำพร้าที่มีชีวิตและชั้นหนังแท้จะขัดขวางการแพร่ผ่านของสารโมเลกุลใหญ่ขนาด 40 กิโลดอลตันขึ้นไป จากการศึกษาครั้งนี้แสดงให้เห็นถึงประโยชน์ของการใช้ไมโครนีดเดิ้ลชนิดรูกลวงเพื่อเพิ่มการนำส่งยาผ่านผิวหนังโดยเฉพาะสารโมเลกุลใหญ่ที่มีคุณสมบัติชอบน้ำและให้ข้อมูลที่เป็นประโยชน์ต่อการพัฒนาระบบนำส่งที่มีประสิทธิภาพโดยอาศัยไมโครนีดเดิ้ลชนิดรูกลวง

สาขาวิชาเทคโนโลยีเภสัชกรรม บัณฑิตวิทยาลัย มหาวิทยาลัยศิลปากร

ลายมือชื่อนักศึกษา ..... ปีการศึกษา 2554

ลายมือชื่ออาจารย์ที่ปรึกษาวิทยานิพนธ์ 1. ..... 2. .....

ACKNOWLEDGEMENTS

The author wishes to express sincere appreciation to every people who contributed in diverse ways to the completion of this research. First of all, I would like to express my deepest gratitude to my thesis advisor, Assoc. Prof. Dr. Tanasait Ngawhirunpat for his supervision, valuable guidance, and encouragement throughout my study. He provided me good opportunities and support in various ways. My sincere gratitude also goes to my thesis co-adviser, Assoc. Prof. Dr. Praneet Opanasopit for her helpful support, invaluable suggestion, and kindness given to me during my study. I am very much indebted to both of them.

My next gratitude and appreciation goes to Prof. Dr. Kenji Sugibayashi for giving me a great opportunity to work at his laboratory, Faculty of Pharmaceutical Sciences, Josai University, Japan. He shared the great attitude and supported me a lot in my research works and also in my living in Japan. I also would like to acknowledge Assoc. Prof. Dr. Hiroaki Todo for his precious suggestions and caring during my stay in Japan. I also cannot forget to thank all laboratory members there for their warm welcoming, help, and fellowship. I will keep in touch with them and keep the memorable time there.

I would like to especially thank Prof. Dr. Mont Kumpugdee-Vollrath for supporting my work at University of Applied Sciences (BHT), Berlin, Germany. It was one of the great times in my life while I had been working there.

I gratefully acknowledge the Commission of Higher Education (Thailand), the Thailand Research Funds through the Golden Jubilee Ph.D. Program (Grant No. PHD/0104/2549), the TRF–DAAD Research Based Mobility Scheme Project (D/08/04910) and the Graduate School, Silpakorn University (Annual Government Budget Expenditures for the fiscal year 2011) for the financial support throughout my study. A big thank you goes to Miss Areerut Sripattanaporn for her helpful assistance in preparing skin membrane.

I would like to manifest the gratefulness to every teachers and staffs in Faculty of Pharmacy, Silpakorn University for the knowledge and generous support. I also would like to pass my heartfelt thanks to all my friends and members of the Pharmaceutical Development of Green Innovation Group (PDGIG) who made my time in Silpakorn University so precious. I am very appreciated with you all. Our friendship will certainly last long in my heart.

I wish to give my special thanks to my beloved family who are always beside me. Thank you for their all along support, love, caring, blessing, encouragement, and belief in me. Finally, an apology is offered to those whom I cannot mention personally one by one here.

TABLE OF CONTENTS

LIST OF TABLES

LIST OF FIGURES

LIST OF ABBREVIATIONS

%w/w	percent weight by weight
°C	degree Celsius
μg	microgram(s)
μL	microliter(s)
μm	micrometer(s)
θ	theta
Ave.	average
CAL	Calcein sodium
cc	cubic centimeter(s)
cm	centimeter(s)
cm^{-1}	wavenumbers
cm^2	square centimeter(s)
Conc.	concentration
D_{SC}	diffusion coefficient of FD-4 in the SC layer
D_{Skin}	diffusion coefficient of FD-4 in skin by employing a hollow microneedle as a delivery method
D_{ved}	diffusion coefficient of FD-4 in viable epidermis and dermis layers
e.g.	exemplī grātiā (Latin); for example
Eq.	equation
et al.	and others
etc.	et cetera (Latin); and other things/ and so forth
FD-4	Fluorescein isothiocyanate (FITC)-dextrans MW 4,000
FD-10	Fluorescein isothiocyanate (FITC)-dextrans MW 10,000
FD-40	Fluorescein isothiocyanate (FITC)-dextrans MW 40,000
G	(needle) gauge
g	gram(s)
h	hour(s)

LIST OF ABBREVIATIONS

i.d.	inner diameter
i.e.	id est (Latin); that is
kDa	kilodalton
kg	kilogram(s)
L	liter(s)
mA	milliampere(s)
mg	milligram(s)
min	minute(s)
mL	milliliter(s)
mm	millimeter(s)
mM	millimolar(s)
ms	millisecond(s)
MW	molecular weight
ng	nanogram(s)
nm	nanometer(s)
nmol	nanomole(s)
o.d.	outer diameter
PBS	phosphate buffer solution
pH	potentia hydrogenii (Latin); power of hydrogen
R^2	coefficient of determination
rpm	revolutions per minute
s	sec(s)
SC	stratum corneum
S.E.	standard error
V	volt(s)

CHAPTER 1
INTRODUCTION

1.1 Statement and significance of the research problem

The two major routes of drug administration, oral delivery and injection, are not always feasible in routine practical use. Drug degradation and possible first-pass effect by the enzymatic system existed in the gastrointestinal tract and liver associated with oral delivery are the main obstacles that inhibit the development of drug substances into an oral formulation. Injection, compared with other routes of administration, is the fastest and effective way to deliver the drugs throughout the body. Patients, however, are not typically able to self-administer and suffer from pain as well as risk of infection. Transdermal drug delivery has emerged over many years as an alternative pathway for systemic drug delivery which overcomes the difficulties occurred by the conventional drug delivery systems as mentioned above and provides controlled delivery of drugs over the period of time. Because of its great advantages, it has become one of the highly research field among the various drug delivery systems.

Although the skin is a large and logical target for drug delivery, its basic functions limit its utility for this purpose. Only a limited number of drugs, essentially the small molecular weight drugs and lipophilic molecules can cross the skin at therapeutic rates by means of the conventional transdermal patches with little or no enhancement (Prausnitz and Langer, 2008: 1261–1268). To expand the range of candidate drugs in which they can be potentially administered through the skin, particularly for hydrophilic drugs, peptides, and macromolecules including new therapeutic agents employing oligonucleotides, DNA, or vaccine, a lot of attempts have been made to develop the methods for increasing the skin permeability, including chemical enhancers (Williams and Barry, 2004: 603–618) or physical enhancement techniques such as iontophoresis (Kalia et al., 2004: 619–658),

electroporation (Denet, Vanbever, and Préat, 2004: 659–674), phonophoresis (Prausnitz, Mitragotri, and Langer, 2004: 115–124), and microneedles (Prausnitz, 2004: 581–587). Although the mechanisms are all different, these methods share the common goal to disrupt the stratum corneum (SC) structure in order to create holes big enough for molecules to pass through (Prausnitz, 2004: 581–587). Many researchers have reported the potentially increasing effect of transdermal delivery when the physical enhancement methods were applied. Among of them, the recent technique employing microneedles, needles in micron dimensions generally range from 100–1000 μm, is in of great interest because they are minimally invasive devices and can effectively deliver a variety of compounds (Prausnitz, 2004: 581–587), especially for the macromolecules across the skin (Wu, Todo, and Sugibayashi, 2006: 102–108). The method uses the concepts of drug delivery from the user-friendly delivery of transdermal patches accompanying with the broad effectiveness of hypodermic injections. Although the needles in micron scale are too small, they can be efficacious because the most significant barrier to diffusion is the outermost skin layer, the SC, which is just 10 to 20 μm thick (Prausnitz, Mikszta, and Raeder-Devens, 2006: 239–256). By employing microneedles, therefore, the skin barrier is completely bypassed and facilitating drug transport can be achieved through the holes created by the needles. The drug is loaded into the viable epidermis or dermis, where the drug can diffuse rapidly for local delivery to skin or systemic distribution via uptake by dermal capillaries. Although safety studies need to be performed, it is proposed that micron-scale holes in the skin are likely to be safe, given that they are smaller than holes made by hypodermic needles or minor skin abrasions encountered in daily life (Prausnitz, 2004: 581–587). Microneedles application does not also typically cause bleeding as well as any severe pain at injection sites (Kaushik et al., 2001: 502–504).

There are two types of microneedles i.e. solid and hollow needles, which can be fabricated in a number of different ways using a variety of materials to produce a range of different geometries (Prausnitz, Mikszta, and Raeder-Devens, 2006: 239–256). By employing solid microneedles, two steps of drug delivery based on the patch application are commonly needed. Skin is pierced to create the pathways for

facilitating drug transport and then the patch-based drug dosage form is placed on the pre-treated skin. Hollow-typed microneedle patches provide an additional functionality over solid microneedle ones, because they can be used to deliver the therapeutic drugs across the skin by either a passive or an active system. As a passive system, a single step of enhanced drug delivery can be achieved through the internal holes of hollow microneedles over time. When used in an injection or infusion scenario, hollow microneedles permit delivery that is more rapid than traditional adhesive patches and can be modulated over time via active delivery controlled by hand or pump (Prausnitz, Mikszta, and Raeder-Devens, 2006: 239–256). Many studies emphasized solid (silicon and metal) needles, but more recent efforts have shifted to solid polymer needles and hollow needles. Increasing of drugs permeated through the microneedles-treated skin has been established with a wide range of compounds, including small (Henry et al., 1998: 922–925; Sivamani et al., 2005: 152–156; Verbaan et al., 2007: 238–245) and large molecular drugs (Cormier et al., 2004: 503–511; Verbaan et al., 2007: 238–245; Wu, Todo, and Sugibayashi, 2006: 102–108), proteinaceous drugs (Ito et al., 2006a: 82–88; Matriano et al., 2002: 63–70; Park, Allen, and Prausnitz, 2005: 51–66), antisense oligonucleotides (Lin, 2001: 1789–1793), DNA (Mikszta et al., 2002: 415–419), vaccines (Mikszta et al., 2005: 278–288), and even drug-loaded nanoparticles (Chabri et al., 2004: 869–877; Gill et al., 2007: 227–237; McAllister et al., 2003: 13755–13760). Although microneedles assist in penetrating the SC barrier and offer several microchannels facilitating drug transport across the skin, the release of macromolecular drugs at the desired therapeutic rate might not be achieved by only (enhanced) passive diffusion from the patch-based drug reservoir due to the small diffusional area produced by needles (Wu, Todo, and Sugibayashi, 2007: 189–195). It is necessary to further improve the transdermal delivery of drugs of large molecular weight by contributing push pressure to propel the drug toward the skin, similar to the conventional topical injection. Wu et al. (2007: 189–195) reported that the combination of solid microneedle pretreatment and subsequent iontophoresis significantly enhance fluorescein isothiocyanate-dextrans (FD) flux compared with microneedle pretreatment alone or iontophoresis alone.

It is difficult, however, to determine the penetration-enhancing effect as well as the parameters affecting the delivery efficiency produced by each enhancing technique and also by each individual microneedle. Yoshida et al. (2007: 142–147) carried out the study to investigate the dermatopharmacokinetics and systemic drug disposition after topical intracutaneous (i.c.) injection of sodium salicylate and concluded that injection volume is one of the factors which can be utilized to control the drug migration rate from the injection site. Al-Qallaf et al. (2007: 2951–2967) found that different surface areas of the hollow microneedle array-patch system affect the blood concentration of human growth hormone (hGH). It is obvious that in order to determine the optimum design of hollow microneedles system, information on the effect of several factors related to the delivery efficiency, for instance, various needle parameters including injection conditions (e.g. length of microneedle/ injection depth, needle numbers, distance between each needle, hollow size, pressure of injection, etc.), physicochemical properties of drugs (e.g. molecular weight, lipophilicity, etc.), and formulations must be considered. However, using the hollow microneedles device to perform the experiment is complicated because many needle parameters, as mentioned above, might affect the drug delivery efficiency or dermatokinetics of drug. Single hollow microneedle was often used at laboratory scale for small proof-of-concept studies.

The objective of the present study was to evaluate the influence of variables related to the hollow microneedle system on the *in vitro* drug release behavior of hydrophilic permeants from skin. Unless otherwise mentioned, Fluorescein isothiocyanate (FITC)-dextrans 4000 (FD-4), was used as a model large hydrophilic permeant. A single 33-gauge hypodermic needle, where the diameter was almost the same to the arrayed microneedles recently reported (Harvey et al., 2011: 107–116; McAllister et al., 2003: 13755–13760; Wang et al., 2006: 1080–1087; Wu, Todo, and Sugibayashi, 2006: 102–108, 2007: 189–195), was used as a single type hollow microneedle in order to reduce the effect of needle parameters. Furthermore, 33-guage steel (hypodermic) needle is mechanically robust, safety in FDA-approved device and can remove needle manufacturing factors. The effects of injection volume, number of injections, and different concentrations on the *in vitro* drug release

from skin were assessed. Moreover, the effect of molecular size of the model hydrophilic drugs was also investigated.

1.2 Objective of this research

1) To study the feasibility of using a hollow microneedle for facilitating hydrophilic drug delivery through the skin barrier

2) To examine the influence of various parameters i.e. injection volume, number of injections, different concentrations, and molecular weight (MW) of the model hydrophilic compounds on the *in vitro* drug release behavior from hollow microneedle-treated skin

1.3 The research hypothesis

1) A hollow microneedle can facilitate drug transport through the skin barrier and enhance transdermal delivery of even large hydrophilic permeants.

2) Injection volume, number of injections, molecular weight (MW) of the model hydrophilic drugs, and different concentrations influence the *in vitro* drug release behavior from hollow microneedles-treated skin.

CHAPTER 2
LITERATURE REVIEWS

2.1 The structure and function of skin

Skin is the outermost layer of the human organism separating the internal from the external environment. It is the largest organ of the body, accounting for more than 10% of body mass (Walters and Roberts, 2002: 1–39). One of its most important purposes is to function as a barrier; i.e., to prevent the entry of foreign materials and invasion of pathogens into and the loss of endogenous substances such as water out of the body. It would be very useful to be able to predict the rate at which materials penetrate the skin, to access potential toxicological hazards and also to improve the way in which the drugs are administered transdermally. The structure of human skin is illustrated in Figure 1. The major skin layers, from inside to outside, comprise the fatty subcutaneous layer (hypodermis), the dermis of connective tissue and the stratified avascular cellular epidermis (El Maghraby, Barry, and Williams, 2008: 203–222).

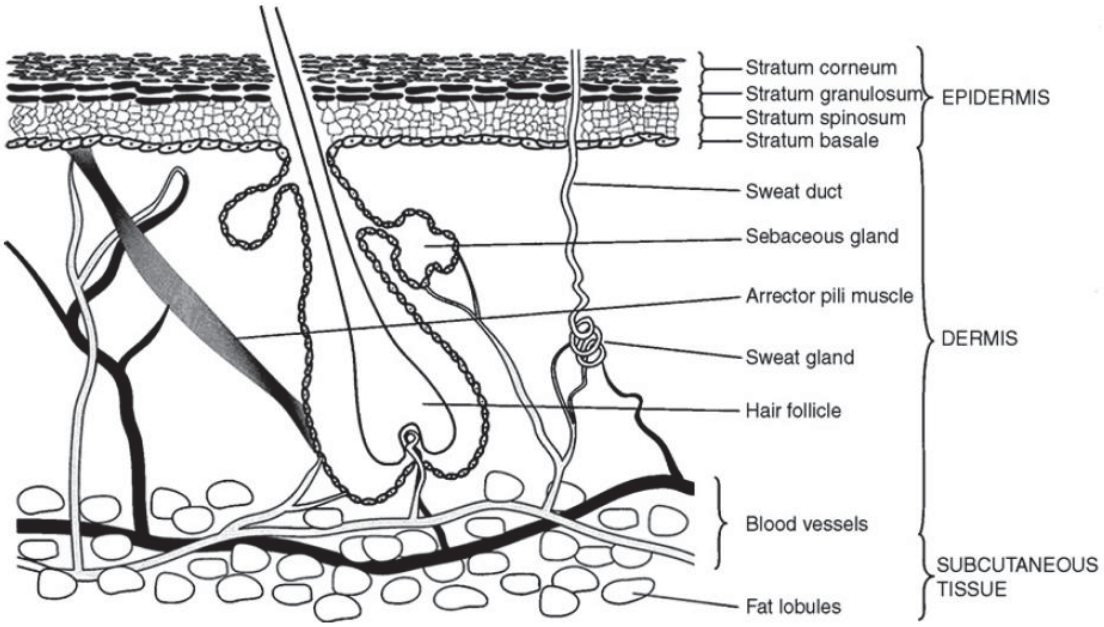

Figure 1 A diagrammatical representation of a cross-section through human skin showing the different cell layers and appendages (El Maghraby, Barry, and Williams, 2008: 205).

2.1.1 The subcutaneous fat layer

The subcutaneous fat layer or hypodermis is the deepest layer of the skin and consists of the subcutaneous tissue filled with fat cells, fibroblasts, and macrophages (Narasimha Murthy and Shivakumar, 2010: 1–36). This layer bridges between the overlying dermis and the underlying body constituents. In most areas of the body this layer is relatively thick, typically in the order of several millimeters (Williams, 2003: 1–25). This layer serves as a heat insulator, a shock absorber, and an energy storage region.

2.1.2 The dermis

The dermis is typically 3–5 mm thick and is the major component of human skin. It is composed of a network of connective tissue, predominantly collagen fibrils (70%) providing support and cushioning, and elastic connective tissue providing flexibility, embedded in a semigel matrix of mucopolysaccharides (Walters and Roberts, 2002: 1–39; Williams, 2003: 1–25). In terms of transdermal drug delivery, this layer is often viewed as essentially gelled water, and thus provides a minimal barrier to the delivery of most polar drugs (Williams, 2003: 1–25). There are numerous structures embedded within the dermis; blood and lymphatic vessels, nerve endings, pilosebaceous units (hair follicles and sebaceous glands), and sweat glands, as shown in Figure 1. The hair follicles and sweat ducts open directly into the environment at the skin surface and provide the so-called appendageal route of skin permeation (El Maghraby, Barry, and Williams, 2008: 203–222), (see Section 2.3). In addition, this layer is filled with a sparse cell population of scattered fibroblasts, macrophages, leukocytes, and mast cells (Narasimha Murthy and Shivakumar, 2010: 1–36).

2.1.3 The epidermis

The epidermis is a complex multiply layered membrane, consisting of several types of cell (corneocytes, melanocytes, Langerhans cells, and Merkel cells) and a variety of catabolic enzymes (esterases, phosphatases, proteases, nucleotidases, and lipases) (Narasimha Murthy and Shivakumar, 2010: 1–36). The stratified

epidermis is about 100–150 μm thick and comprises five histologically distinct layers, which from inside to outside are the stratum germinativum (basal layer), stratum spinosum (spinous layer), stratum granulosum (granular layer), stratum lucidum and the stratum corneum (SC, horny layer) (El Maghraby, Barry, and Williams, 2008: 203–222; Williams, 2003: 1–25). Because the SC cells are dead, the epidermis without the SC is usually termed the viable epidermis. The viable epidermis is made up of keratinocytes at various stages of differentiation. Typically, it takes 14 days for a daughter cell from the stratum basale to differentiate into a SC cell, and the SC cells are typically retained for a further 14 days prior to shedding (Williams, 2003: 1–25). The phospholipid content in skin decreases while the sphingolipid and cholesterol content gradually increases as the cells differentiate during their migration to the surface (Narasimha Murthy and Shivakumar, 2010: 1–36).

The SC is the heterogeneous outermost layer of skin and is approximately 10–20 μm thick. It is nonviable epidermis and consists of 15–25 flattened, stacked, hexagonal, and cornified cells embedded in a mortar of intercellular lipid, represented as a 'brick and mortar' model (Walters and Roberts, 2002: 1–39; Williams, 2003: 1–25). The SC is recognized as a rate limiting barrier in transdermal permeation of most molecules and is often viewed as a separate membrane in topical and transdermal drug delivery studies (Williams, 2003: 1–25). The barrier nature of the SC depends critically on its unique constituents; 75–80% of protein, 5–15% of lipid, and 5–10% unidentified on a dry weight basis (Williams, 2003: 1–25). The majority of the intracellular protein in the SC is composed of insoluble keratin filaments (around 70%) and the components of the cornified cell envelope (around 5%). The intercellular lipids of the SC exist as a continuous lipid phase and arrange in multiple lamellar structure. A remarkable feature is the lack of phospholipids and the predominance of ceramides (41%) and choresterol (27%), together with free fatty acids (9%), cholesteryl esters (10%), and cholesteryl sulfate (2%) (Walters and Roberts, 2002: 1–40). Many studies reveal that relatively polar lipids play a critical role in maintaining the barrier integrity of the SC (Narasimha Murthy and Shivakumar, 2010: 1–36). The composition of the SC intercellular lipids is summarized in Table 1.

Table 1 Lipid content of the stratum corneum intercellular space.[a]

Lipid	% (w/w)	mol %
Cholesterol esters	10.0	7.5[b]
Cholesterol	26.9	33.4
Cholesterol sulfate	1.9	2.0
Total cholesterol derivatives	38.8	42.9
Ceramide 1	3.2	1.6
Ceramide 2	8.9	6.6
Ceramide 3	4.9	3.5
Ceramide 4	6.1	4.2
Ceramide 5	5.7	5.0
Ceramide 6	12.3	8.6
Total ceramides	41.1	29.5
Fatty acids	9.1	17.0[b]
Others	11.1	10.6[c]

[a]Walters and Roberts, 2002: 20.

[b]Based on C_{16} alkyl chain.

[c]Based on MW of 500.

2.2 The transdermal permeation process

The process of percutaneous absorption involves multiple potential steps from a molecule's first application to the skin surface until it appears in the systemic circulation. The two key determinants for a solute crossing a membrane are solubility and diffusivity (Roberts, Elizabeth Cross, and Pellett, 2002: 89–195). The relative solubility of a solute in two domains determines its partition coefficient and, therefore, the likelihood of the solute being taken up into the SC from a vehicle. The diffusivity is a measure of how easily the solute will traverse through a given barrier and is affected by binding, viscosity of the environment, and the tortuosity of the path.

In the first step of transport process, the drug is typically applied to the skin in a vehicle. The molecule adjacent to the SC surface will partition into the

membrane dependent on their physicochemical properties. Since only molecules adjacent to the skin can partition from the vehicle into the membrane, further drug delivery is dependent upon molecules within the vehicle randomly redistributing to provide further molecules adjacent to the SC surface. In an extreme case, the diffusion of drug through the vehicle can limit the rate of transdermal drug delivery. The additional considerations will apply if the vehicle contains suspended particles. For poorly water-soluble drugs delivered from an aqueous system, dissolution of drug particles to maintain a saturated solution may be the rate-limiting step to transdermal drug delivery (Williams, 2003: 27–49).

Once the permeant has partitioned into the outer layer of the SC, the drug then diffuses through the SC. At the SC/viable epidermis junction there is another partitioning step as the molecules move into the viable epidermis before further diffusion through it to the epidermis/dermis junction. Again, there is partitioning followed by diffusion through the dermis tissue where the systemic absorption can take place. In addition to these multiple partitioning and diffusion processes for transdermal drug delivery, there are other potential fates for molecules entering human skin. Permeants may bind with various elements of the skin. For example, drug binding to keratin within the SC could provide a reservoir effect. Drug degradation or activation may occur at metabolic sites. Further, depending on the nature of the drug, the permeant may not enter the systemic circulation but may partition into the subcutaneous fatty layer. Indeed, some molecules may even reach muscles (Williams, 2003: 27–49).

2.3 Basic mathematical principles in skin permeation

Since all compounds are thought to transfer the skin by a passive diffusion mechanism (to date, no active transport mechanisms have been reported), it is then possible to apply the Fick's laws of diffusion to the data obtained from the skin transport experiments (Guy and Hadgraft, 1985: 3–15; Watkinson and Brain, 2002: 61–88; Williams, 2003: 27–49; Yamashita and Hashida, 2003: 1185–1199). In the transport process, the molecules move in response to a thermodynamic force arising from a concentration gradient. Fick's first law is to assume that the rate of transfer of

diffusing substance through unit area of a section is proportional to the concentration gradient:

$$J = -D\frac{\partial C}{\partial x} \tag{1}$$

where J is the rate of transfer per unit area, $\partial C/\partial x$ is the concentration gradient (C is the concentration of diffusing substance, x is the space coordinate), and D is the diffusion coefficient. In real situations steady-state conditions are unlikely to be established during the penetration of drugs across the skin. As such the law is not readily usable; Fick's second law is employed to analyze the flux and concentration profiles under these conditions. Fick's second law can be derived from Eq. 1:

$$\frac{\partial C}{\partial t} = D\frac{\partial^2 C}{\partial x^2} \tag{2}$$

where t is time. Thus, the rate of change in concentration with time at a given point in a system is proportional to the rate of change in the concentration gradient at that point. Solutions to this second-order differential equation are complex and depend on the boundary conditions for the experiment. The simplest boundary conditions are as follows:

$$\begin{aligned} t > 0 \quad x = 0 \quad & C = KC_v \\ x = h \quad & C = 0 \end{aligned}$$

where K is the skin–vehicle partition coefficient, C_v is the concentration of the solute in the vehicle and constant over time, and h is the thickness of the skin. The diffusive flow begins at the high-concentration side (the donor side, $x = 0$) of the membrane and occurs in the direction of decreasing x toward the opposite side of the membrane where $x = h$ and $C = 0$ (sink receptor phase) for all time t. There is no diffusant material within the membrane before the ingress of the permeant being modeled,

implying that $C(0<x<h)$ equals zero at $t = 0$. After the sufficient time, steady-state permeation across the membrane is achieved when the concentration gradient of the permeant across the membrane is constant. Under these conditions, Eq. 2 can be simplified to Eq. 3:

$$\frac{dQ}{dt} = J = \frac{DC_0}{h} \tag{3}$$

where Q is the cumulative amount of permeant passing through a unit area of the membrane in time t, C_0 is the concentration of the permeant in the first layer of the membrane in contact with the donor solution (at skin surface). The graphic plot of the cumulative amount of diffusant, Q, passing per unit area through a membrane at long times, approaches linearity and its slope yields the steady-state flux J (dQ/dt). In practical terms, it is very difficult to determine the C_0. The value C_0 can be replaced with a term that links it to the concentration in the vehicle C_v (which is usually known) through the partition coefficient K, as expressed by Eq. 4:

$$\frac{dQ}{dt} = J = \frac{DKC_v}{h} \tag{4}$$

This equation is more practical and widely applied in examining the transdermal drug delivery data. The lag time (t_{lag}; the period during which the rate of permeation across the membrane is increasing) can be obtained from extrapolation of the pseudo-steady-state portion of the permeation profile (a plot of Q against time) to the intercept on the time axis, as described by Eq. 5:

$$t_{lag} = \frac{h^2}{6D} \tag{5}$$

Eq. 5 is only applicable to situations where there are no significant interactions, such as binding between the permeant and the components of the skin.

The permeability coefficient (P) of the permeant through a membrane, which is often used to assess the membrane permeability of drugs, can be defined by:

$$P = \frac{KD}{h} \tag{6}$$

which can be substituted into Eq. 4 to give:

$$\frac{dQ}{dt} = J = PC_v \tag{7}$$

where the pseudo-steady-state flux J is simply obtained from the gradient of the linear portion of the permeation profile as described above, and if the concentration of the permeant in the applied vehicle is known then the permeability coefficient can be determined. Other parameters such as the diffusion coefficient can also be used to characterize the permeation of drugs across the skin but are more difficult to calculate accurately due to the difficulty in measuring the membrane thickness.

2.4 Transport pathways through the stratum corneum

There are three potential pathways postulated for the diffusion of permeants through the intact SC: (a) intercellular (paracellular) pathway; (b) transappendageal pathway; and (c) transcellular pathway (Roberts, Elizabeth Cross, and Pellett, 2002: 89–195; Williams, 2003: 27–49) (Figure 2). Typically, all molecules traverse the SC by a combination of all three routes. The relative contributions of these pathways to the total flux will depend on the molecules physicochemical characteristics. An additional potential pathway (d) that enabling the large molecular transport via micron-scale holes in skin created by microneedles (see Section 2.5) and thermal poration is also illustrated in Figure 2.

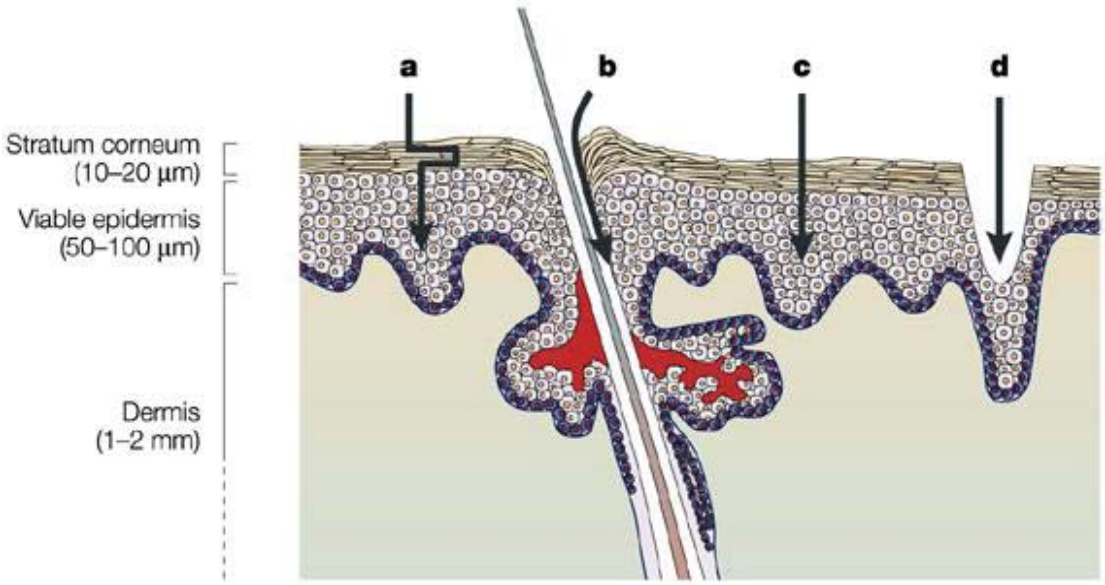

Figure 2 The possible drug permeation pathways through the SC: (a) Intercellular pathway; (b) Transappendageal pathway; (c) Transcellular pathway; (d) Micropores generated by microneedles and thermal poration to provide pathways for enhancing drug transport (Prausnitz, Mitragotri, and Langer, 2004).

2.4.1 Intercellular pathway

The intercellular pathway is a continuous and highly tortuous way through the intercellular lipid domain. It is now generally accepted that, most molecules penetrate through skin via this intercellular microroute and therefore various enhancing techniques aim to disrupt, possibly in the presence of a chemical enhancer, or bypass its well-organized molecular architecture (Barry, 2001: 101–114; Roberts, Elizabeth Cross, and Pellett, 2002: 89–195). The pathlength for intercellular permeation has been proposed ranging from 150 to 500 μm, which is considerably greater than the SC thickness.

2.4.2 Transappendageal pathway

The transappendageal route is also known as a shunt route, including the permeation through the sweat glands and across the hair follicles with their associated

sebaceous glands. Because of the low fractional appendageal area (around 0.1% of the total skin surface), this pathway usually contributes negligibly to steady state drug flux (Barry, 2001: 101–114). However, with finite dosing and at short time periods after drug application, the relative contribution of the appendages will be significantly greater since molecules will not have had time to cross the bulk of the SC (Williams, 2003: 27–49). Transappendageal pathway may also be important for ions and large polar molecules that poorly traverse the intact SC. Moreover, these shunt routes are also important for delivering vesicular structures to the skin and for targeting to the pilosebaceous units. One of the most considerable determinants of targeted follicular transport is the particle size of applied materials in which the degree of follicular penetration was inversely dependent on the particle size and the optimum size at which microspheres selectively entered the follicles was 3–10 μm (Roberts, Elizabeth Cross, and Pellett, 2002: 89–195; Rolland et al., 1993: 1738–1744). Low-voltage electrical enhancement by iontophoresis can provide the transport pathways through hair follicles and sweat ducts more accessible (Prausnitz, Mitragotri, and Langer, 2004: 115–124).

2.4.3 Transcellular pathway

The transcellular pathway can be defined as the pathway where molecules permeate across the intact SC through the keratinized cells. The transport process faces numerous repeating hurdles because the keratinocytes are bound to a lipid envelop that attaches to the intercellular multiply bilayered lipid domain. Thus, the molecules require not only partitioning into and diffusion through the hydrated keratin but also into and across the intercellular lipids. It is obvious that the process of multiple partitioning and diffusion steps between hydrophilic and hydrophobic domains is generally unfavorable for most drugs (Williams, 2003: 27–49). Moreover, the keratin also provides the potential binding sites for the solutes. For highly hydrophilic molecules, the transcellular route may predominate at pseudo-steady state. However, the rate-limiting barrier for permeation via this pathway remains the multiply intercellular lipid bilayers (Williams, 2003: 27–49). High-voltage enhancement by electroporation has been shown to occur via the transcellular

pathway by disrupting the lipid bilayers (Prausnitz, Mitragotri, and Langer, 2004: 115–124).

2.5 Percutaneous penetration enhancers

The range of drugs that can be delivered in therapeutic doses via the skin for both local and systemic therapies is limited by a highly efficient and effective barrier of the SC. The simple equation for steady-state flux (Eq. 4; as described above in Section 2.3) is useful when considering factors controlling the SC permeation rates. According to Eq. 4, the ideal properties needed for a molecule to penetrate the SC well can be accessed. There are: low molecular mass, preferably less than 600 Da, adequate solubility in oil and water, high but balanced (optimal) partition coefficient, and low melting point, correlating with good solubility as predicted by ideal solubility theory (Barry, 2001: 101–114, 2006: 3–16). If the permeant does not possess appropriate partitioning, diffusivity or solubility properties, then the use of penetration enhancers are favorably. Figure 3 summarizes some techniques for overcoming the barricade offered by an intact SC (Barry, 2006: 6). Drug permeation across the skin could be enhanced by adapting one or more of these several strategies.

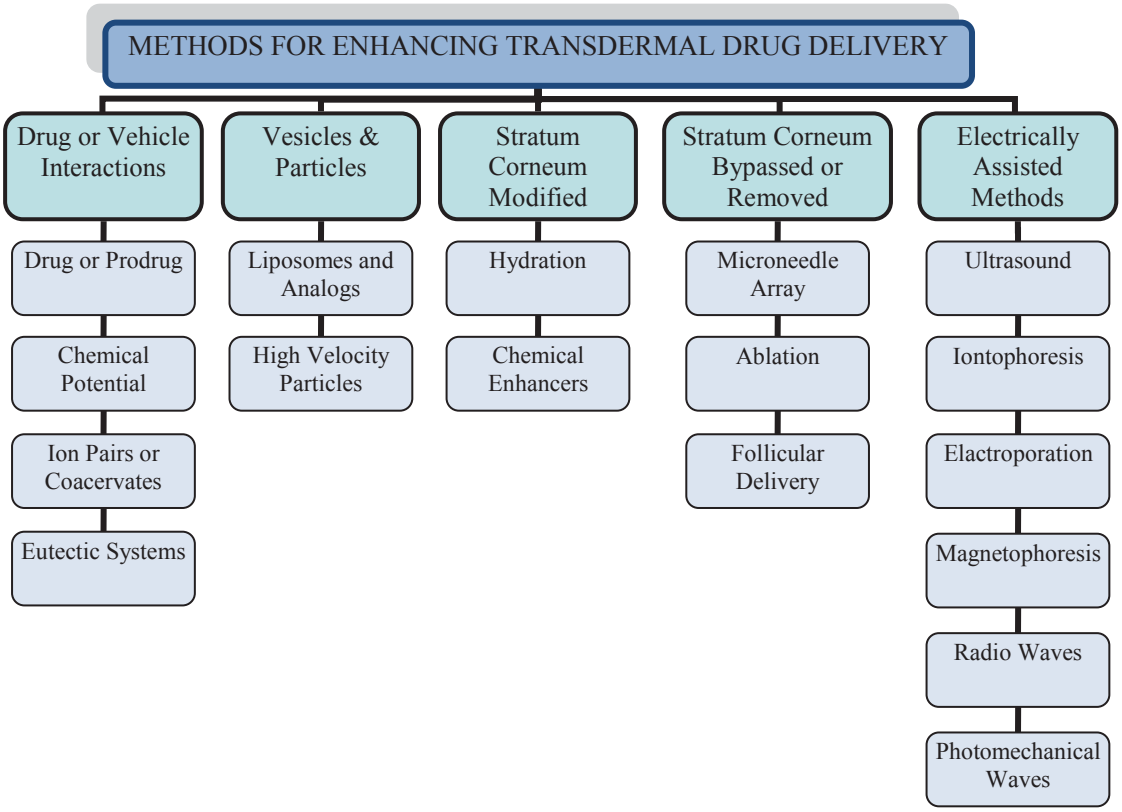

Figure 3 Some methods for enhancing transdermal drug therapy (Barry, 2006: 6).

Permeation enhancement methods showing in Figure 3 can be classified roughly into two categories; the chemical enhancers and the physical enhancers.

2.5.1 Chemical enhancers

Substances that help promoting drug diffusion through the SC and epidermis are referred to as chemical penetration enhancers. The literature reveals numerous classes of chemical compounds that have been accessed for their ability to promote or enhance the permeation of biomolecules across the skin (Chattaraj and Walker, 1995: 7–8). Various elegant formulations that may contain substances which have penetration enhancing activity are also addressed. For example, vesicles are often prepared from phospholipids; phospholipids themselves have some penetration enhancing activity. Likewise, penetration enhancers have been formulated into eutectic systems or into slow or sustained release delivery systems (Williams and Barry, 2004: 603–618). Table 2 provides an overview of some of different chemical

classes that have been used as penetration enhancers and examples of substances within each specific chemical class (Chattaraj and Walker, 1995: 7–8).

Table 2 Some of chemical classes used as penetration enhancers.*

Chemical Class	Examples
Sulfoxides	Dimethlsulfoxide, decylmethylsulfoxide
Alcohols	Alkanol: ethanol, propanol, butanol, pentanol, hexanol, octanol, nonanol, decanol, 2-butanol, 2-pentanol, benzyl alcohol Fatty alcohol: caprylic, decyl, lauryl, 2-lauryl, myristyl, cetyl, steryl, oleyl, linoleyl, linolenyl alcohol
Fatty acids	Linear: valeric, heptanoic, pelagonic, caproic, capric, lauric, myristic, stearic, oleic, caprylic Branched: isovaleric, neopentanoic, neoheptanoic, neononanoic, trimethyl hexanoic, neodecanoic, isostearic
Fatty acid esters	Aliphatic-isopropyl *n*-butyrate, isopropyl *n*-hexanoate, isopropyl *n*-decanoate, isopropyl myristate, isopropyl palmitate, octyldodecyl myristate Alkyl: ethyl acetate, butyl acetate, methyl acetate, methyl valerate, methyl propinoate, diethyl sebacate, ethyl oleate
Polyols	Propylene glycol, polyethylene glycol, ethylene glycol, diethylene glycol, triethylene glycol, dipropylene glycol, glycerol, propanediol, butanediol, pentanediol, hexanetriol
Amides	Urea, dimethylacetamide, diethyltoluamide, dimethylformamide, dimethyloctamide, dimethyldecamide Biodegradable cyclic urea: 1-alkyl-4-imidazolin-2-one Pyrrolidone derivatives: 1-methyl-2-pyrrolidone, 2-pyrrolidone, 1-lauryl-2-pyrrolidone, 1-methyl-4-carboxy-2-pyrrolidone, 1-hexyl-4-carboxy-2-pyrrolidone, 1-lauryl-4-carboxy-2-pyrrolidone, 1-methyl-4-methoxycarbonyl-2-pyrrolidone, 1-hexyl-4-methoxycarbonyl-2-pyrrolidone, 1-lauryl-4-methoxycarbonyl-2-pyrrolidone, *N*-cyclohexylpyrrolidone, *N*-dimethylaminopropylpyrrolidone, *N*-cocoalkylpyrrolidone, *N*-tallowalkylpyrrolidone

Table 2 (continued) Some of chemical classes used as penetration enhancers.*

Chemical Class	Examples
Amides	Biodegradable pyrrolidone derivatives: Fatty acid esters of *N*-(2-hydroxyethyl)-2-pyrrolidone
	Cyclic amides: 1-dodecylazacycloheptan-2-one (Azone®), 1-geranylazacycloheptan-2-one, 1-farnesylazacycloheptan-2-one, 1-geranylgeranylazacycloheptan-2-one, 1-(3,7-dimethyloctyl)azacycloheptan-2-one, 1-(3,7,11-trimethyldodecyl)azacyclohaptan-2-one, 1-geranylazacyclohexan-2-one, 1-geranylazacyclopentan-2,5-dione, 1-farnesylazacyclopentan-2-one
	Hexamethylenelauramide and its derivatives
	Diethanolamine, triethanolamine
Surfactants	Anionic: Sodium laurate, sodium lauryl sulfate
	Cationic: Cetyltrimethyl ammonium bromide, Tetradecyltrimethylammonium bromide, benzalkonium chloride, octadecyltrimethylammonium chloride, cetylpyridinium chloride, dodecyltrimethylammonium chloride, hexadecyltrimethylammonium chloride
	Nonionics: Poloxamer (231, 182, 184), Brij (30, 93, 96, 99), Span (20, 40, 60, 80, 85), Tween (20, 40, 60, 80), Myrj (45, 51, 52), Miglyol 840
	Bile salts: Sodium cholate, sodium salts of taurocholic, glycolic, desoxycholic acids
	Lecithin
Terpenes	Hydrocarbons: D-Limonene, α-pinene, β-carene
	Alcohols: α-Terpineol, terpinen-4-ol, carvol
	Ketones: Carvone, pulegone, piperitone, menthone
	Oxides: Cyclohexene oxide, limonene oxide, α-pinene oxide, cyclopentene oxide, 1,8-cineole
	Oils: Ylang ylang, anise, chenopodium, eucalyptus
Alkanones	*N*-heptane, *N*-octane, *N*-nonane, *N*-decane, *N*-undecane, *N*-dodecane, *N*-tridecane, *N*-tetradecane, *N*-hexadecane

Table 2 (continued) Some of chemical classes used as penetration enhancers.*

Chemical Class	Examples
Organic acids	Salicylic acid and salicylates (including their methyl, ethyl, and propyl glycol derivatives), citric and succinic acid

* Chattaraj and Walker, 1995: 7–8

Although many chemicals have been evaluated as penetration enhancers in human or animal skins, to date none has proven to be ideal. The ideal penetration enhancers should have the following characteristics (Chattaraj and Walker, 1995: 5–20; Narasimha Murthy and Shivakumar, 2010: 1–36; Williams and Barry, 2004: 603–618)

- Be both pharmacologically and chemically inert and chemically stable
- A high degree of potency with specific activity and reversible effects on the skin properties
- Be both predictable and reproducible on the activity and duration of action
- Show compatibility with formulation and system components
- Work rapidly and uni-directionally, i.e. should allow therapeutic agents into the body whilst preventing the loss of endogenous material from the body
- Be non-irritating, non-sensitizing, non-allergenic, non-toxic, and non-comedogenic
- Be odorless, tasteless, colorless, and cosmetically acceptable

It is difficult to select rationally a penetration enhancer for a given permeant. Penetration enhancer potencies appear to be drug specific, or at best may be predictive for a series of compounds that have the similar physico-chemical properties (Williams and Barry, 2004: 603–618). The exact mechanism(s) by which many chemical penetration enhancers function remains to be clearly elucidated. It is almost certain that they will have multiple effects once absorbed into the SC. The potential mechanisms of action of the enhancers can range from direct effects on the skin to modification of the formulation. By directly acting on the skin, enhancers can

act by altering skin lipids and/or proteins and/or by affecting partitioning behavior; termed the lipid–protein partititioning theory (Barry, 1991: 237–248, 2001: 101–114) as depicted in Figure 4. In addition, chemical enhancers can act indirectly by modification of the thermodynamic activity of the vehicle and solubilising the permeant in the donor solution (e.g. with surfactants) (Williams and Barry, 2004: 603–618).

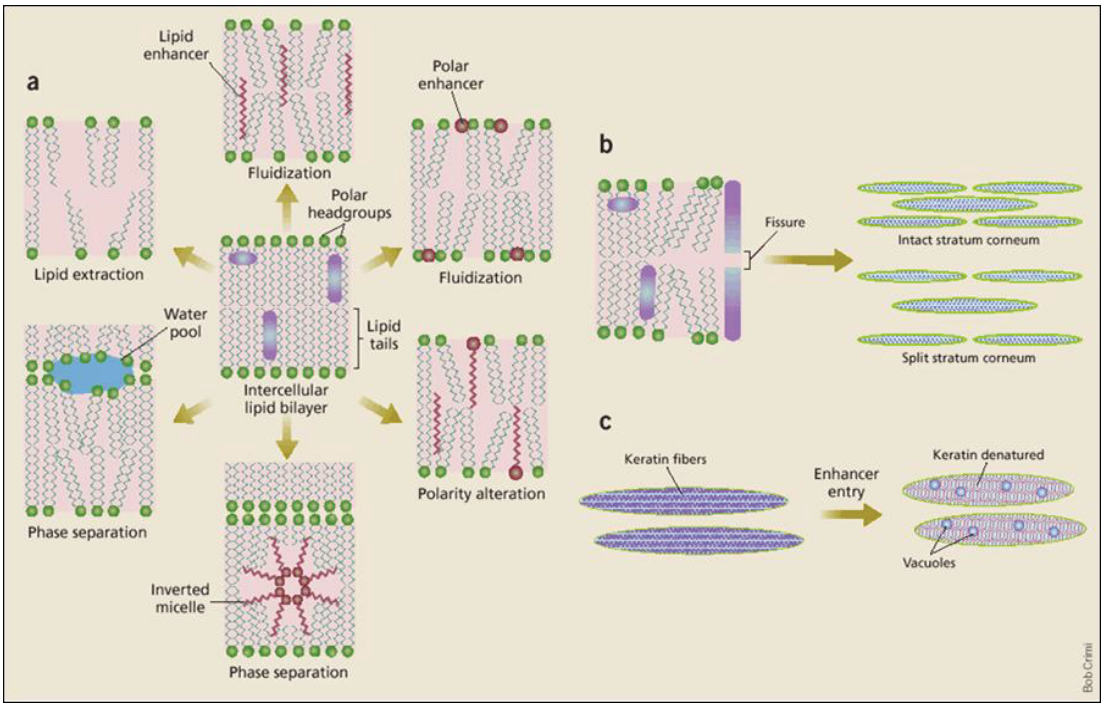

Figure 4 Some actions of penetration enhancers on the human SC: (a) Action at intercellular lipids. Some of the ways by which chemical penetration enhancers attack and modify the lamellar intercellular lipid domain of the SC; (b) Action at desmosomes and protein structures. Such dramatic disruption by enhancers (particularly potent solvents) as they split the SC into additional squames and individual cells would be clinically unacceptable; (c) Action within corneocytes. Swelling, further keratin denaturation and vacuolation within individual horny layer cells would not be so drastic but would usually be cosmetically challenging (Barry, 2004: 165).

2.5.2 Physical enhancers

The uncertainty of the chemical means of penetration enhancement makes the use of the physical approaches attractive. By the physical means, the SC can be modified by bypassing or removing this tissue layer via microneedles (which is of particular interest, see Section 2.5) and thermal ablation. Thermal ablation or thermal poration refers to the selective removal of the SC without damaging the deeper tissue layers by heating the skin surface briefly (e.g. << 1 s). The formation of micropores of 30 μm diameter and 70 μm depth and the absence of necrosis in surrounding tissue has been addressed using selective ablation techniques (Arora, Prausnitz, and Mitragotri, 2008: 227–236). Electrically assisted methods, i.e. iontophoresis, ultrasound, and electroporation, are also promising. Ionized drugs and complex macromolecules such as proteins or peptides may be induced to penetrate the SC at a faster rate than normal by an iontophoresis technique. A small electrical current (approximately 0.5 mA/cm^2) is applied across the membrane. The charged permeant is repelled from the electrode of similar polarity into the SC, which acts as the electrical conduit to the companion electrode (Smith and Maibach, 1995: 1–4). Iontophoretic flux is obtained not only by electrorepulsion but also electroosmotic solvent flow (Wu, Todo, and Sugibayashi, 2007: 189–195). The application of ultrasound (at low frequency) on skin makes the intercellular and transcellular pathways more permeable by cavitation and fluidizing the SC lipids and/or increasing the convective flow (Prausnitz, Mitragotri, and Langer, 2004: 115–124; Wang et al., 2005: 179–191). This method is also known as phonophoresis or sonophoresis. High-voltage (50–500 V) enhancement at short time (< 1 s) by electroporation has been shown to occur via transcellular pathways by disorganizing the SC lipid structure (Prausnitz, Mitragotri, and Langer, 2004: 115–124). The creation and/or the enlargement of aqueous pathways during electroporation has been extensively proposed and observed in many studies (Wang et al., 2005: 179–191). Table 3 shows the comparative efficacy of some delivery methods in terms of increase in drug transport, sustained drug release, pain sensation, and complexity (Bariya et al., 2012: 11–29). Although all these methods have been individually shown to enhance the transdermal drug transport, their combinations have been widely studied and found to

enhance the transdermal transport more effectively than each of them alone (Mitragotri, 2000: 1354–1359).

Table 3 Comparative efficacy of different approaches to drug delivery across the skin.*

Delivery method	Increased transport	Sustained delivery	No pain/ irritation	Low capacity/ complexity
Hypodermic needle	+++	++	+	+++
Chemical enhancer	+	+++	++	+++
Iontophoresis	++	+++	+++	+
Electroporation	++	+++	++	+
Ultrasound	++	+++	+++	+
Microneedles	++	+++	+++	+
Thermal poration	++	+++	+++	+

+, Low efficacy; ++, Moderate efficacy; +++, High efficacy.

* Adapted from Bariya et al., 2012: 13.

2.6 Microneedles

For over 150 years, syringes and hypodermic needles have been used to deliver drugs into patients. The hollow needle was firstly invented in 1844, and the first injection was applied shortly after (McAllister, Allen, and Prausnitz, 2000: 289–313). The needle's impact as a drug delivery vehicle is still strong today, partly because many therapeutic agents cannot be administered orally due to their poor absorption in the intestine and/or sensitiveness to the enzymatic degradation. Currently, the smallest needles available for injections are used widely for insulin administration, measuring 30 gauge for conventional syringes and 31 gauge for pen injectors. The outer diameters of 30- and 31-gauge needles are 305 μm and 254 μm, respectively (Becton Dickinson, Franklin Lakes, New Jersey) (McAllister, Allen, and Prausnitz, 2000: 289–313).

Microneedles are needle-like structures with an approximate external diameter of not more than 300 μm and lengths up to 1 mm (Bariya et al., 2012: 11–29; van der Maaden, Jiskoot, and Bouwstra, 2012). These structures are used to

pierce the upper layer of the skin to enable (trans)dermal drug delivery. The concept employs an array of needles in micron-scale that are sufficiently large to deliver drug effectively, but small enough to avoid causing pain (Prausnitz, Mikszta, and Raeder-Devens, 2006: 239–256). Although the microneedles concept was first proposed and patented by Alza Corporation in the 1976 (Gerstel and Place, 1976), it was not demonstrated until the microfabrication tools became available in 2000s for making such small structures (Prausnitz, 2004: 581–587). Microscopic needles are efficacious because the rate-limiting barrier to transdermal delivery is the outermost layer of skin, the SC, which is just 10 to 20 μm thick. The advantages and disadvantages of microneedles are summarized in Table 4 (Bariya et al., 2012: 11–29).

Table 4 Advantages and Disadvantages of microneedles.

Advantages	Disadvantages
Be able to deliver large molecules	Lower in Dosage accuracy than hypodermic needles
Avoidance of first-pass metabolism	Careful use of device may be needed
The process is, by itself, biologically nontoxic and minimally invasive.	Penetration depth could vary due to the thickness variation of the SC and other skin layers between individuals
Painless administration and no fear of needle	The external environment, such as hydration of the skin, could affect delivery
Ease of administration	Repetitive injection may collapse the veins
Faster healing at injection site than with a hypodermic needle	The tip of microneedle may break off and remain within the skin
Decrease of microbial penetration as compared with a hypodermic needle	Small amount of drug (less than 1 mg) can be administered by bolus
Targeting the specific skin area for desired drug delivery	Compressed dermal tissue can block hollow microneedles
Enhanced drug efficacy may result in dose reduction	
Good tolerability without long-term oedema or erythema	
Enable rapid drug delivery by coupling with an electrically controlled micropump	
Delivery rate can be controlled more effectively as compared with drug delivery via the SC	

2.6.1 Microneedle fabrication

Microneedles can be fabricated in a number of different ways using a variety of materials to create a range of different geometries, including both solid and hollow microneedles (Donnelly, Raj Singh, and Woolfson, 2010: 187–207; Prausnitz, Mikszta, and Raeder-Devens, 2006: 239–256) (Figure 5–6). Moreover, they have been fabricated in-plane, where the microneedle is parallel to the substrate surface, and out-of-plane, where the microneedle is perpendicular to the substrate surface (Kaushik et al., 2010: 135–164). The materials that have been used in fabrication methods are silicon (wafers), stainless steel, titanium, nickel-iron, glass, and numerous polymers. Each material requires a slightly different method of fabrication and has diversely physical characteristics. The first produced microneedles for drug delivery were made out of silicon wafers by lithography and plasma etching. The processing methods for silicon have been extensively studied in the microelectronics industry and are suitable for the highly-reproducible mass production of microneedles. (Prausnitz, Mikszta, and Raeder-Devens, 2006: 239–256; van der Maaden, Jiskoot, and Bouwstra, 2012). Another benefit of silicon microneedles is that they are usually much sharper than polymeric and metal microneedles (van der Maaden, Jiskoot, and Bouwstra, 2012). The disadvantages of silicon needles include the expensive micro-fabrication processes and claenroom processing and the risk of needles breaking due to the fragile nature of silicon (Prausnitz, Mikszta, and Raeder-Devens, 2006: 239–256; van der Maaden, Jiskoot, and Bouwstra, 2012). Other microneedle production processes by laser cutting, molding, chemical etching, and other techniques, have been lately introduced for the generation of cheaper and biocompatible microneedles, including metal, polymer, and polysaccharide-based microneedles. One of the most common materials in fabrication of metal needles is the stainless steel, which is biocompatible, inexpensive, and mechanically strength (Verbaan et al., 2007: 238–245). Metals are especially attractive materials for making hollow needles where the structural strength is needed (Davis et al., 2004: 1155–1163). The metal needles are also known to be safe in FDA-approved devices. Polymeric needles utilize the engineering plastics, biodegradable polymers, and water-soluble polymers such as polycarbonate, polylactic-coglycolic acid, and

carboxymethyl cellulose, respectively (Arora, Prausnitz, and Mitragotri, 2008: 227–236). Polymer microneedles could have important benefits over microcroneedles made of other materials, because polymers are inexpensive, can be biocompatible, and they are amenable to mass production. Drugs may be incorporated into the biodegradable polymeric microneedles for controlled drug delivery (Park, Allen, and Prausnitz, 2005: 51–66, 2006: 1008–1019). However, polymeric microneedles are generally weaker than those prepared from silicon or metal, thus, the selection of an appropriate polymer and microneedle design are critical for making needles that easily penetrate the skin without breaking (Prausnitz, Mikszta, and Raeder-Devens, 2006: 239–256).

2.6.2 Type of approach

There are four general approaches of (trans)dermal drug delivery by microneedles depending on the microneedle design (Arora, Prausnitz, and Mitragotri, 2008: 227–236; Bariya et al., 2012: 11–29; Gill and Prausnitz, 2007: 227–237; van der Maaden, Jiskoot, and Bouwstra, 2012), as schematically shown in Figure 7. The limitations, advantages, and disadvantages of each approach are summarized in Table 5.

2.6.2.1 *Solid microneedles*

There are three main mechanisms in which the solid microneedles can be used to administer the therapeutic drugs into the skin. They are the “poke and patch” approach, the “poke and release” approach, and the “coat and poke” approach.

Solid microneedles were firstly used in the poke and patch approach (Figure 7a). In this method microneedles are pierced onto the skin surface. Once the microchannels exist in the SC, a reservoir of drug is applied onto the site of microneedle application and allowed to diffuse through the formed microchannels. Oh et al. (2008: 1040–1045) performed the study comparing the application modes of solid polycarbonate (PC) microneedles in which the PC microneedle was inserted into the skin ahead of applying the drug formulation or, the drug was directly loaded onto skin and then the PC microneedle was inserted or, the drug was applied into skin with the PC microneedle, simultaneously. It was shown that the highest permeation profile

was obtained when the drug was applied into skin together with the microneedle. Another study of Martanto et al. (2004: 947–952) which comparing the removal of microneedle array before applying the drug solution and leaving the microneedle array in skin for various time while applying the drug solution revealed that shorter microneedle insertion time resulted in a larger pharmacological effect. For the poke and patch approach, it is important that the micropores stay open during the drug application period. It has been reported that residual micropores after microneedle removal in *in vivo* rat skin were completely close within 15 h. However, under an occlusive condition, the barrier recovery can be delayed for up to 72 h (Kalluri and Banga, 2011: 82–94). Passive transport of drugs through the micropores does not always lead to a high bioavailability of drugs; therefore, this approach has been combined with iontophoresis or electroporation to further enhance the drug delivery through skin compared to each technique alone (Chen Huabing et al, 2009: 63–72; Wu, Todo, and Sugibayashi, 2007: 189–195; Yan, Todo, and Sugibayashi, 2010: 77–83).

The second mechanism, coat and poke, involves coating the microneedle arrays with drug solution using a dip-coating method and then inserting them into skin (Figure 7b). This coating can dissolve or release rapidly after insertion into skin. The coating solution usually contains drug, viscosity agent, surfactant, and solvent (Kaushik et al., 2010: 135–164). A board range of drugs, including calcein, vitamin B, bovine serum albumin, plasmid DNA, modified vaccinia virus, and microparticles, have been coated onto the microneedles (Gill and Prausnitz, 2007: 227–237). However, a limited amount of drugs could be coated over the microneedles (only about 1 mg) (Bariya et al., 2012: 11–29). Therefore, this approach is only applicable for very potent drugs, such as vaccines (van der Maaden, Jiskoot, and Bouwstra, 2012). This approach is also required an extensive optimization for uniform coating.

Further research resulted in the development of a poke and release approach (Figure 7c). Microneedles were fabricated out of the biodegradable or water-soluble polymers. Model drugs have been encapsulated within the microneedles for controlled drug release system (Lee, Park, and Prausnitz, 2008: 2113–2124; Park, Allen, and Prausnitz, 2006: 51–66). The advantage of this

approach is that the drug release could be modified by using a variety of available polymers. The administration of a large amount of drug was still not feasible with all these approaches, which led to the development of the hollow microneedles (Bariya et al., 2012: 11–29).

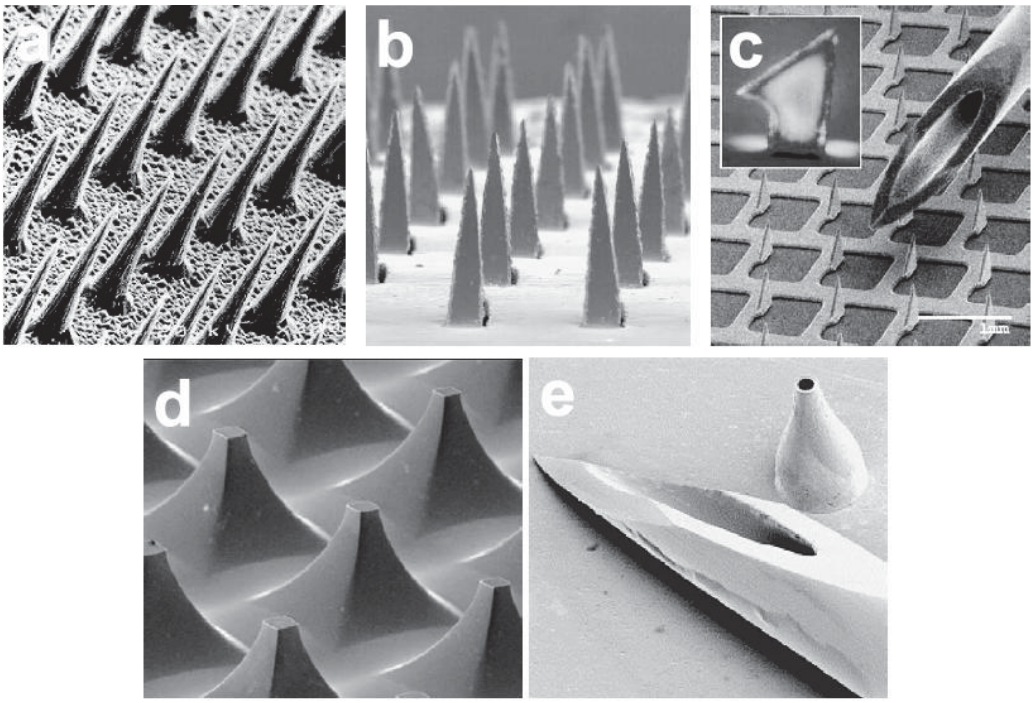

Figure 5 Images of microneedles used for transdermal drug delivery: (a) Solid microneedles (150 μm tall) etched from a silicon wafer were used to demonstrate microneedles for transdermal delivery; (b) Solid microneedles (1000 μm tall) laser-cut from a stainless steel sheet were used to deliver insulin to diabetic rats; (c) Solid microneedles ("microprojection array", 330 μm tall) acid-etched from a titanium sheet were coated with protein antigen for vaccine delivery *in vivo*; similar needles were used to deliver oligonucleotides *in vivo*; (d) Solid microneedles (''microenhancer array'', 200 μm tall) chemically etched from a silicon wafer were dipped in plasmid DNA solution for vaccine delivery *in vivo*; (e) Hollow microneedles (500 μm tall) formed by electrodeposition of metal onto a polymer mold were used for needle insertion and fracture force measurements (Prausnitz, 2004: 584).

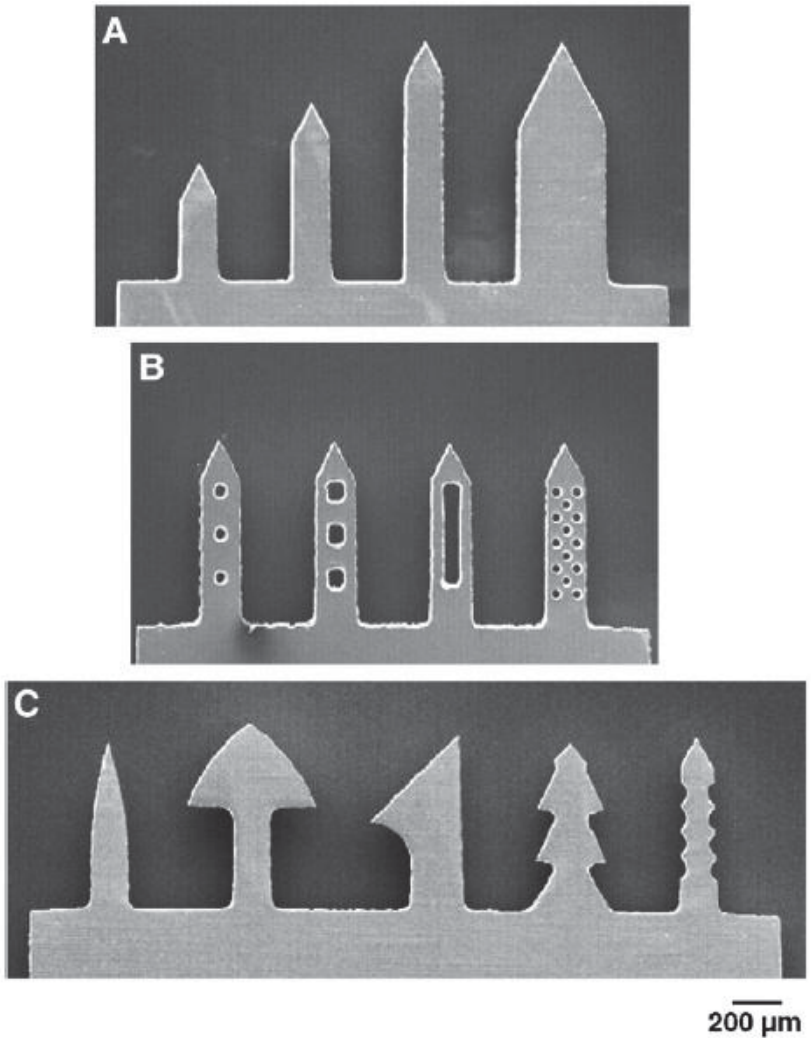

Figure 6 Fabrication of different microneedle geometries. Scanning electron micrographs of: (A) microneedles having different lengths and widths at a constant tip angle of 55°; (B) microneedles with 'pockets' of different shapes and sizes etched through the microneedle shaft; and (C) microneedles with complex geometries, such as contoured surfaces in the form of barbs and serrated edges (Gill and Prausnitz, 2007, 232).

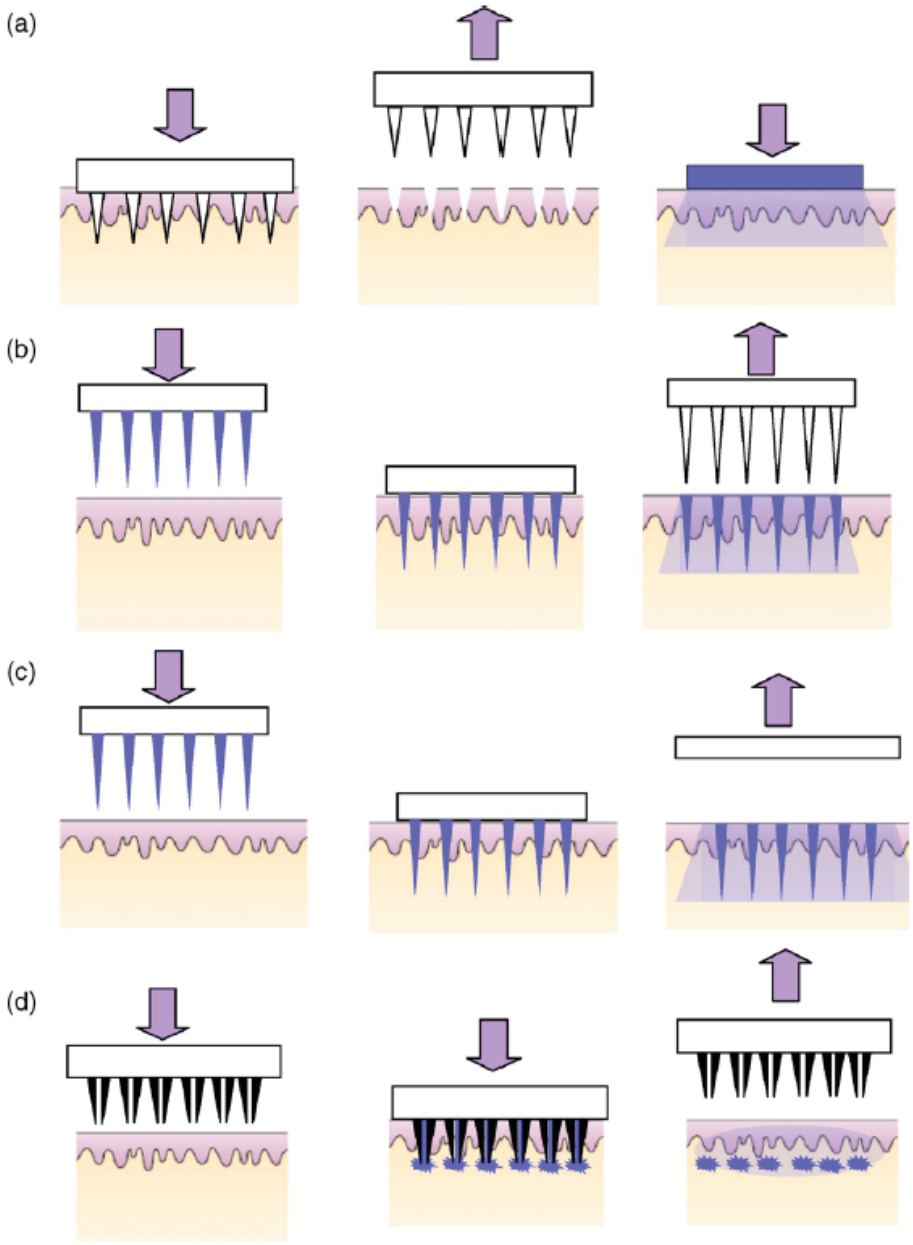

Figure 7 Schematic of drug delivery using different designs of microneedles: (a) solid microneedles for permeabilizing skin via formation of micron-sized holes across stratum corneum. The needle patch is withdrawn followed by application of drug-containing patch; (b) solid microneedles coated with dry drugs or vaccine for rapid dissolution in the skin; (c) polymeric microneedles with encapsulated drug or vaccine for rapid or controlled release in the skin; (d) hollow microneedles for injection of drug solution (Arora, Prausnitz, and Mitragotri, 2008: 232).

Table 5 Main features of the different approaches of drug delivery by microneedles.*

Drug delivery approach	Rate-limiting step of drug delivery	Main advantages	Main disadvantages
Poke and Flow	Solvent flow through microneedle bore or at higher volume; Pressure resistance of the skin	Rate of drug delivery can be regulated e.g. via a pump, if solvent flow is rate-limiting Delivery of high volume Integration into lab-on-a-chip systems possible Precise dosing No or limited reformulation of the drug needed	Risk of clogging Impaired microneedle strength Increased risk of leakage for arrays More complex device
Poke and Patch	Diffusion of the drug through the micropores generated by microneedles into the skin, dependent on the pore size and number, and concentration of the drug in the patch	Technically simple No pump or encapsulation/coating process is required Extended release	Low fraction of the drug may be delivered (only of interest for drugs with high potency) Two-step administration process No precise dosing Reformulation of the drug needed
Poke and Release	Dissolving microneedles: dissolution rate Porous microneedles: diffusion of drug from the pores	Small amount of drug may be lost during the encapsulation/absorption process No patch or pump is required No sharp waste (dissolving microneedles) Precise dosing	Impaired microneedle strength (increased fracture and deformation of microneedle geometry) Often less sharp microneedles (decreased penetration ability) Small dose Reformulation of the drug needed
Coat and Poke	Detachment of the coating from microneedle surface or, at thicker coatings: Dissolution rate of the coating	Microneedle strength is retained after coating No patch or pump is required Precise dosing	Requires an efficient coating procedure Small dose Reformulation of the drug needed Reduction of microneedle sharpness/penetration ability

* van der Maaden, Jiskoot, and Bouwstra, 2012: in press

2.6.2.2 *Hollow microneedles*

Hollow microneedles deliver drugs into skin via the "poke and flow" approach (Figure 7d). They offer an additional benefit over solid microneedles, that is the possibility to transport drugs through a hollow bore of microneedle by diffusion or, for more rapid rates of delivery, by pressure-driven flow. In the latter case, the drug in solution is actively delivered into skin by injection or infusion in a similar manner of hypodermic needles. However, by reducing the size of needles into micron scale, pain and tissue trauma associated with hypodermic needle injection was reduced greatly (Kaushik et al., 2010: 135–164). Furthermore, hollow microneedles can be integrated with a microfluidic chip or a micropump to direct the content of the drug reservoir into skin in a controllable manner (van der Maaden, Jiskoot, and Bouwstra, 2012). Figure 8 shows the patent distributions of microneedles based on their type. A greater number of these patent applications are focused on the design of, and delivery through, hollow microneedles since a higher amount of drug can be delivered from such microneedles as compared with others (Bariya et al., 2012: 11–29). A drawback of the poke and flow approach is that the hollow microneedles have a risk of clogging at the tip opening and are usually weaker than solid microneedles. Moreover, their small geometry can restrict flow rate for rapid injection.

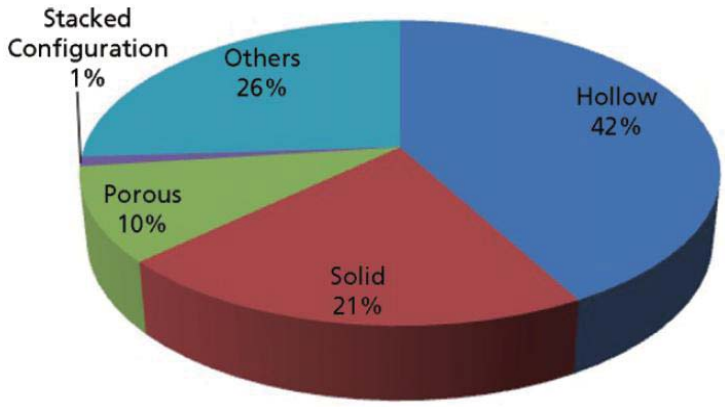

Figure 8 Division of patents filed based on type of microneedles (Bariya et al., 2012: 24).

2.6.3 Design parameters

The design of the microneedles is critical for achieving successful drug delivery and constrained by a number of parameters. Microneedles must be capable of easily inserting into skin without breaking. Therefore, the most important factor is the strength of microneedles. The type of material used to fabricate the needles affects this physical property as aforementioned. Microneedle geometry is also important. In particular, the elastic nature of skin can prevent microneedles from penetration by folding around the needles during microneedle application, especially for the blunt and short microneedles (van der Maaden, Jiskoot, and Bouwstra, 2012). It has been reported that sharpness of needle tip (needle tip area) linearly affects the insertion force of microneedle into skin (Davis et al., 2004: 1155–1163). Other parameters, including microneedle length, width, and shape, influence the microneedle fracture force (Arora, Prausnitz, and Mitragotri, 2008: 227–236).

Microneedles can also be designed to minimize pain. Gill et al. (2008: 585–594) reported that microneedle length had strongly effect on pain, where a 3-fold increase in needle length (480 to 1450 μm) resulted in a 7-fold increase in pain score (from 5 to 40% of the 26G hypodermic needle). The number of microneedles also affected the pain score, in which increasing the number of microneedles 10-fold increased pain by over 2-fold.

Fabrication methods for microneedles need to be designed appropriately. As a single-use, disposable device, manufacturing costs should be low (Arora, Prausnitz, and Mitragotri, 2008: 227–236). Furthermore, in order to obtain sufficient and reproducible penetration and the possibility of self-administration, microneedle applicator should be used (van der Maaden, Jiskoot, and Bouwstra, 2012).

Various factors influence the drug delivery efficiency while designing the microneedle-based delivery systems. Oh et al. (2008: 1040–1045) examined the effect of needle length (200 and 500 μm) and needle density (45, 99, and 154 ea/cm^2) on the level of the calcein, a model low molecular weight drug, permeation. The amount of permeated calcein increased with increasing the length and density of the microneedles. They also suggested that the material composed of microneedles may show an effect on the enhancement of skin permeation. The effect of different needle

lengths (100–1100 μm) and needle densities (400–11,900 needles/cm^2) on drug flux was also determined by Yan et al. (2010: 7–12) which was shown that the microneedle pretreatment of skin with needles longer than 600 μm and lower needle densities (< 2000 needles/cm^2) were more effective in increasing drug flux. Li et al. (2010: 122–129) performed the transport studies using the super-short solid microneedles with a length of 70–80 μm and revealed that the permeated amount of drug increased as the insertion force increased. Skin permeation of drug also increased when the microneedles number increased, however, no linear correlation between these two parameters was observed. This finding was consistent with the result of Wu, Todo, and Sugibayashi (2006: 102–108) study. Dermarollers®, a solid microneedle device, was used to perforate the skin for enhancing the hydrophilic drug permeation. It was observed that when combining the Dermarollers® with the invasome formulations, drug penetration through skin was further enhanced, compared to the aqueous solutions of the model drugs (Badran et al., 2009: 511–523). Coulman et al. (2009: 190–200) described the significant impact of the surface charge and microchannel size on the permeation characteristics of a nanoparticle formulation through the Isopore® membrane, the synthetic membrane used to represent the human skin containing micropores such as those created by the microneedle array device. Verbaan et al. (2007: 238–245) used an electric applicator for piercing the short microneedles (300 μm) with a predefined velocity into skin and reported the dependence of drug transport rate on the piercing velocity and shape of microneedles (solid/hollow). In their study, manual piercing of the needles did not show the appearance of drug transport into skin. They also observed that the needle density (4×4, 6×6, and 9×9) did not affect on drug flux. Matriano et al. (2002: 63–70) reported that the quantity of a model protein antigen, ovalbumin, delivered into skin from the coated Macroflux® microprojection array patch system can be controlled by the formulation of coating solution, the patch system size, and patch wearing time. Xie, Xu, and Gao (2005: 184–190) studied the enhancement of transdermal transport of drug dispersed in the chitosan films from coated microneedles and found that the drug permeation rate increased with increasing the drug loading dose and decreasing the chitosan concentration or the thickness of the film. The linear correlation between

the drug release rate and the amount of drug containing in the dissolving microneedle patch was observed by Lee, Park, and Prausnitz (2008: 2113–2124).

For hollow microneedles, it is important that a sufficient and constant flow rate is generated for delivering drugs into skin, without affecting the needle strength. It was determined that microneedle insertion resulted primarily in skin indentation up to a certain length of microneedles, and only a fraction of the microneedle actually went into the skin causing a significant dermal tissue compression, which limited the drug flow through the microneedle bore. Martanto et al. (2006: 104–113) performed the study by using a single glass hollow microneedle for intradermal fluid infusion and showed that the flow resistance can be overcome by partially retracting the needle after insertion into skin, infusing at high pressure, and co-injection with the hyaluronidase, an enzyme that degrades hyaluronic acid in the extracellular matrix of the skin. Moreover, using a beveled microneedle with a bore opening on the side of the microneedle tip may avoid the need to force fluid into the compressed tissue layer comparing with the microneedle with a bore opening at a blunt tip, and thereby increase the infusion rate (Wang et al., 2006: 1080–1087).

For designing a microneedle system, optimizing various transport parameters (e.g. properties of drugs, formulations, skin thickness, injection conditions etc.) as well as the physical dimensions of the system (e.g. needle length, needle numbers, surface area of the patch, etc.) enhances the efficiency of the transdermal drug delivery techniques.

2.6.4 Application of microneedles

Microneedles have been studies *in vitro*, in animals, and in humans for a variety of applications. Microneedle puncture has been shown to increase skin permeability with a board range of compounds, including small molecular weight drugs, DNA, proteins, and even nanoparticles (McAllister et al., 2003: 13755–13760; Mikszta et al., 2002: 415–419; Verbaan et al., 2007: 238–245). Wermeling et al. (2008: 2058–2063) demonstrated the systemic administration of naltrexone, a potent mu-opioid receptor antagonist used to treat opiate and alcohol dependence, in human study. Solid microneedles have been coated with a variety of compounds ranging

from low molecular weight drugs, DNA, proteins, inactivated pathogens, and microparticles (Bal et al., 2010: 266–282; Chen Xianfeng et al., 2009: 212–220; Cormier et al., 2004: 503–511; Gill and Prausnitz, 2007: 227–237). Human clinical trials by Zosana Pharmaceuticals (Freemont, CA, USA) had completed Phase II clinical trials for delivery of parathyroid hormone from coated Macroflux® microneedles, which evidenced the excellent safety and efficacy. This product is now ready for Phase III study (Arora, Prausnitz, and Mitragotri, 2008: 227–236; Bariya et al., 2012: 11–29). Dissolving polymer microneedles have also encapsulated various compounds such as erythropoietin (Ito et al., 2006b: 255–261), proteins (Ito et al., 2006a: 82–88; Park, Allen, and Prausnitz, 2006: 1008–1019), and enzyme (Lee, Park, and Prausnitz, 2008: 2113–2124). Encapsulated proteins and enzyme in polymeric microneedles were shown to have good stability for at least 1 month after storage at room temperature. Hollow microneedles have been used to deliver insulin into skin *in vivo* and shown to reduce blood glucose level in diabetic rats (McAllister et al., 2003: 13755–13760). Besides that delivery of insulin by such microneedles in human studies has also reported (Gupta, Felner, and Prausnitz, 2009: 329–337, 2011: 451–456; Pettis et al., 2011a: 435–442, 2011b: 443–450). Smart and Subramanian (2000: 549–559) used the single silicon microneedle to extract nanoliter quantities of blood from human for monitoring the blood glucose level. NanoPass Technologies have used their Micronjet® hollow microneedles for the delivery of insulin, influenza vaccine, and lidocaine (for local anesthesia) in clinical studies. BD Medical-Pharmaceutical systems studied a rabies vaccine delivery in a clinical trial by using the BD 34G hollow microneedles (van der Maaden, Jiskoot, and Bouwstra, 2012). Human clinical trials on influenza vaccination employing hollow microneedles have completed Phase III and have been submitted for registration in Europe (Arora, Prausnitz, and Mitragotri, 2008: 227–236). Other vaccine delivery studies include ChimeriVax™-JE for yellow fever, DNA plasmid encoding hepatitis B surface antigen, recombinant Protective Antigen (rPA) of *Bacillus anthracis*, and DNA plasmid encoding four vaccinia virus genes. In all these studies, microneedles generated the same immune responses at lower doses compared to those generated by conventional subcutaneous or intramuscular injections (Prausnitz et al., 2009: 369–

393). Synergistic effect of microneedles combined with vesicular structures and other physical methods such as iontophoresis, sonophoresis, and elctroporation, have also been addressed (Bariya et al., 2012: 11–29; Chen Huabing et al., 2009: 63–72; Matriano et al., 2002: 63–70, Qiu et al., 2008: 144–150; Wu, Todo, and Sugibayashi, 2007: 189–195; Yan, Todo, and Sugibayashi, 2010: 77–83).

Bariya et al. (2012: 11–29) summarized some immunobiologicals, bioactive macromolecules (biopharmaceuticals), and drugs administered via microneedles with different delivery approaches as shown in Table 6. Moreover, the examples of microneedle-based transdermal products with their possible use have also been reviewed by this research team (Table 7). Although a large number of studies demonstrated that microneedles are the promising transdermal drug delivery system, until now there are no microneedle-based (trans)dermal drug delivery systems on the market (van der Maaden, Jiskoot, and Bouwstra, 2012).

2.6.5 Safety

The use of microneedles is considered to be safe due to their small size and, thus, lack of significant damage to sensory nerves and blood vessels located in the dermis layer, which means negligible pain and bleeding. Although there have not been the published data on safety from ongoing human clinical trials, their progression through Phases II and III suggests an acceptable safety profile (Arora, Prausnitz, and Mitragotri, 2008: 227–236). Other data from animal and human studies have been reported and generally shown no significant adverse reactions to microneedles. Kaushik et al. (2001: 502–504) reported the painless and no bleeding on the use of microneedles in human subjects. Wermeling et al. (2008: 2058–2063) performed a human study on the delivery of naltrexone, which is used to treat opioid and alcohol addiction, by microneedles and reported the well-tolerated with mild systemic and application site side effects. Bal et al. (2008: 193–202) studied the safety of microneedle arrays in human in terms of skin irritation (skin redness and blood flow) and pain sensation and concluded that microneedles were painless and caused only minimal skin irritation. Donnelly et al. (2009: 2513–2522) performed the study on microbial penetration and found that microneedle puncture resulted in

significantly less microbial penetration than 21G hypodermic needle puncture. Moreover, no microorganisms crossed the viable epidermis in microneedle-treated skin. Burton et al. (2011: 31–40) demonstrated the rapid intradermal delivery of drug formulation using a hollow microneedle device in animal models and reported the good tolerability and recover of skin with no long-term edema or erythema. Gupta et al. (2011: 148–155) studied on the kinetics of skin resealing after insertion of microneedles in human subjects and revealed the rapid resealing of microneedle-treated sites within 2 h. Further studies are needed to fully assess the safety of microneedles.

Table 6 Application of microneedles.*

	Active constituent/ product	Delivery approach	Description
Immunobiologicals	Influenza vaccine	Coat and poke	Adjuvant increases cellular immunogenicity, safety and self life.
	Hepatitis B vaccine	Poke and release	Antigenicity was maintained at high temperature.
	Human IgG	Poke and release	Transportation of macromolecules through skin was enhanced.
	Anthrax, botulism, plague and staphylococcal toxins	Poke and flow	To avoid physical and chemical incompatibility of such multiple/combination vaccine.
	Tetanus toxoid	Poke and release	Due to enhanced immunogenicity dose can be reduced by four times.
	Ovalbumin	Coat and poke	Antigenicity was increased.
	Flavivirus vaccine	Poke and flow	Vaccination was safer and well tolerated.
Biopharmaceuticals .	L-Carnitine	Poke and patch	Bioavailability of L-carnitine was increased and controlled delivery could be achieved.
	Recombinant human growth hormone and desmopressin	Poke and release	Absorption, bioavailability and stability were increased.
	Albumin	Poke and flow	MEMS syringe were used to successfully delivery of macromolecules.
	Low molecular weight heparin, calcein, erythropoietin	Poke and release	Bioavailability and stability were increased.

Table 6 (continued) Application of microneedles.*

	Active constituent/ product	Delivery approach	Description
Biopharmaceuticals	Insulin	Poke and release	Increased in bioavailability and rapid onset of action.
	Calcein and bovine serum albumin	Poke and release	Controlled release in skin for hours to month.
	Insulin	Poke and patch	Insulin was successfully delivered in animal with 80% reduction in blood glucose.
	Desmopressin	Coat and poke	Efficient, controlled and less variable delivery of desmopressin was achieved.
Drugs	L-Ascorbic acid	Poke and release	Faster hair growth due to 10.54 fold increased in penetration.
	Galanthamine	Poke and patch	Enhanced drug delivery.
	Aspirin	Poke and patch	Polymeric microneedle rollers were fabricated.
	Docetaxel	Poke and patch	Administration in form of liposomes increases the bioavailability and reduces lag time.
	Pilocarpine	Coat and poke	Rapid and extensive pupil constriction with higher bioavailability.
	Riboflavin	Coat and poke	Studied various parameters of coating of riboflavin on microneedles.

* Bariya et al., 2012: 20.

Table 7 Commercial status of microneedle-based transdermal products.*

Brand name	Manufactured by	Applications
VaxMat	TheraJect Inc., USA	It is dissolvable microneedles and can deliver hundreds of micrograms of drug rapidly through the stratum corneum into the epidermal tissue.
Micro-Trans	Valeritas Inc., USA	It can deliver the drug into dermis without limitations of drug size, structure, charge or the patient's skin characteristics.
Nanoject	Debiotech, Switzerland	Useful for intradermal and hypodermic drug delivery and for interstitial fluid diagnostics.
Janisys	Janisys, Ireland	Actively delivers drugs from transdermal patches and multiple drugs can be administered via one patch.
BD Soluvia	Becton Dickinson, USA	It is a prefillable microinjection system for accurate intradermal delivery of drugs and vaccines.
Onvax	Becton Dickinson, USA	It is a skin micro abrader having plastic microneedles for disruption of stratum corneum for the delivery of vaccines.
MicronJet	NanoPass Inc., Israel	It can be used with any standard syringe for painless delivery of drugs, protein, and vaccines approved for this delivery route.
Macroflux	Zosano Pharma Inc., USA	Metallic microneedles for the delivery of peptides and vaccines.
MicroCor	Corium International Inc., USA	It can be used to deliver small as well as large molecules like proteins, peptides, and vaccines.

Table 7 (continued) Commercial status of microneedle-based transdermal products.*

Brand name	Manufactured by	Applications
Microstructured transdermal system technology (MTS)	3 M Corp., USA	The technology can be used to administer drugs including monoclonal antibodies in solid or liquid dosage form.
AdminPen	AdminMed, USA	Liquid pharmaceutical formulation or cosmetics can be conveniently injected in to the skin.
NanoCare	NanoPass Inc., Israel	It is a small hand-held device for rejuvenation of skin and to boosts the cosmetic effect of topical applications.
MTS-Rollers	Clinical Resolution Laboratory Inc., USA	It is used for transdermal delivery of cosmetics in deeper skin layers.

* Bariya et al., 2012: 25.

CHAPTER 3
MATERIALS AND METHODS

3.1 Materials

1) Calcein sodium; CAL (Tokyo Chemical Industry, Tokyo, Japan)

2) Deuterium oxide; D_2O (99.9%, NMR grade) (Wako Pure Chemical Industries, Osaka, Japan)

3) Disodium ethylenediamine; EDTA·2Na (Dojindo Laboratories, Kumamoto, Japan)

4) Diethyl ether (BDH Prolabo chemicals, VWR International Ltd., Belgium)

5) Fluorescein isothiocyanate (FITC)-dextrans 4,000; FD-4 (Sigma Aldrich®, St. Louis, MO, USA)

6) Fluorescein isothiocyanate (FITC)-dextrans 10,000; FD-10 (Sigma Aldrich®, St. Louis, MO, USA)

7) Fluorescein isothiocyanate (FITC)-dextrans 40,000; FD-40 (Sigma Aldrich®, St. Louis, MO, USA)

8) Liquid nitrogen (S.S. Enterprises Co., Ltd., Thailand)

9) Nembutal®; Pentobarbitone Sodium Injectable Solution (CEVA SANTE ANIMALE, France**)**

10) Optimal cutting temperature compound; Tissue-Tek® OCT™ Compound (Sakura Finetek, Torrance, CA, U.S.A.)

11) All other chemicals were commercially available and analytical grade.

- Acetonitrile (Lab Scan, Dublin, Ireland)
- Disodium hydrogenphosphate dodecahydrate; $Na_2HPO_4 \cdot 12H_2O$ (Ajax Finechem, Australia)
- Ethanol absolute (Scharlau Chemie S.A., Spain)
- Evans blue (Sigma Aldrich®, St. Louis, MO, USA)
- Isopentane (2-methylbutane) (Lab Scan, Dublin, Ireland)
- Potassium dihydrogenphosphate; KH_2PO_4 (Ajax Finechem, Australia)
- Sodium chloride; NaCl (Ajax Finechem, Australia)

12) Male Wistar rats, weighing 200–250 g (National Laboratory Animal Center (NLAC), Mahidol University, Nakhon Pathom, Thailand)

3.2 Equipments

1) 1.5 mL Microcentrifuge tube; Eppendorf® tubes (CORNING®; Corning Incorporated, NY, USA) and holder

2) 26-guage hypodermic needle; 26G × ½" (NIPRO Corporation, Osaka, Japan)

3) Analytical balance (Model CP224S and CP3202S, SARTORIUS, Germany)

4) Beaker (PYREX®, USA)

5) Centrifuge (MULTIFUGE 1S-R, Kendro, Germany)

6) Cylinder (PYREX®, USA)

7) Digital thickness gauge (Type 25 mm – 0.001/1" – .00005, Sylvac, Switzerland)

8) Dropper

9) Electric clipper (WAHL®; Model 9217, WAHL CLIPPER CORP., USA)

10) Embedding mold container; Tissue-Tek® Cryomold® Intermediate 15×15×5 mm (Sakura Finetek, Torrance, CA, U.S.A.)

11) Fine forceps

12) Fourier Transform Infrared spectrophotometer (IRAffinity–1, Shimadzu, Japan)

13) Franz diffusion cell 6 mL

14) Freezer/Refrigerator –20°C

15) Freezing microtome (Leica CM3050S; Finetec, Japan)

16) Hollow microneedle (Gift from Terumo Co., Tokyo, Japan)

17) Homogenizer (ULTRA-TURRAX® T10 basic) equipped with a S10N-10G probe (IKA®, Germany)

18) Ice bath

19) Intelli-Mixer RM-2L (ELMI Ltd., Latvia)

20) Kimwipes® disposable wipers (Kimberly-Clark Professional, Australia)

21) Microfuge® 16 Centrifuge (Beckman Coulter, Inc., Germany)

22) MICROLITER™ Syringe #705 (HAMILTON CO., Reno, Nevada, USA)

23) Micropipette 2–20 μL, 20–200 μL, 100–1000 μL, 1–5 mL, and micropipette tip

24) Multi stirrer and magnetic bar

25) Parafilm (BEMIS®, WI, USA)

26) pH Meter (Sartorius Professional Meter PP-15, Germany)

27) Phase-contrast microscope (IX71; Olympus, Japan)

28) Polyethylene tubing (INTRAMEDIC™, Becton Dickinson and Company, USA)

29) Scalpel (ZENTECH, Germany)

30) Scissors (ZENTECH, Germany)

31) Shaver (Panasonic ES4033s, Panasonic Electric Works Wanbao (Guangzhou) Co., Ltd., China)

32) Side-by-side diffusion cell 3 mL

33) Silicone sheet

34) Spectrofluorophotometer RF 1501 (Shimadzu, Japan).

35) Supporting board

36) TERUMO® syringe (1 cc/mL) (Terumo (Philippines) Corporation, Laguna, Philippines)

37) Test tube (PYREX®, USA)

38) Thermo-regulated water bath (WiseCircu® Fuzzy Control System; Model WCR-P6, DAIHAN Scientific Co., Ltd., Korea)

39) Volumetric flask (PYREX®, USA)

40) Vortex mixer (VX100, Labnet)

41) Watch glass

3.3 Methods

3.3.1 Preparation of skin

Male Wistar rats, weighing 200–250 g, were used in all animal experiments. The animals were supplied by National Laboratory Animal Center (NLAC), Mahidol University (Nakhon Pathom, Thailand). They were housed in controlled environment with a 12 h light-dark cycle. The ventilation, temperature, and humidity were controlled by HVAC (Heating, Ventilating, Air conditioning) system at temperature range of 24 ± 2 °C, relative humidity of 55 ± 10%, and air changes per hour 10–15 ACH. The noise level was maintained less than 85 decibels. The rats were fed on commercial diet (No. CP 082) produced by Perfect Companion Group Co., Ltd. (Bangkok, Thailand). The chlorinated RO Water was provided as drinking water (chlorine concentration 10–12 ppm) which was free from *Pseudomonas aeruginosa*. The protocols used to generate animal experimental data were approved by the ethics committee for the use of laboratory animals, Faculty of Pharmacy, Silpakorn University (Protocol Number: 0003/2010). Experiments were performed in accordance with the Guideline for Animal Experimentation of OECD (OECD, 2004). The rats were anesthetized by intraperitoneal (i.p.) injection of pentobarbitone sodium (50 mg/kg), and the hair on their back was shaved. The upper part of full-thickness skin was carefully excised from the dorsal region of the rats, and excess subcutaneous fat was carefully trimmed off. The excised skin, 1.0–1.3 mm in thickness, was immediately used for experiments.

3.3.2 Preparation of a hollow microneedle

The hollow microneedles, Nanopass^{TM} (33-gauge hypodermic needle, o.d., 0.20 mm), were kindly provided by Terumo Co. (Tokyo, Japan). A hollow microneedle was manufactured from a microneedle connected to a 27-gauge hypodermic needle (i.d., 0.22 mm; o.d., 0.40 mm; Terumo Co.). The needle was fixed with a triangular silicone sheet to maintain an angle of insertion (θ) of 40° and constant insertion depth in the skin barrier, as shown in Figure 9.

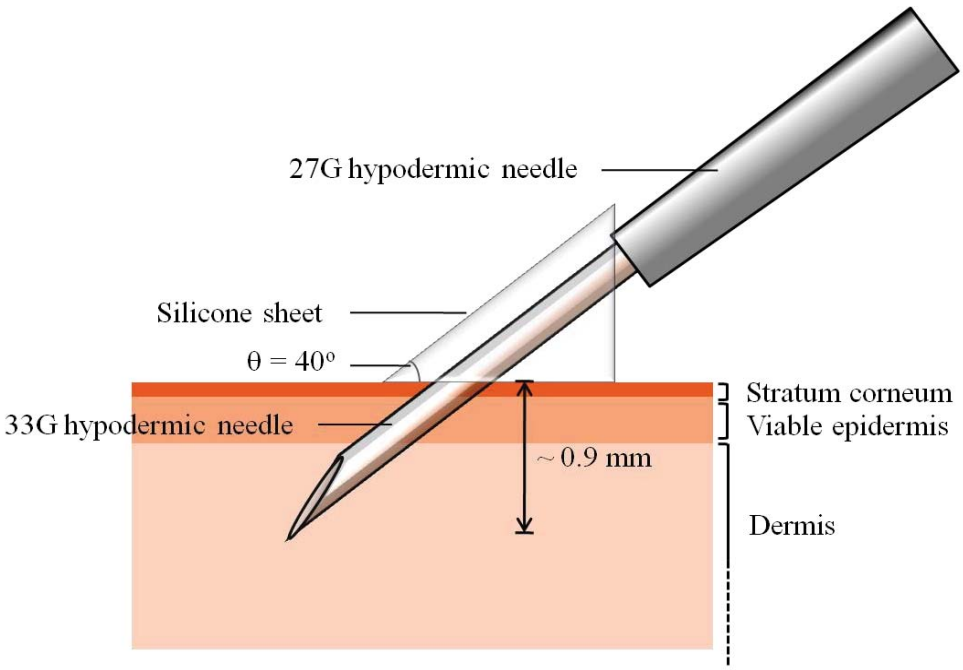

Figure 9 Schematic representation of a hollow microneedle insertion into skin.

3.3.3 Preparation of buffer solution

The composition of phosphate buffer solution (PBS) used in this study is shown in Table 8. Inorganic salts were dissolved in distilled water separately to form acidic and basic solution, respectively. Then, the basic solution was placed onto a magnetic stirrer and measured for the pH simultaneously. The acidic solution was used to adjust the pH of solution to 7.4 by gradually adding into the basic solution. For the release study of CAL, EDTA·2Na 0.3722 g was adding into 1000 mL pH 7.4 PBS to make 1 mM EDTA·2Na in pH 7.4 PBS.

3.3.4 Histological imaging

To visualize hollow microneedle penetration into the skin and the pathway of fluid injection, a small amount of Evans blue was injected into the skin by a hollow microneedle. After removing the microneedle, the skin sample was frozen in isopentane (2-methylbutane) cooled by dry ice with optimal cutting temperature compound (Tissue-Tek® OCT™ Compound) in an embedding mold container. A

freezing microtome was used to make the vertical sections of 10 μm thickness. These sections were examined histologically using a phase-contrast microscope.

Table 8 Phosphate buffer solution (PBS) formulation.

Component		PBS	
Inorganic salts	M.W.	g/L	mL
Basic solution			
$Na_2HPO_4.12H_2O$	358.14	9.5504	
NaCl	58.44	5.0984	
Distilled water			800
Acidic solution			
KH_2PO_4	136.1	0.9072	
NaCl	58.44	1.4	
Distilled water			200

3.3.5 *In vitro* skin release studies

The extent and rate of drug release from skin were investigated to examine the effect of different four variables (a–d) related to the hollow microneedle-based delivery system on the drug dermatopharmacokinetics. FD-4 (1 mM) was used as a model high molecular hydrophilic compound for testing in this study. *In vitro* release studies were carried out after the following treatments:

(a) different volumes of FD-4 solution (5, 10, and 20 μL) were administered into the excised dorsal skin by single injection;

(b) different numbers of injections (10 μL single injection, 5 μL two injections, and 2.5 μL four injections) were administered into the excised skin. Distance between each injection point was 0.5 cm;

(c) different FD-4 concentrations (1, 2, 4, and 10 mM) were injected into the excised skin by single injection. The test was divided into two groups, in which either 10 μL of each concentration or 5 μL of 2 mM, 2.5 μL of 4 mM, and 1 μL of 10

mM of FD-4 solution was administered into the skin. The total amount of FD-4 loaded into skin was adjusted to be equally (10 nmol) in the latter;

(d) different molecular sizes of the test compounds (10 μL of either FD-40 (MW 40000) solution, FD-10 (MW 10000) solution, FD-4 (MW 4000) solution, CAL (MW 623) solution, or D_2O (MW 20.03)) were injected into the excised skin by single injection.

In the injection process, the skin was stretched onto a support board with four tissue-mounting pins to simulate skin tension *in vivo*. The skin containing injected solution was then mounted in a vertical diffusion cell (an average effective diffusion area of 2.02 cm^2) with the SC side facing the donor compartment (without drug solution), which was covered with Parafilm to establish an occlusive condition. The receiver solution was approximately 6.0 mL of pH 7.4 PBS, which was stirred with a magnetic stirrer bar driven by a constant-speed synchronous motor and maintained at 32 °C using a thermoregulated water bath throughout the experiment. For the release study of CAL, 1 mM EDTA·2Na in pH 7.4 PBS was used instead of pH 7.4 PBS. The receiver solution (0.5 mL) was withdrawn at predetermined time of 5, 10, 15, 20, 30 min, 1, 2, 3, 4, 5, 6, 7, 8 h after starting the release experiment, and the same volume of PBS was added to the receiver compartment to keep the volume constant. The sampling solution was centrifuged at 200 rpm for 5 min before determination.

3.3.6 Determination of drug remaining in skin

After the release study was ended over a period of 8 h, the amount of drug remaining in the skin was measured by isolating the skin from the diffusion cell. The skin was cut into small pieces with scissors and fine forceps, and homogenized (at 12,000 rpm for 5 min) with 2 mL PBS to extract the drug under an ice bath. Acetonitrile (2mL) was then added and mixed with the skin homogenized solution using a vortex shaker to precipitate protein. After centrifugation at 15,000 rpm for 5 min, the clear supernatant was taken for analysis.

3.3.7 Quantitative Assay

The concentrations of FD-4, FD-10, and FD-40 in each receiver sample were analyzed using a spectrofluorophotometer (RF 1501; Shimadzu, Japan) at an excitation wavelength of 495 nm and a fluorescent emission wavelength of 515 nm. CAL samples were analyzed using a spectrofluorophotometer at an excitation wavelength of 490 nm and a fluorescent emission wavelength of 515 nm. D_2O was determined by the intensity of O–D stretching vibrational band at 2512 cm^{-1} infrared spectroscopic spectra (Wu, Todo, and Sugibayashi, 2007: 189–195).

3.3.8 Diffusivity of FD-4 in skin

3.3.8.1 *Analysis of diffusivity from drug release profiles*

The hollow microneedle system is defined as a way to directly load drugs into skin and provide a drug depot in skin, as in a topical injection. Thus, the dermatopharmacokinetics after the application of this device may be different from that of conventional topical application (Yoshida et al., 2007: 142–147). The FD-4 release behavior from FD-4–loaded skin was observed. Release experiments were carried out under perfect sink conditions, and release profiles were classified by considering the skin to be a homogeneous single membrane. The obtained release data were analyzed using the mathematical model proposed by Higuchi. According to Higuchi (1962: 802–804), the cumulative amount of drug released from the drug-loaded skin into the bulk solution per unit application area, Q (nmol/cm^2), under sink condition is as follows:

$$Q = hC_0\left[1 - \frac{8}{\pi^2}\sum_{m=0}^{\infty}\frac{1}{(2m+1)^2}\exp\left(-\frac{D_{Skin}(2m+1)^2\pi^2 t}{4h^2}\right)\right] \quad (8)$$

where h is the thickness of skin (cm), C_0 is the initial drug concentration in the skin (nmol/ml), and D_{Skin} is the effective diffusion coefficient of drug in skin by employing a hollow microneedle as a delivery method (cm^2/h), t is the time after application, m is the integer, as indicated, goes from 0 to ∞.

The most practical application of Eq. 8 is expressed as the simplified form when the percentage of drug released is not too large, i.e., up to 30% of dose release. It can be easily shown that (Higuchi, 1962: 802–804):

$$Q = 2C_0\sqrt{\frac{D_{Skin}t}{\pi}} \tag{9}$$

D_{Skin} can be calculated from Eq. 9, and the drug release rate can be determined from the simplified Higuchi model:

$$Q = kt^{1/2} \tag{10}$$

where k is the kinetic constant indicative of the release rate (nmol/cm^{2}h$^{1/2}$). Higuchi describes drug release as a diffusional process based on the Fick's law, square root time dependent. Eqs. 9 and 10 are confined to the description of the first 30% of the release curve.

3.3.8.2 *Analysis of diffusivity from skin permeation profiles*

To examine the diffusion coefficient of FD-4 in viable epidermis and dermis layers, D_{ved}, stripped skin excised from the rats was used as a model skin, which was supposed to be a homogenous single membrane (defined as the one-layered diffusion model). The stripped skin was set in a diffusion cell, and FD-4 solution was applied to the donor cell on the epidermal side of the skin to determine the skin permeation profile of FD-4.

The concentration of FD-4, C_{ved}, in the stripped skin at a position, x, and time, t, can be calculated using Fick's second law of diffusion (Eq. 11).

$$\frac{\partial C_{ved}}{\partial t} = D_{ved}\frac{\partial^2 C_{ved}}{\partial x^2} \tag{11}$$

where D_{ved} is the diffusion coefficient of FD-4 in the viable epidermis and dermis layers. Based on the differential equation, Eq. 11 can be changed to Eq. 12, as

described in details by Hada et al. (2005: 341–350) and Sugibayashi et al. (2010: 134–142)

$$C_{ved_{i,j+1}} = rD_{ved}C_{ved_{i-1,j}} + (1-2rD_{ved})C_{ved_{i,j}} + rD_{ved}C_{ved_{i+1,j}} \quad (12)$$

where $C_{ved\ i,j}$ is FD-4 concentration at i-th position and j-th time in the stripped skin, r is $\Delta t/\ \Delta x^2$; Δx is $x_{i+1} - x_i$, and Δt is $t_{j+1} - t_j$. In addition, the skin permeation rate to the receiver compartment, J, can be expressed by Eq. 13. The cumulative amount of FD-4 permeated per unit area, Q, is expressed by Eq. 14.

$$J_j = -D_{ved}\frac{C_{n+1,j} - C_{n,j}}{\Delta x} \quad (13)$$

$$Q_j = Q_{j-1} + J_j \Delta t \quad (14)$$

where n is the number of divisions of skin. Then, J_j was calculated using Microsoft® Excel by setting $n = 10$. In this calculation, Δt was set to be less than 0.5 for $D_{\mathrm{Skin}}\ \Delta t/\ \Delta x^2$. Q_j was calculated from J_j using Eq. 14. The diffusion coefficient, D_{ved}, was obtained by fitting the observed data using the least squares method performed by the solver function of Microsoft® Excel. The calculation condition was 100 s for the calculation limit, 100 times for repeated calculation, 0.000001 for accuracy, 5% basic tolerance and 0.001 for convergence. The pseudo-Newtonian method was used as an algorithm (Hada et al., 2005: 341–350; Sugibayashi et al., 2010: 134–142).

Full-thickness skin of the rats was used instead of stripped skin to calculate the diffusion coefficient of FD-4 in the SC layer, D_{SC}. A two-layered diffusion model was established herein to analyze the FD-4 permeation profiles. FD-4 concentration in the SC layer can be expressed by Fick's second law of diffusion as follows:

$$\frac{\partial C_{sc}}{\partial t} = D_{sc}\frac{\partial^2 C_{sc}}{\partial x^2} \quad (15)$$

FD-4 concentration, C_{ved}, in the viable epidermis and dermis layers at a position, x and time, t can be expressed by Eq. 11. Equation 15 is changed to Eqs. 16 and 17 by differential calculus (Hada et al., 2005: 341–350; Sugibayashi et al., 2010: 134–142)

$$Csc_{i,j+1} = rD_{sc}Csc_{i-1,j} + (1-2rD_{sc})Csc_{i,j} + rD_{sc}Csc_{i+1,j} \quad (16)$$

$$Cved_{i,j+1} = rD_{ved}Cved_{i-1,j} + (1-2rD_{ved})Cved_{i,j} + rD_{ved}Cved_{i+1,j} \quad (17)$$

Similar analysis was carried out in the two-layered model using the least squares method to obtain the diffusion coefficient of FD-4 in SC, D_{SC}. In this calculation, diffusivity in the viable epidermis and dermis layers, D_{ved}, was fixed to the already estimated value by the stripped skin permeation experiment.

3.3.9 Statistical analysis

In vitro drug release measurements were collected from three to five experiments. Values are expressed as the mean ± standard error (S.E.). Statistical significance of differences between groups in the amount of drug released from skin was examined using one-way analysis of variance (ANOVA) followed by Student's *t*-test. The significance level was set at $p < 0.05$.

CHAPTER 4
RESULTS AND DISCUSSION

4.1 Characterization of hollow microneedle injection

4.2 Effect of injection volume on the release behavior of FD-4 from skin

4.3 Effect of number of injections on the release behavior of FD-4 from skin

4.4 Effect of concentration on the release behavior of FD-4 from skin

4.5 Effect of different molecular sizes of the test compounds on the release behavior from skin

4.6 Effect of hollow microneedle-assisted delivery on the diffusivity of FD-4 within skin

4.1 Characterization of hollow microneedle injection

To investigate piercing of the skin barrier and delivering the drug through the barrier by a hollow microneedle, FD-4 solution was injected into the excised back skin of Wistar rats. The needle was fixed with a triangular silicone sheet to maintain an angle of insertion (θ) of 40º and constant insertion depth in the skin barrier, as shown in Figure 9. The microneedle tip was inserted easily into the skin using gentle force, and no bending was observed after removing the needle. Up to 20 μL (single injection) of FD-4 solution was successfully injected into skin without any leakage from the skin surface or from the bottom (dermal) side of the skin (Figure 10A and 10B). The presence of FD-4 solution in skin was visualized by the appearance of a greenish-yellow region spread around the injection site. Increasing the injection volume resulted in a broader greenish-yellow region. After injection and removing the needle, the skin was frozen instantly in liquid nitrogen and sectioned vertically to observe the FD-4 deposition in the skin. Figure 10C shows the diffusion characteristics of FD-4 solution through the tissue adjacent to the injection site.

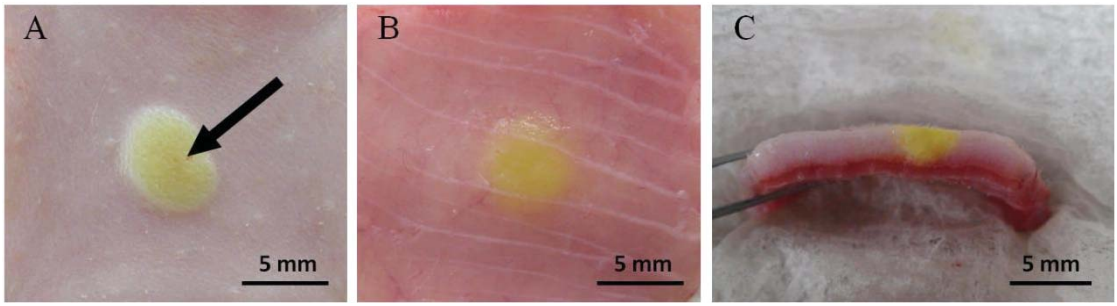

Figure 10 Photographs of the excised dorsal rat skin after injection of 20 μL of FD-4 solution using a hollow microneedle: (A) top surface; (B) bottom surface; (C) the vertical section. The black arrow in (A) indicates the needle insertion site. The greenish-yellow regions represent FD-4 localization within skin.

In Gupta, Felner, and Prausnitz (2009: 329–337) study, the appearance of an intradermal injection (needle insertion to 1 mm depth) by a glass hollow

microneedle into human subjects was observed immediately after bolus infusion of 15 units insulin. The skin wheal became apparently and a raised wheal extended approximately 5 mm from the point of insertion. In comparison, visual observation of the subcutaneous catheter infusion site did not show any skin wheal.

Next, a histological study was performed by examining skin sections under a light microscope after loading a small amount of Evans blue into the skin using a hollow microneedle. Figure 11 shows a typical cross section of a skin piece. The blue dye in the skin corresponded to the needle insertion across the stratum corneum and upper epidermis as well as into the superficial dermis.

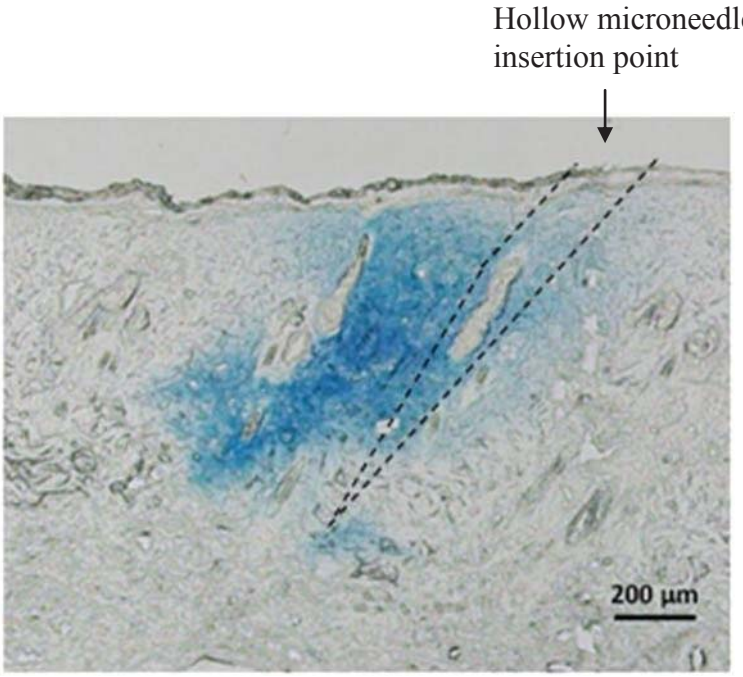

Figure 11 Histological section of the excised dorsal rat skin pierced with a hollow microneedle *in vitro*. A small amount of Evans blue was injected into skin. The paths of fluid injection are indicated by the presence of blue dye. Dotted lines show where the hollow microneedle was inserted. A hollow microneedle could be inserted forwards or backwards in this histological section.

In other studies, hollow microneedles were used in a different way to transfer the drug solutions into skin. For example, McAllister et al. (2003: 13755–13760) used a single glass hollow microneedle to inject insulin into the skin of hairless rats *in vivo*. A single glass microneedle (900-μm length and 60-μm bore diameter) was drilled with a circular motion into the dorsal skin to a depth of 500–800 μm for 30 min. Up to 32 μL of fluid could be flowed into skin at a pressure of 10 psi. Moreover, a dose-dependent response was observed, where infusion at larger pressure resulted in a larger drop in blood glucose. Smaller amounts of low molecular weight dye as well as 2.8-μm fluorescence-labeled latex particles could also be injected into skin by using lower pressure or shorter periods of time. Gupta, Felner, and Prausnitz (2009: 329–337) carried out the study to deliver the insulin solution into human subjects through a hollow microneedle. A microneedle connected to a programmable syringe pump at the rate of 1 mL/min was inserted at a 90° angle into the abdominal skin at the 1 mm depth to deliver 15 units of 50-U insulin intradermally. The results of their study showed that microneedle-based delivery was as least as effective as subcutaneous catheter delivery. Häfeli et al. (2009: n. pag.) fabricated the hollow microneedle arrays (200 μm in length) connected to a 12.5 μL flexible poly-dimethylsiloxane reservoir to deliver the two different agents as the model substances for application in vaccination delivery. A miniature syringe with 6 or 8 needles was successfully used to deposit the approximately 1 μm polystyrene microspheres and the 67 kDa human serum albumin into the skin *in vitro* and *in vivo*, respectively, by manually pressing a finger on the deformable drug reservior. Laurent et al. (2010: 5850–5856) used the Becton Dickinson intradermal delivery device (a glass syringe with a 30G hollow microneedle varying in length from 1–3 mm) to deliver rabies vaccine into human subjects. The needle was inserted into skin at a 90° angle. A reduced intradermal dose following a microneedle injection generated the humoral immune response as strong as a standard intramuscular dose of the commercial rabies vaccine.

4.2 Effect of injection volume on the release behavior of FD-4 from skin

To evaluate the effect of the injection volume, 5, 10, and 20 μL FD-4 solution were loaded into the skin using a hollow microneedle. The passive diffusion of 1 mM FD-4 solution across the intact full-thickness skin was also performed for comparison. Figure 12 shows the time course of the cumulative amount of FD-4 released in the unit area of skin. It was shown that the larger amount of FD-4 can be delivered into skin by using a hollow microneedle to puncture the skin and inject the FD-4 solution into skin. The cumulative amount of FD-4 released was increased as the higher volume of FD-4 injected. The amount of FD-4 released through the skin over 8 h from FD-4–loaded skins of 5, 10, and 20 μL was enhanced approximately by more than 50-fold (1.46 nmol/cm^2), 85-fold (2.57 nmol/cm^2), and 180-fold (5.35 nmol/cm^2), respectively, comparing with the total amount of FD-4 permeated across the intact skin (0.03 nmol/cm^2). In Yan, Todo, and Sugibayashi study (2010: 77–83), they found an approximate 7-fold and 20-fold higher in FD-4 permeability of skin pretreated with microneedles (3×3 of each 400 μm long), and followed by the conventional electroporation (ON-SKIN EP; 200 V, 10 ms, 10 pulses), respectively, compared to the passive FD-4 permeated across the intact skin. Besides that they fabricated the microneedles to serve as a microelectrode for electroporation (IN-SKIN EP), which forms an electric field inside the skin barrier. IN-SKIN EP showed 140-fold FD-4 permeability compared to the passive permeation. The results of these studies revealed the higher drug transport through skin following a hollow microneedle injection.

Table 9 shows the percentage of FD-4 released from skin over 8 h after administration by a hollow microneedle. More than 65% FD-4 solution was released from the skin over 8 h in all cases. Since diffusion in skin is the primary mechanism of drug release from skin, FD-4–loaded skin might be treated as a drug-loaded matrix. In this respect, the Higuchi model was applicable and further used to analyze the obtained drug release data. Figure 13 shows the graphic plot of the cumulative amount of FD-4 released per unit area from skin against the square root of time. The linear relationships (R^2 = 0.897–0.980) were obtained, indicating that the release of FD-4 followed the Higuchi diffusion model validated when the drug release was less

than 30%. The drug release rate (*k*) can be calculated from the slope of the graphic plot (Figure 13). The release kinetics of FD-4 from FD-4–loaded skin derived by the simplified Higuchi model are summarized in Table 10. From the results, it was shown that increasing the injection volume from 5 to 20 µL increased the FD-4 release rate almost proportionally (Figure 14). These results, however, were not a virtual effect of injection volume. Because the higher the volume of FD-4 solution injected, the higher the FD-4 amount delivered into skin.

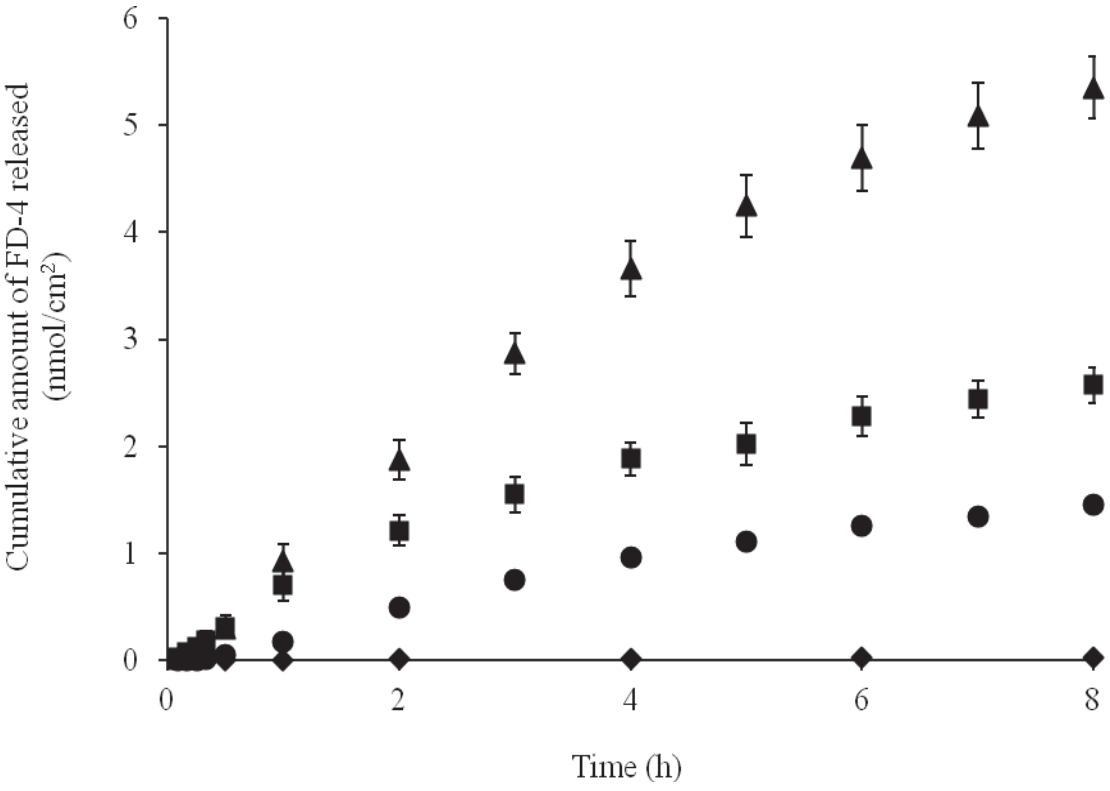

Figure 12 Effect of injection volume on the release profile of FD-4 from skin after administration of FD-4 solution of 5, 10, and 20 µL. Symbols: ●, 5 µL; ■, 10 µL; ▲, 20 µL; ◆, Passive diffusion. Each point represents the mean ± S.E. of four experiments.

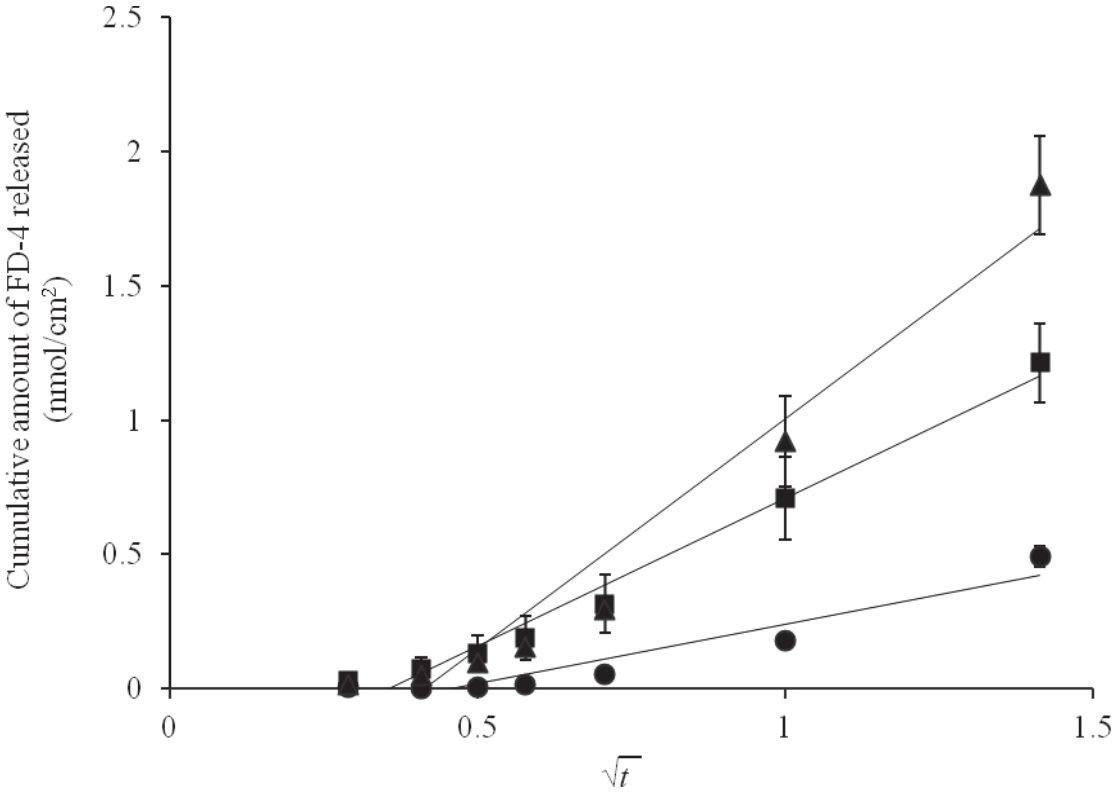

Figure 13 Analysis of the effect of injection volume on the FD-4 release profile using the simplified Higuchi model. Symbols: ●, 5 μL; ■, 10 μL; ▲, 20 μL. Solid lines represent the calculated values by the following equations: ●; $Q = 0.44 \times \sqrt{t} - 0.20$ ($R^2 = 0.897$), ■; $Q = 1.10 \times \sqrt{t} - 0.39$ ($R^2 = 0.980$), ▲; $Q = 1.71 \times \sqrt{t} - 0.71$ ($R^2 = 0.947$). Each point represents the mean ± S.E. of four experiments.

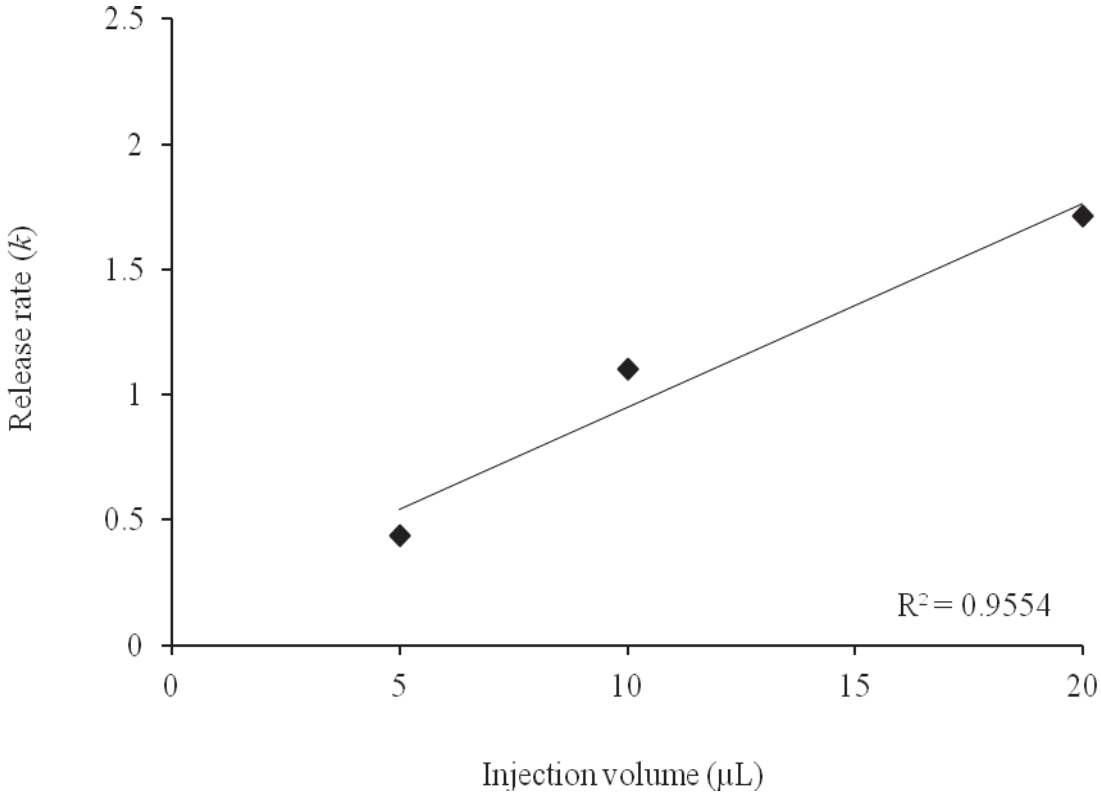

Figure 14 Relationship between injection volume and release rate of FD-4 from skin following a hollow microneedle injection.

4.3 Effect of number of injections on the release behavior of FD-4 from skin

In order to further examine the effect of number of injections, the total injection volume was set to be constant at 10 μL. Release studies were performed using different injection conditions, i.e. one of 10 μL, two of 5 μL, and four of 2.5 μL. Figure 15 shows the time course of the accumulated amount of FD-4 released in the unit area of skin. Two 5 μL injections showed a higher amount of FD-4 released than one 10 μL and four 2.5 μL injections. However, the statistical analysis of the FD-4 release data showed no significant differences among these three groups. The percentage of FD-4 release was in the range of 66.2–77.7% which two 5 μL injections also exhibited an insignificantly higher in the percentage of FD-4 release than the others (Table 9). The effect of number of injections on the drug release from skin was

analyzed in a similar manner as above. The release profiles were found to follow Higuchi kinetics with R^2 of 0.980–0.984 (Figure 16). The FD-4 release rate (k) was shown to be slightly different between groups, k = 0.96–1.15 (Table 10). The results demonstrated that dividing the amount of FD-4 loaded into skin by multiple injections did not affect the release rate and the total amount of drug released from skin.

Since the number of injections did not affect on the drug release rate when the identical total volume of drug solution was delivered into skin. Thus, the single hollow microneedle may be preferred over hollow microneedle arrays, because with a single microneedle there is a lower risk of leakage (van der Maaden, Jiskoot, and Bouwstra, 2012).

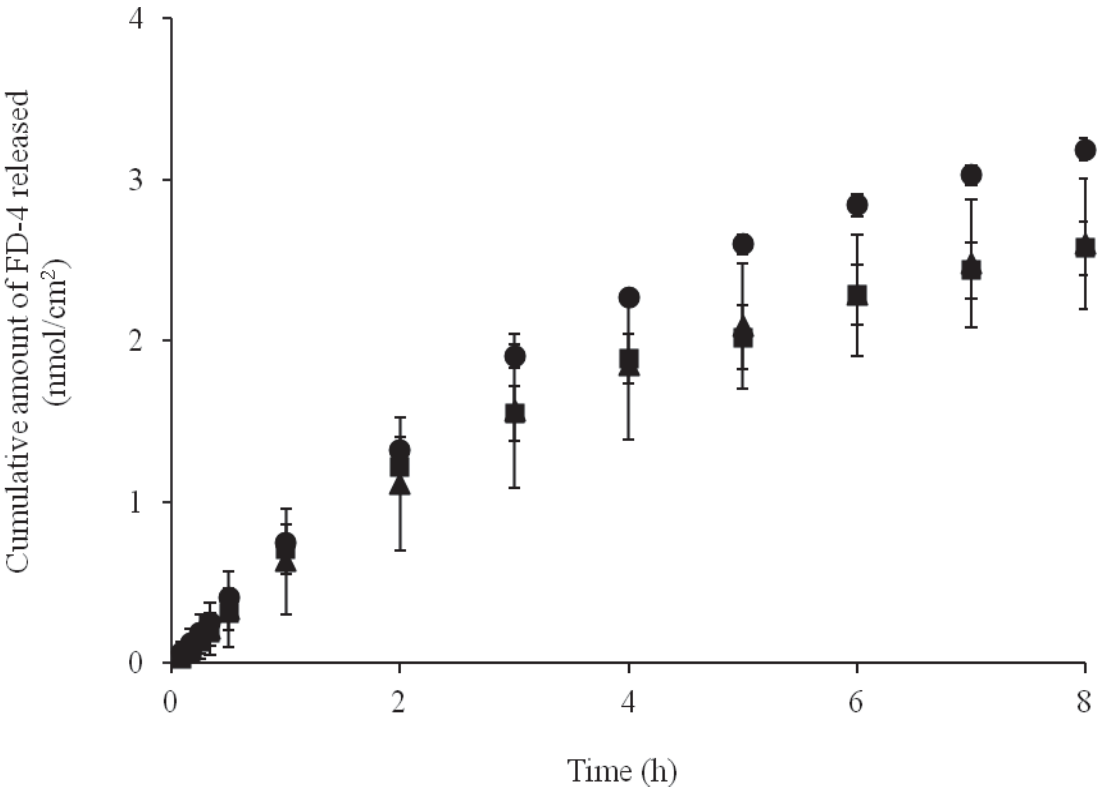

Figure 15 Effect of number of injections on the release profile of FD-4 from skin. Symbols: ■, one of 10 µL; ●, two of 5 µL; ▲, four of 2.5 µL. Each point represents the mean ± S.E. of three to four experiments.

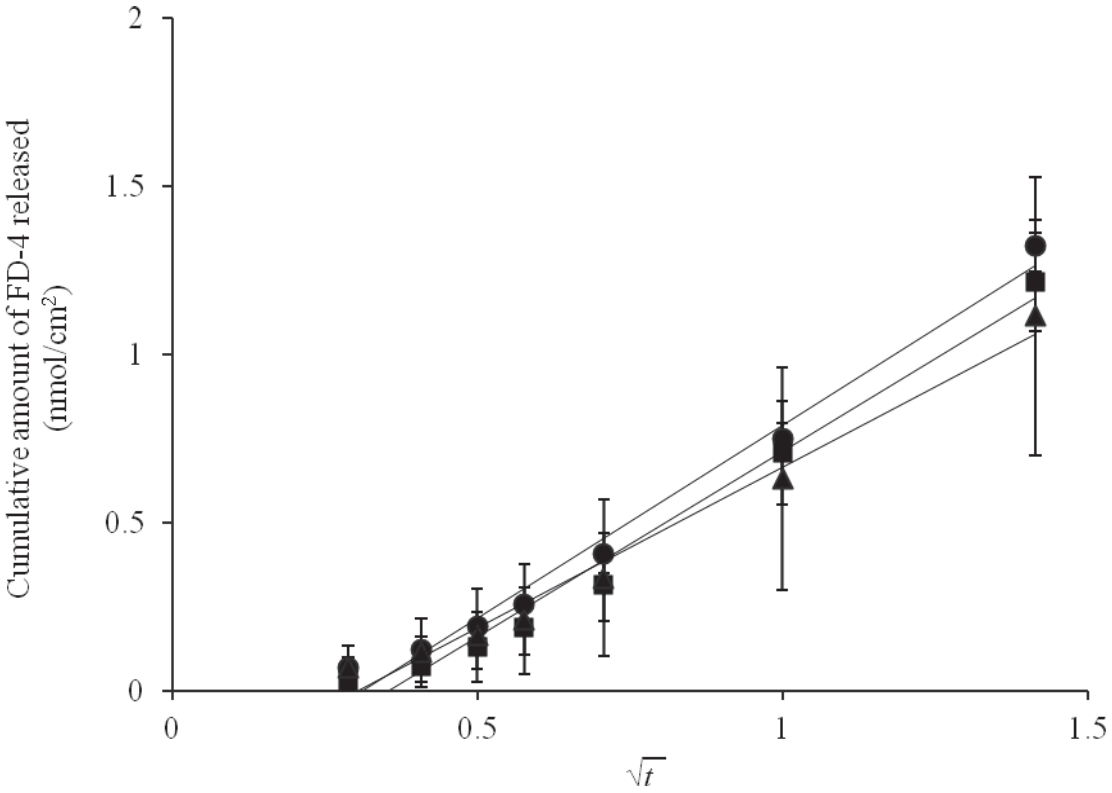

Figure 16 Analysis of the effect of number of injections on the FD-4 release profile using the simplified Higuchi model. Symbols: ■, one of 10 μL; ●, two of 5 μL; ▲, four of 2.5 μL. Solid lines represent the calculated values by the following equations: ■; $Q = 1.10 \times \sqrt{t} - 0.39$ ($R^2 = 0.980$), ●; $Q = 1.15 \times \sqrt{t} - 0.36$ ($R^2 = 0.984$), ▲; $Q = 0.96 \times \sqrt{t} - 0.29$ ($R^2 = 0.981$). Each point represents the mean ± S.E. of three to four experiments.

Table 9 The percentage of FD-4 released from skin over 8 h after administration by a hollow microneedle.

Injection volume (μL)	%	Number of injections [a]	%
5	65.1 ± 3.7	1 (10 μL)	66.2 ± 4.2
10	66.2 ± 4.2	2 (each 5 μL)	77.7 ± 2.1
20	69.3 ± 3.1	4 (each 2.5 μL)	67.7 ± 10.8

Concentration (mM)	Injection volume [b] (μL)	%	Injection volume [c] (μL)	%
1	10	66.2 ± 4.2	10	66.2 ± 4.2
2	10	70.0 ± 3.0	5	68.1 ± 6.3
4	10	63.3 ± 3.9	2.5	70.3 ± 4.6
10	10	76.9 ± 3.9	1	76.3 ± 6.1

[a] The total volume of injection was adjusted to 10 μL.

[b] The volume of injection was set to be constant at 10 μL.

[c] The total amount of FD-4 injected was adjusted to be equally at 10 nmol.

Mean ± S.E. with 3 to 4 measurements

Table 10 Release kinetics of FD-4 from FD-4–loaded skin derived by the simplified Higuchi model.

Simplified Higuchi Model $Q = kt^{1/2}$						
	Injection volume (μL)	Kinetic constant (k)	R^2	Number of injections [a]	Kinetic constant (k)	R^2
	5	0.440	0.897	1 (10 μL)	1.100	0.980
	10	1.100	0.980	2 (each 5 μL)	1.146	0.984
	20	1.714	0.947	4 (each 2.5 μL)	0.955	0.981
Concentration (mM)	Injection volume [b] (μL)	Kinetic constant (k)	R^2	Injection volume [c] (μL)	Kinetic constant (k)	R^2
1	10	1.100	0.980	10	1.100	0.980
2	10	1.969	0.975	5	0.805	0.956
4	10	3.136	0.903	2.5	0.739	0.918
10	10	10.487	0.942	1	0.665	0.890

[a] The total volume of injection was adjusted to 10 μL.

[b] The volume of injection was set to be constant at 10 μL.

[c] The total amount of FD-4 injected was adjusted to be equally at 10 nmol.

Mean ± S.E. with 3 to 4 measurements.

4.4 Effect of concentration on the release behavior of FD-4 from skin

To evaluate the effect of concentration parameter, various concentrations of FD-4 solution over a range of 1 to 10 mM were loaded into skin by a hollow microneedle. Based on the Fick's diffusion laws, molecules move in response to the concentration gradient, thus, the release rate should also depend on the concentration of FD-4 solution delivered into skin. Figure 17 shows the time course of the cumulative amount of FD-4 released per unit area of skin, in which the FD-4 solution was injected at a constant fixed volume of 10 μL. From the release profiles, it was observed that the cumulative amount of FD-4 released in the unit area of skin was increased as the higher concentration of FD-4 delivered. The plots of the initial drug release data (30% of dose release) versus the square root of release time gave a straight line with R^2 of 0.903–0.980 (Figure 18). The drug release rate (k) increased almost proportionally to the higher amount of drug injected (Figure 19), which was correspondent with the results of the effect of different injection volumes and of Lee, Park, and Prausnitz (2008: 2113–2124) study. They observed an approximate 3 times greater in drug release rate from human cadaver skin following the application of the dissolving microneedle patch containing 30% w/w of drug than the patch containing 10% w/w of drug.

When the injection volume was adjusted to give an equal amount of FD-4 delivered into skin, there were no significant differences on the cumulative release of FD-4 in the four concentrations of drug delivery (Figure 20). In this case, the total amount of FD-4 delivered was equally in all skin samples, meaning that there was the same FD-4 concentration loaded in the skin. The drug release rate of the first 30% release, however, was tended to be slower when the smaller volume of the higher FD-4 concentration was injected (Figure 21 and Table 10). These findings may be due to the faster drug diffusion through skin of the large volume injection in an early release time (decreasing in the diffusional pathlength). The effect of different concentrations on the percentage of FD-4 release is shown in Table 9. In all cases, more than 63.0% of FD-4 was released from the skin over 8 h and no significant differences on the percentage of FD-4 release were observed.

From the results, it can be concluded that the release rate of FD-4 from skin increased with the higher amount of FD-4 injected (FD-4 concentration in skin). When delivering the same total amount of drug into skin, release rate was tended to be slower when the smaller volume of the higher FD-4 concentration was injected, however, the total amount of FD-4 released from skin were not significant difference. With the small amount of drugs can be delivered into skin through a microinjection system, the drug release rate could be modified by adjusting the drug concentration with an identical injection volume.

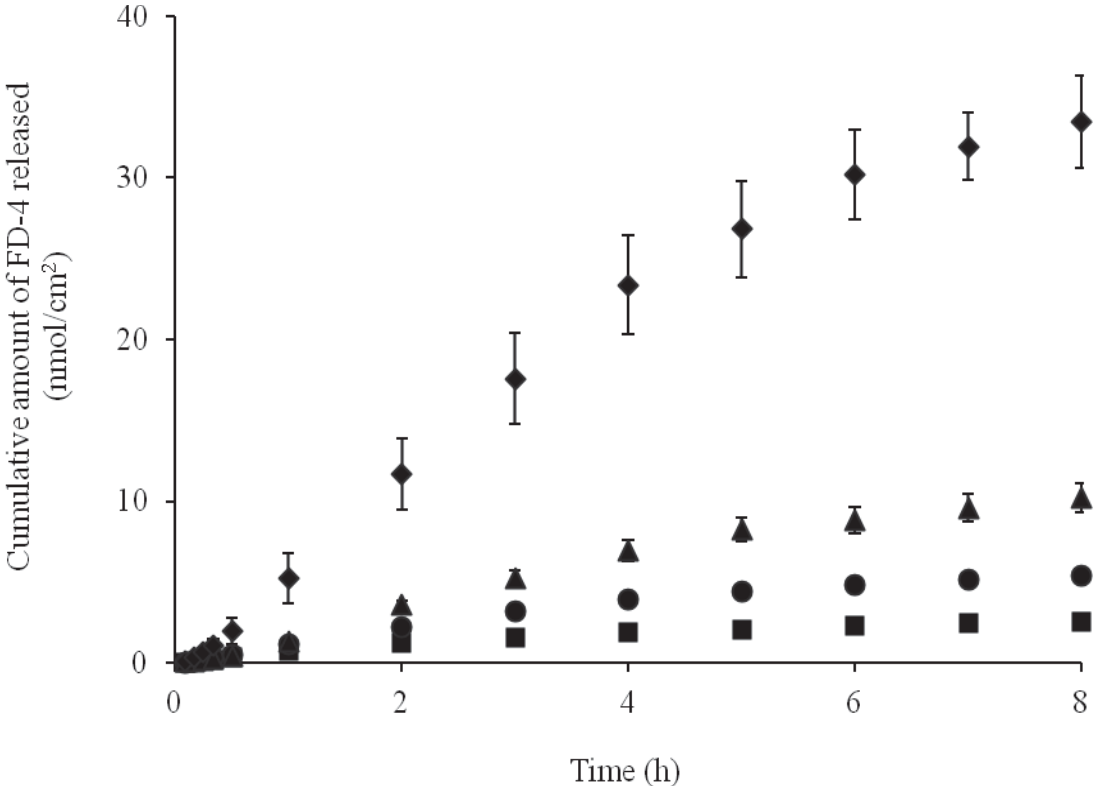

Figure 17 Effect of concentration on the release profile of FD-4 from skin following a 10-μL hollow microneedle injection. Symbols: ■, 1 mM; ●, 2 mM; ▲, 4 mM; ◆, 10 mM. Each point represents the mean ± S.E. of three to four experiments.

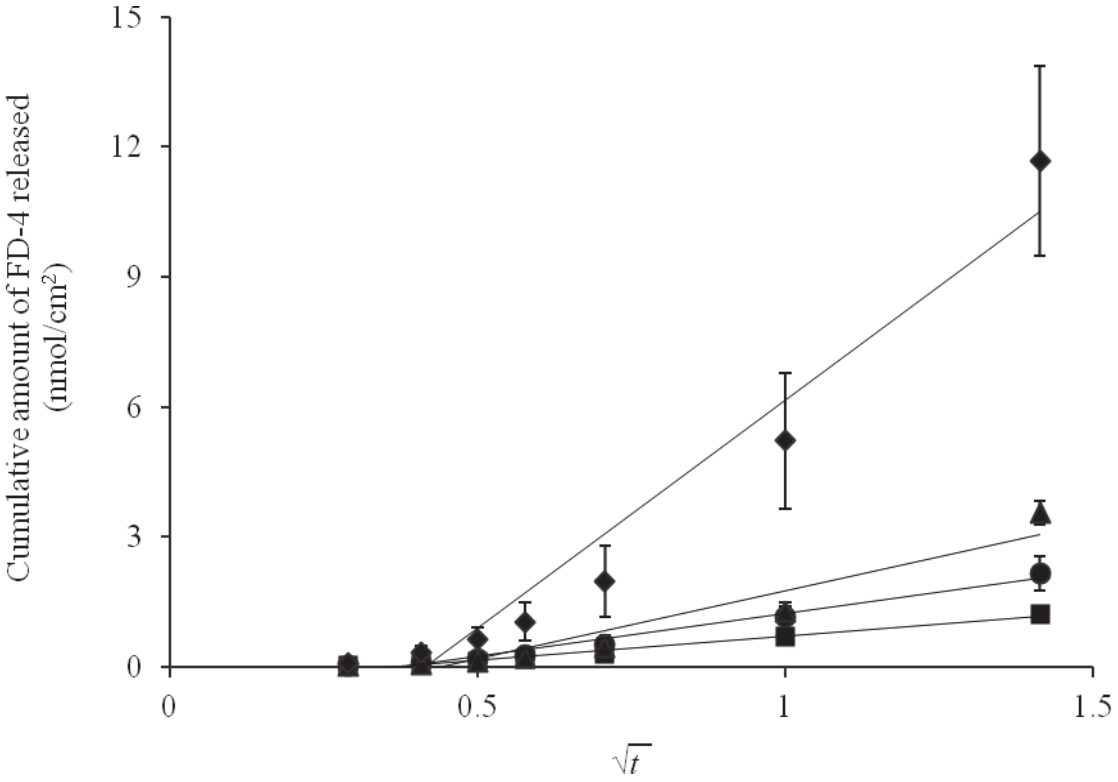

Figure 18 Analysis of the effect of FD-4 concentration on the release profile following a 10-μL hollow microneedle injection using the simplified Higuchi model. Symbols: ■, 1 mM; ●, 2 mM; ▲, 4 mM; ◆, 10 mM. Solid lines represent the calculated values by the following equations: ■; $Q = 1.10 \times \sqrt{t} - 0.39$ ($R^2 = 0.980$), ●; $Q = 1.97 \times \sqrt{t} - 0.74$ ($R^2 = 0.975$), ▲; $Q = 3.14 \times \sqrt{t} - 1.37$ ($R^2 = 0.903$), ◆; $Q = 10.49 \times \sqrt{t} - 4.33$ ($R^2 = 0.942$). Each point represents the mean ± S.E. of three to four experiments.

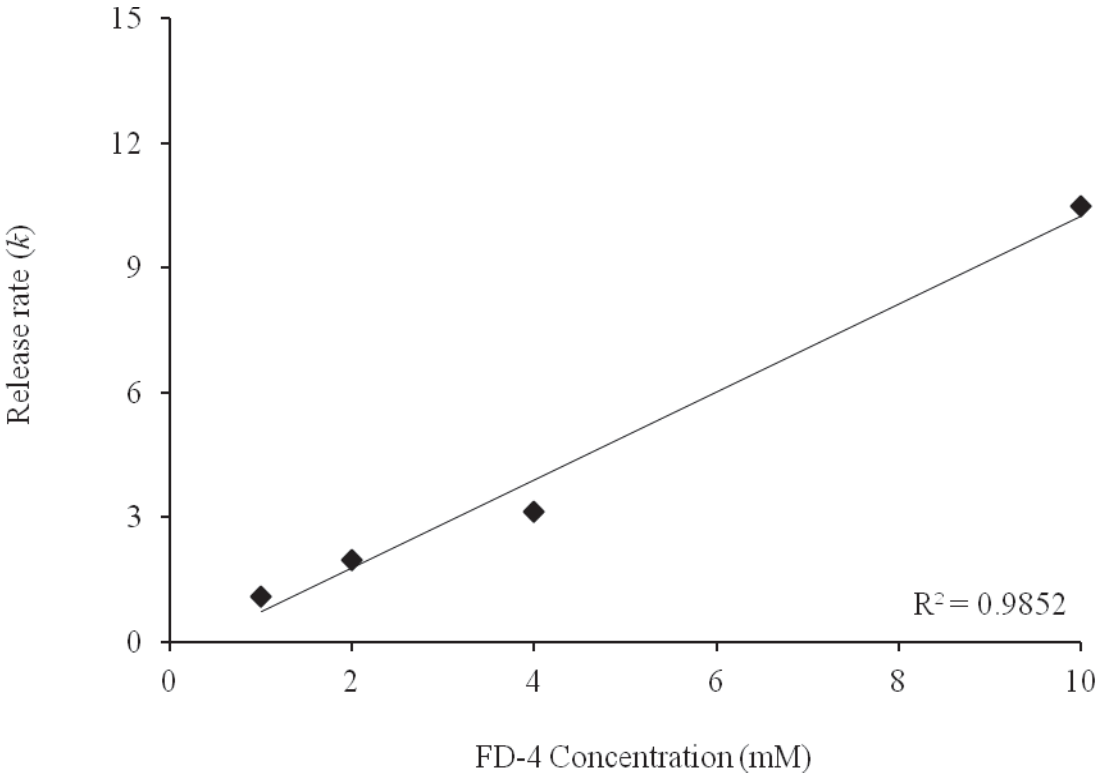

Figure 19 Relationship between concentration and release rate of FD-4 from skin following a hollow microneedle injection.

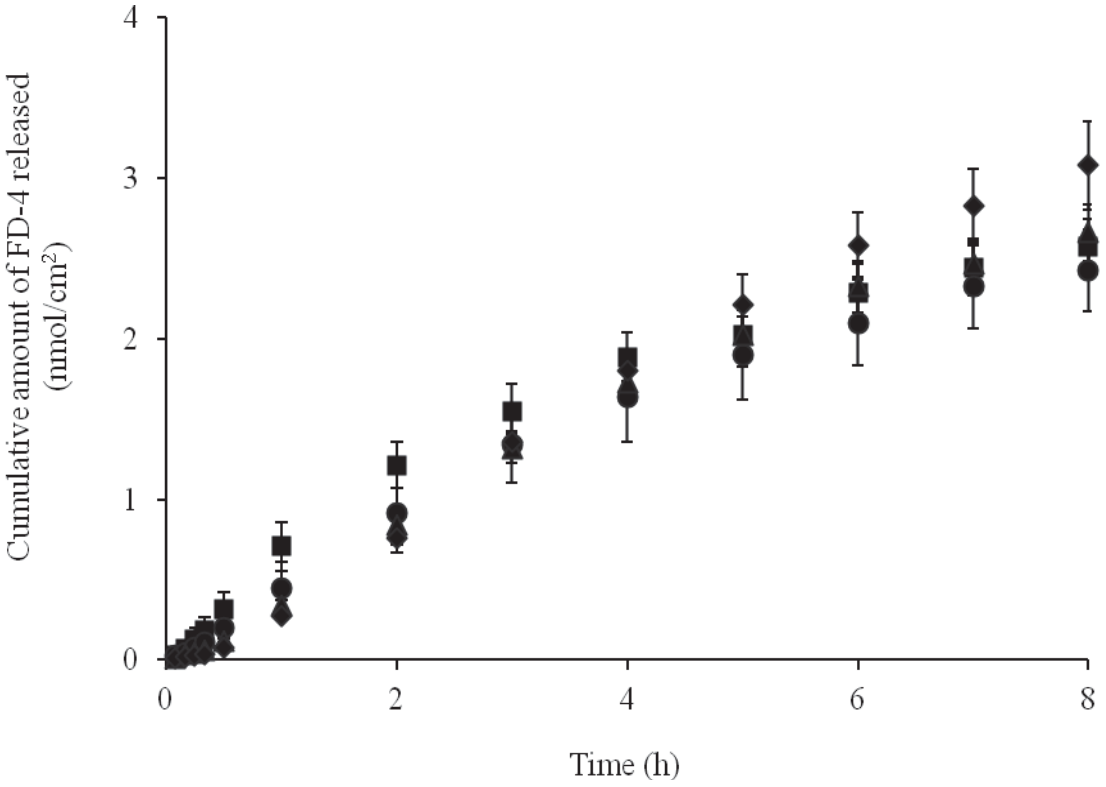

Figure 20 Effect of concentration on the release profile of FD-4 from skin following a hollow microneedle injection of the identical total amount of FD-4 (10 nmol) into skin. Symbols: ■, 1 mM; ●, 2 mM; ▲, 4 mM; ◆, 10 mM. Each point represents the mean ± S.E. of three to four experiments.

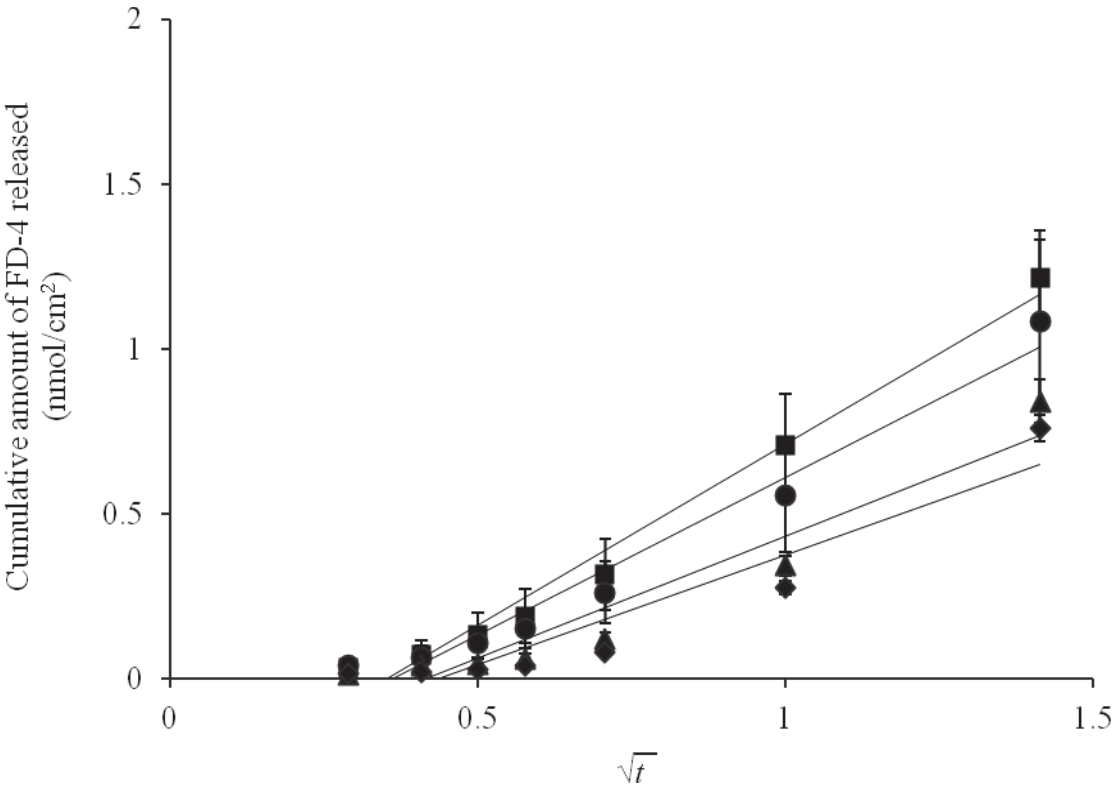

Figure 21 Analysis of the effect of FD-4 concentration on the release profile following a hollow microneedle injection of the identical total amount of FD-4 (10 nmol) using the simplified Higuchi model. Symbols: ■, 1 mM; ●, 2 mM; ▲, 4 mM; ◆, 10 mM. Solid lines represent the calculated values by the following equations: ■; $Q = 1.10 \times \sqrt{t} - 0.39$ ($R^2 = 0.980$), ●; $Q = 0.96 \times \sqrt{t} - 0.35$ ($R^2 = 0.965$), ▲; $Q = 0.74 \times \sqrt{t} - 0.31$ ($R^2 = 0.917$), ◆; $Q = 0.66 \times \sqrt{t} - 0.29$ ($R^2 = 0.890$). Each point represents the mean ± S.E. of three to four experiments.

4.5 Effect of different molecular sizes of the test compounds on the release behavior from skin

Study of the transport of drug substances within the deeper skin layers lags behind that of transport in SC. Only SC has been recognized as a rate-limiting barrier for skin permeation of drugs, particularly hydrophilic drugs. By employing a hollow microneedle, drugs are directly loaded into the lower epidermis or dermis layer and bypass the SC, as explained above. Thus, hydrophilic molecules can be expected to readily diffuse through the lower layers of skin which contain a larger amount of water than the SC. In this study, the molecular weight dependence on the release of hydrophilic model compounds from skin after administration by a hollow microneedle was determined. Small molecules, D_2O, CAL, and three macromolecular compounds, FD-4, FD-10, and FD-40, having a molecular weight of 20.03, 623, 4000, 10000 and 40000 Da, respectively, were selected to be model substances. In this study, D_2O was used as received (99.9% without any dilutions), however, the sample solution of D_2O released from skin into 6.0 mL vertical diffusion cell was unable to detect. Therefore, 3.0 mL side-by-side diffusion cell was selected for the test of D_2O. Other model drugs were used at 1 mM solutions. The experimental results are shown in Figure 22 and 23. D_2O was released rapidly in the first hour of experimental period (Figure 22). Due to its property as a very small molecule, it was released fastest among the model compounds. The amount of CAL released from skin was significantly higher than that of FD-4, FD-10, and FD-40 ($p < 0.05$) (Figure 23). The release of FD-4 and FD-10 from drug-loaded skins was not significantly different. However, they were substantially higher compared to the release of FD-40 from skin ($p < 0.05$). The percentage of model drugs released in 8 h of the experimental time is shown in Figure 24. More than 85% of D_2O was released from the treated skin within an hour. The percent cumulative release over 8 h was in the order of D_2O (100.0%) > CAL (85.7%) > FD-4 (66.2%) ≈ FD-10 (65.0%) > FD-40 (43.7%) (Figure 24). Analysis of drug release profile using the simplified Higuchi model revealed the release rate of CAL, FD-4, FD-10, and FD-40 of 2.075, 1.100, 0.846, and 0.675 $nmol/cm^2h^{1/2}$, respectively (Figure 25). Since the simplified Higuchi model is confined to the description of the first 30% of the release curve. D_2O was released more than 50% at the first sampling

time of 15 min. Therefore, the release rate of D_2O could not be determined in this study.

These results clearly showed that the molecular sizes of drug compounds affect drug release from skin. Alternatively, molecular size has a marked influence on drug diffusivity within the deeper layers of skin, with increasing bulky molecules decreasing in diffusivity. Yoshida et al. (2008: 5–11) also showed the molecular weight dependence on the apparent diffusion coefficients in skin after intracutaneous injection. However, there were no differences in the amount of drug released from skin at 8 h of the compounds having a molecular weight range of 4–10 kDa. These results also supported the results of Ito et al. (2010: 845–851) that the viable epidermis and dermis retarded the penetration of macromolecules with the molecular size of 40 kDa and greater. Moreover, Ogiso et al. (1994: 1676–1681) reported the dependency of the permeability of polar solutes through the stripped skin on the molecular size dependent. They also suggested that the viable epidermis and dermis restricted the penetration of macromolecules, such as FD-70. However, the model substances in their study were FD-4, FD-10, and FD-70.

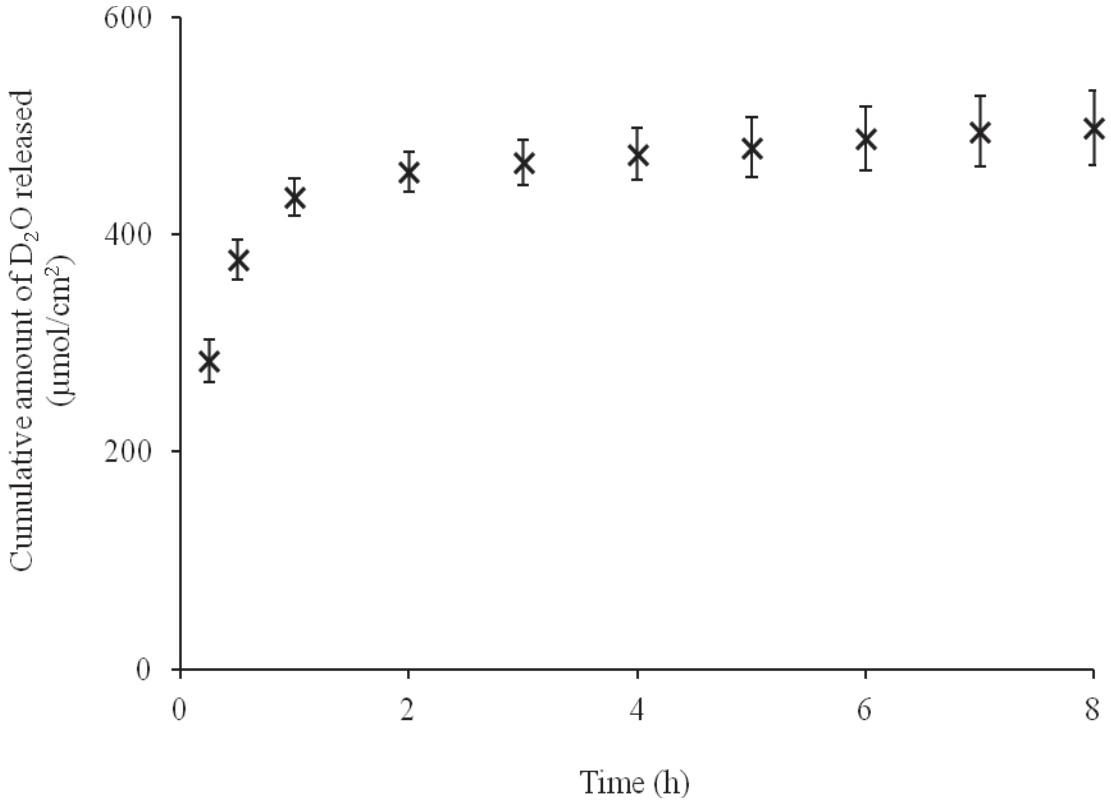

Figure 22 Cumulative amount of D_2O released per unit area from skin following a 10-μL hollow microneedle injection. Each point represents the mean ± S.E. of three to five experiments.

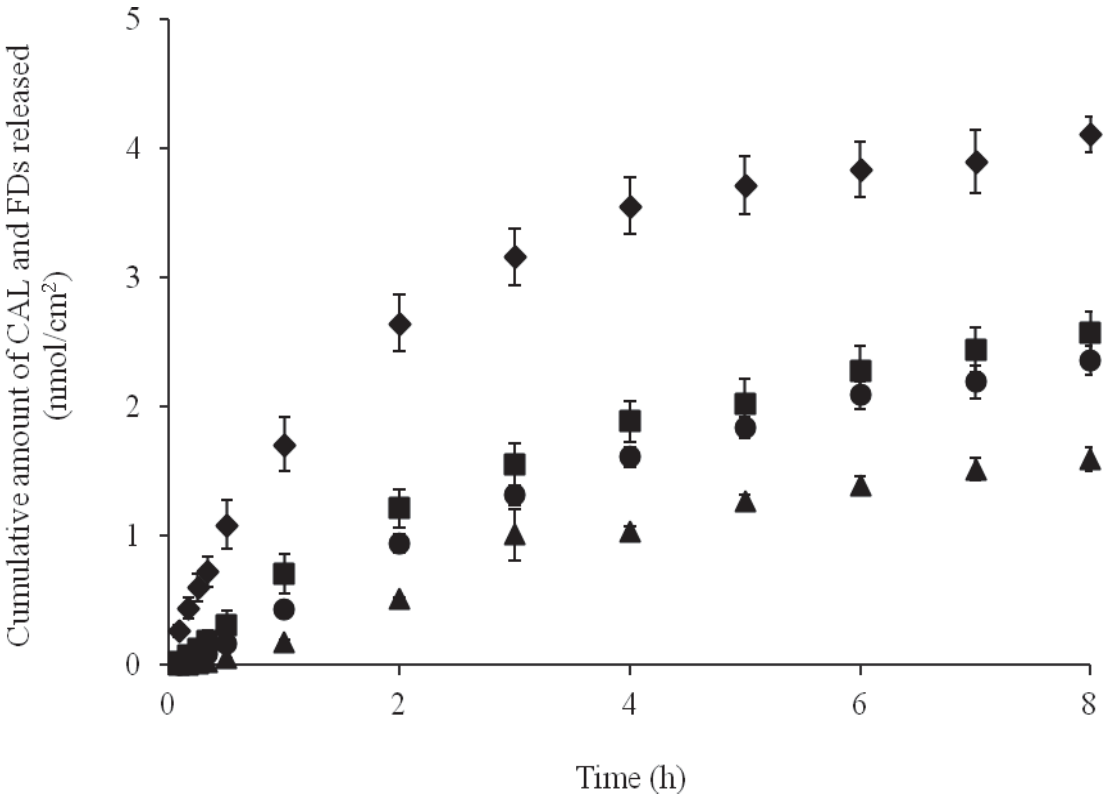

Figure 23 Cumulative amount of CAL and FDs released per unit area from skin following a 10-μL hollow microneedle injection. Symbols: ◆, CAL; ■, FD-4; ●, FD-10; ▲, FD-40. Each point represents the mean ± S.E. of three to five experiments.

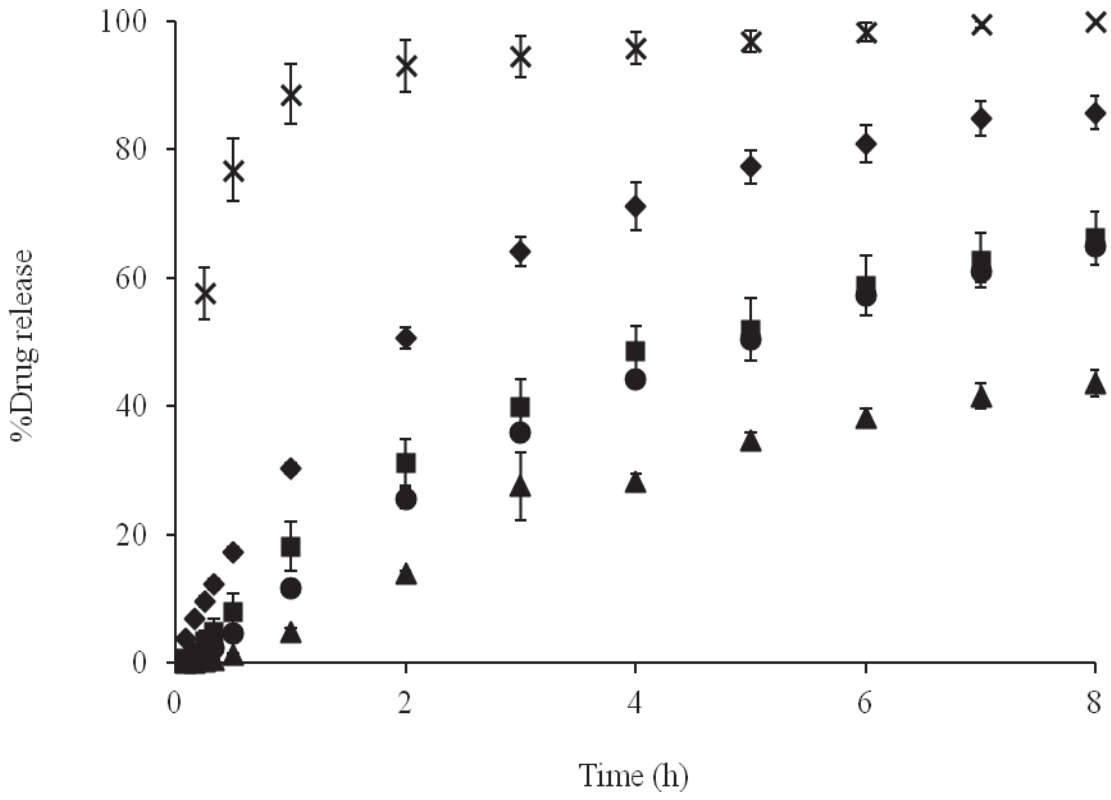

Figure 24 Effect of different molecular sizes of the hydrophilic model compounds on the percentage of drug release from skin. Symbols: ✕, D_2O; ◆, CAL; ■, FD-4; ●, FD-10; ▲, FD-40. Each point represents the mean ± S.E. of three to five experiments.

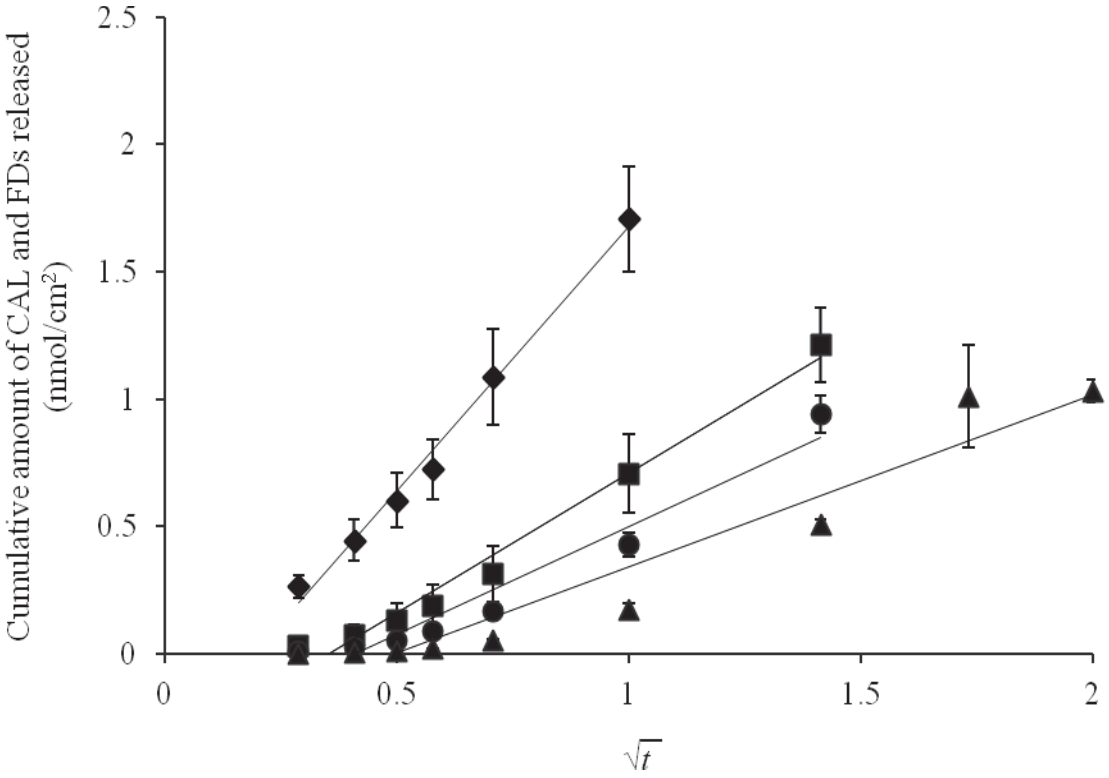

Model substance	k (nmol/cm^{2}h$^{1/2}$)	R^2
CAL	2.075	0.991
FD-4	1.100	0.980
FD-10	0.846	0.947
FD-40	0.675	0.930

Figure 25 Analysis of the effect of different molecular sizes of the hydrophilic model compounds on the release profile using the simplified Higuchi model. Symbols: ◆, CAL; ■, FD-4; ●, FD-10; ▲, FD-40. The table expresses the release kinetics (k) derived from the graphic plots.

4.6 Effect of hollow microneedle-assisted delivery on the diffusivity of FD-4 within skin

The study was further performed to determine the diffusion coefficient of the model macromolecular compound, FD-4. The diffusion coefficient of FD-4 solution in skin (D_{Skin}) was examined from the gradients of Higuchi plots (see 'Diffusivity of FD-4 in Skin' in Chapter 3). D_{Skin} was calculated to be 3.9×10^{-4} cm^2/h. A comparison was performed with the diffusion coefficient of FD-4 in the stratum corneum layer (D_{SC}) and in viable epidermis and dermis layers (D_{ved}), which were 5.1×10^{-7} and 6.0×10^{-4} cm^2/h, respectively. As a result, D_{Skin} was in the same order of magnitude as D_{ved} and much higher than D_{SC}. Because the SC provides a marked skin barrier, its resistance to drug diffusion in this skin layer is the highest, causing the lowest diffusivity of FD-4. By employing a hollow microneedle device, the surface of the skin barrier (SC) was bypassed; thus, FD-4 solution was capable to deliver into the lower epidermis or dermis, where the permeation resistance of FD-4 must be much lower than that on the SC; therefore, FD-4 can easily diffuse through the deeper layers of skin. These results exhibited the utility of hollow microneedles for overcoming the barrier function of SC and enhancing the delivery of hydrophilic compounds, especially the large molecular compounds into skin.

CHAPTER 5
CONCLUSIONS

A strategy employing microneedles have recently emerged as a minimally invasive device for disrupting the SC structure and creating holes for molecules to pass through. Although solid-type microneedles are simpler to make, hollow-type microneedles have the potential to deliver material more precisely by injection through the well-defined bore of hollow microneedles (McAllister, Allen, and Prausnitz, 2000: 289–313). The present study demonstrated the utilization of a hollow microneedle for delivering the hydrophilic drugs including the macromolecular compounds into skin. A single 33-gauge hypodermic needle was used instead of the hollow microneedle array. The needle was inserted into the skin with an angle of 40 degree. The present results may not extrapolate to those by the hollow microneedle array. However, the size of 33-gauge hypodermic needle used in this experiment resembles to the hollow microneedle reported by other researchers. Furthermore, both of the device used in this study and typical hollow microneedle array could avoid the SC barrier function by creating pores. The advantage of single needle device is capable to investigate several factors such as administration volume, formulation, and depth penetration of needles.

By employing a hollow microneedle device, the hydrophilic model compounds were favorably loaded into the lower epidermis as well as the superficial dermis of skin. Up to 20 μL (bolus injection) of FD-4 solution was successfully administered into the excised dorsal rat skin without any leakage. The diffusivity of FD-4 after administration by a hollow microneedle was almost the same as its diffusivity in viable epidermis and dermis layers and much larger than that in the SC. Plots of the initial drug release data (30% of dose release) of experiments conducted under perfect sink conditions versus the square of release time gave a straight line (R^2 = 0.890–0.984) which indicated the release mechanism of drug-loaded skin of Fickian

diffusion. Various parameters based on the hollow microneedle system were examined to optimize the delivery device. Overall, the release rates of FD-4 from FD-4–loaded skin were approximately linearly increased with the amount of FD-4 injected and almost the same independent of the volume of injection. The release profiles of different FD-4 concentrations showed no significant differences. However, the FD-4 release rates were tended to decrease with the smaller injection volume of the higher FD-4 concentration injection. The effect of molecular size on the percentage of drug release was in the order of D_2O > Calcein sodium > FD-4 ≈ FD-10 > FD-40. These observations exhibited an influence of molecular size on the drug diffusivity within the deeper layers of skin. The release of FD-40 was significantly lower when the release of macromolecules was compared, indicating the restriction of macromolecules with molecular weight more than 40 kDa penetration through the viable epidermis and dermis.

Other factors such as physicochemical properties of drugs (i.e. lipophilicity and drug binding), type of formulation selected (i.e. aqueous or non-aqueous solution, and solution, emulsion, or suspension), and injection parameters (i.e. injection pressure and infusion rate) must be further investigated to obtain the utilizable information for development an effective and precisely controlled hollow microneedle array-patch system. In that case, moreover, the characterization of a hollow microneedle array-patch system and the investigation of its application in *in vitro* and *in vivo* are also further required.

BIBLIOGRAPHY

Al-Qallaf, Barrak et al. (2007). "Modelling transdermal delivery of high molecular weight drugs from microneedle systems." **Philos Transact A Math Phys Eng Sci** 365, 1861: 2951–2967.

Arora, Anubhav, Mark R. Prausnitz, and Samir Mitragotri. (2008). "Micro-scale devices for transdermal drug delivery." **Int J Pharm** 364, 2: 227–236.

Badran, M. M., J. Kuntsche, and A. Fahr. (2009). "Skin penetration enhancement by a microneedle device (Dermaroller®) in vitro: dependency on needle size and applied formulation." **Eur J Pharm Sci** 36, 4–5: 511–523.

Bal, Suzanne M. et al. (2008). "In vivo assessment of safety of microneedle arrays in human skin." **Eur J Pharm Sci** 35, 3: 193–202.

Bal, Suzanne M. et al. (2010). "Advances in transcutaneous vaccine delivery: do all ways lead to Rome?" **J Control Release** 148, 3: 266–282.

Bariya, Shital H. et al. (2012). "Microneedles: an emerging transdermal drug delivery system." **J Pharm Pharmacol** 64, 1: 11–29.

Barry, Brian W. (1991). "Lipid-Protein-Partitioning theory of skin penetration enhancement." **J Control Release** 15, 3: 237–248.

Barry, Brian W. (2001). "Novel mechanisms and devices to enable successful transdermal drug delivery." **Eur J Pharm Sci** 14, 2: 101–114.

Barry, Brian W. (2004). "Breaching the skin's barrier to drugs." **Nat Biotechnol** 22: 165–167.

Barry, Brian W. (2006). "Penetration Enhancer Classification." In **Percutaneous Penetration Enhancers**, 3–16. Edited by Eric W. Smith and Howard I. Maibach. New York: Taylor & Francis Group.

Burton, Scott A. et al. (2011). "Rapid intradermal delivery of liquid formulations using a hollow microstructured array." **Pharm Res** 28, 1: 31–40.

Chabri, F. et al. (2004). “Microfabricated silicon microneedles for nonviral cutaneous gene delivery.” **Br J Dermatol** 150, 5: 869–877.

Chattaraj, Sarat C., and Roderick B. Walker. (1995). “Penetration Enhancer Classification.” In **Percutaneous Penetration Enhancers**, 5–20. Edited by Eric W. Smith and Howard I. Maibach. New York: CRC Press, Inc.

Chen Huabing et al. (2009). “Iontophoresis-driven penetration of nanovesicles through microneedle-induced skin microchannels for enhancing transdermal delivery of insulin.” **J Control Release** 139, 1: 63–72.

Chen Xianfeng et al. (2009). “Dry-coated microprojection array patches for targeted delivery of immunotherapeutics to the skin.” **J Control Release** 139, 3: 212–220.

Cormier, Michel et al. (2004). “Transdermal delivery of desmopressin using a coated microneedle array patch system.” **J Control Release** 97, 3: 503–511.

Coulman, Sion A. et al. (2009). “Microneedle mediated delivery of nanoparticles into human skin.” **Int J Pharm** 366, 1–2: 190–200.

Davis, Shawn P. et al. (2004). “Insertion of microneedles into skin: measurement and prediction of insertion force and needle fracture force.” **J Biomech** 37, 8: 1155–1163.

Denet, Anne R., Rita Vanbever, and Véronique Préat. (2004). “Skin electroporation for transdermal and topical delivery.” **Adv Drug Deliv Rev** 56, 5: 659–674.

Donnelly, Ryan F. et al. (2009). “Microneedle arrays allow lower microbial penetration than hypodermic needles in vitro.” **Pharm Res** 26, 11: 2513–2522.

Donnelly, Ryan F., Thakur R. Raj Singh, and A. David Woolfson. (2010). “Microneedle-based drug delivery systems: microfabrication, drug delivery, and safety.” **Drug Deliv** 17, 4: 187–207.

El Maghraby, Gamal M., Brian W. Barry, and Adrian C. Williams. (2008). "Liposomes and skin: From drug delivery to model membranes." **Eur J Pharm Sci** 34: 203–222.

Gerstel, M. S., and V. A. Place. (1976). Drug delivery device, US Patent No. 3964482.

Gill, Harvinder S. et al. (2008). "Effect of microneedle design on pain in human volunteers." **Clin J Pain** 24, 7: 585–594.

Gill, Harvinder S., and Mark R. Prausnitz. (2007). "Coated microneedles for transdermal delivery." **J Control Release** 117, 2: 227–237.

Gupta, Jyoti, Eric I. Felner, and Mark R. Prausnitz. (2009). "Minimally invasive insulin delivery in subjects with type 1 diabetes using hollow microneedles." **Diabetes Technol Ther** 11, 6: 329–337.

Gupta, Jyoti, Eric I. Felner, and Mark R. Prausnitz. (2011). "Rapid pharmacokinetics of intradermal insulin administered using microneedles in type 1 diabetes subjects." **Diabetes Technol Ther** 13, 4: 451–456.

Gupta, Jyoti. et al. (2011). "Kinetics of skin resealing after insertion of microneedles in human subjects." **J Control Release** 154, 2: 148–155.

Guy, Richard H., and Jonathan Hadgraft. (1985). "Mathematical Models of Percutaneous Absorption." In **Percutaneous Absorption: Mechanisms–Methodology–Drug Delivery**, 3–15. Edited by Robert L. Bronaugh and Howard I. Maibach. New York: Marcel Dekker, Inc.

Hada Nobuko et al. (2005). "Cultured skin loaded with tetracycline HCl and chloramphenicol as dermal delivery system: mathematical evaluation of the cultured skin containing antibiotics." **J Control Release** 108, 2–3: 341–350.

Häfeli, Urs O., Amir Mokhtari, and Dorian Liepmann. (2009). "In vivo evaluation of a microneedle-based miniature syringe for intradermal drug delivery." **Biomed Microdevices** doi: 10.1007/s10544-009-9311-y

Harvey, Alfred J. et al. (2011). "Microneedle-based intradermal delivery enables rapid lymphatic uptake and distribution of protein drugs." **Pharm Res** 28, 1: 107–116.

Henry, Sebastien et al. (1998). "Microfabricated microneedles: a novel approach to transdermal drug delivery." **J Pharm Sci** 87, 8: 922–925.

Higuchi, William I. (1962). "Analysis of data on the medicament release from ointments." **J Pharm Sci** 51, 8 (August): 802–804.

Ito Yukako et al. (2006a). "Feasibility of microneedles for percutaneous absorption of insulin." **Eur J Pharm Sci** 29, 1: 82–88.

Ito Yukako et al. (2006b). "Self-dissolving microneedles for the percutaneous absorption of EPO in mice." **J Drug Target** 14, 5: 255–261.

Ito Yukako et al. (2010). "Molecular weight dependence on bioavailability of FITC-dextran after administration of self-dissolving micropile to rat skin." **Drug Dev Ind Pharm** 36, 7: 845–851.

Kalia, Yogeshvar N. et al. (2004). "Iontophoretic drug delivery." **Adv Drug Deliv Rev** 56, 5: 619–658.

Kalluri, Haripriya and Ajay K. Banga. (2011). "Formation and closure of microchannels in skin following microporation." **Pharm Res** 28, 1: 82–94.

Kaushik, Diksha et al. (2010). "Microneedles – Minimally invasive transdermal delivery technology." In **Handbook of Non-Invasive Drug Delivery Systems**, 135–164. Edited by Vitthal S. Kulkarni. Elsevier Inc.

Kaushik, Shilpa et al. (2001). "Lack of pain associated with microfabricated microneedles." **Anesth Analg** 92, 2: 502–504.

Laurent, Philippe E. et al. "Safety and efficacy of novel dermal and epidermal microneedle delivery systems for rabies vaccination in healthy adults." **Vaccine** 28, 36: 5850–5856.

Lee, Jeong W., Jung-Hwan Park, and Mark R. Prausnitz. (2008). “Dissolving microneedles for transdermal drug delivery.” **Biomaterials** 29, 13: 2113–2124.

Li Wei-Ze et al. (2010). “Super-short solid silicon microneedles for transdermal drug delivery applications.” **Int J Pharm** 389, 1–2: 122–129.

Lin WeiQi et al. (2001). “Transdermal delivery of antisense oligonucleotides with microprojection patch (Macroflux) technology.” **Pharm Res** 18, 12: 1789–1793.

Martanto, Wijaya et al. (2004). “Transdermal delivery of insulin using microneedles in vivo.” **Pharm Res** 21, 6: 947–952.

Martanto, Wijiya. et al. (2006). “Microinfusion using hollow microneedles.” **Pharm Res** 23, 1: 104–113.

Matriano, James A. et al. (2002). “Macroflux microprojection array patch technology: a new and efficient approach for intracutaneous immunization.” **Pharm Res** 19, 1: 63–70.

McAllister, Devin V. et al. (2003). “Microfabricated needles for transdermal delivery of macromolecules and nanoparticles: fabrication methods and transport studies.” **Proc Natl Acad Sci U S A** 100, 24: 13755–13760.

McAllister, Devin V., Mark G. Allen, and Mark R. Prausnitz. (2000). “Microfabricated microneedles for gene and drug delivery.” **Annu Rev Biomed Eng** 2: 289–313.

Mikszta, John A. et al. (2002). “Improved genetic immunization via micromechanical disruption of skin-barrier function and targeted epidermal delivery.” **Nat Med** 8, 4: 415–419.

Mikszta, John A. et al. (2005). “Protective immunization against inhalational anthrax: a comparison of minimally invasive delivery platforms." **J Infect Dis** 191, 2: 278–288.

Mitragotri, Samir. (2000). "Synergistic effect of enhancers for transdermal drug delivery." **Pharm Res** 17, 11: 1354–1359.

Narasimha Murthy S., and H. N. Shivakumar. (2010). "Topical and Transdermal Drug Delivery." In **Handbook of Non-Invasive Drug Delivery Systems**, 1–36. Edited by Vitthal S. Kulkarni. Elsevier Inc.

OECD. (2004). "Test Guideline 428: Skin absorption: *in vitro* Method." Accessed January 15, 2009. Available from OECD*i*Library http://www.oecd-ilibrary.org/environment/test-no-428-skin-absorption-in-vitro-method_9789264071087-en

Ogiso Taro et al. (1994). "Mechanism of the enhancement effect of n-octyl-beta-D-thioglucoside on the transdermal penetration of fluorescein isothiocyanate-labeled dextrans and the molecular weight dependence of water-soluble penetrants through stripped skin." **J Pharm Sci** 83, 12: 1676–1681.

Oh Jae-Ho et al. (2008). "Influence of the delivery systems using a microneedle array on the permeation of a hydrophilic molecule, calcein." **Eur J Pharm Biopharm** 69, 3: 1040–1045.

Park Jung-Hwan, Mark G. Allen, and Mark R. Prausnitz. (2005). "Biodegradable polymer microneedles: fabrication, mechanics and transdermal drug delivery." **J Control Release** 104, 1: 51–66.

Park Jung-Hwan, Mark G. Allen, and Mark R. Prausnitz. (2006). "Polymer microneedles for controlled-release drug delivery." **Pharm Res** 23, 5: 1008–1019.

Pettis, Ronald J. et al. (2011a). "Intradermal microneedle delivery of insulin lispro achieves faster insulin absorption and insulin action than subcutaneous injection." **Diabetes Technol Ther** 13, 4: 435–442.

Pettis, Ronald J. et al. (2011b). "Microneedle-based intradermal versus subcutaneous administration of regular human insulin or insulin lispro: pharmacokinetics and postprandial glycemic excursions in patients with type 1 diabetes." **Diabetes Technol Ther** 13, 4: 443–450.

Prausnitz, Mark R. (2004). “Microneedles for transdermal drug delivery.” **Adv Drug Deliv Rev** 56, 5: 581–587.

Prausnitz, Mark R. et al. (2009). “Microneedle-based vaccines.” **Curr Top Microbiol Immunol** 333: 369–393.

Prausnitz, Mark R., and Robert Langer. (2008). “Transdermal drug delivery.” **Nat Biotechnol** 26, 11: 1261–1268.

Prausnitz, Mark R., John A. Mikszta, and Jennifer Raeder-Devens. (2006). “Microneedles.” In **Percutaneous Penetration Enhancers**, 239–256. Edited by Eric W. Smith and Howard I. Maibach. New York: Taylor & Francis Group.

Prausnitz, Mark R., Samir Mitragotri, and Robert Langer. (2004). “Current status and future potential of transdermal drug delivery.” **Nat Rev Drug Discov** 3, 2: 115–124.

Qiu Yuqin et al. (2008). “Enhancement of skin permeation of docetaxel: a novel approach combining microneedle and elastic liposomes.” **J Control Release** 129, 2: 144–150.

Roberts Michael S., Sheree Elizabeth Cross, and Mark A. Pellett. (2002). “Skin Transport.” In **Dermatological and Transdermal Formulations**, 89–195. Edited by Kenneth A. Walters. New York: Marcel Dekker, Inc.

Rolland, A. et al. (1993). “Site-specific drug delivery to pilosebaceous structures using polymeric microspheres.” **Pharm Res** 10, 12: 1738–1744.

Sivamani, Raja K. et al. (2005). “Clinical microneedle injection of methyl nicotinate: stratum corneum penetration.” **Skin Res Technol** 11, 2: 152–156.

Smart, Wilson H. and Kumar Subramanian. (2000). “The use of silicon microfabrication technology in painless blood glucose monitoring.” **Diabetes Technol Ther** 2, 4: 549–559.

Smith, Eric W., and Howard I. Maibach. (1995). “Percutaneous Penetration Enhancers: The Fundamentals.” In **Percutaneous Penetration**

Enhancers, 1–4. Edited by Eric W. Smith and Howard I. Maibach. New York: CRC Press, Inc.

Sugibayashi Kenji et al. (2010). "Mathematical model to predict skin concentration of drugs: toward utilization of silicone membrane to predict skin concentration of drugs as an animal testing alternative." **Pharm Res** 27, 1 (January): 134–142.

van der Maaden, Koen, Wim Jiskoot, and Joke Bouwstra. (2012). "Microneedle technologies for (trans)dermal drug and vaccine delivery." **J Control Release** in press, doi: 10.1016/j.jconrel.2012.01.042

Verbaan, Ferry J. et al. (2007). "Assembled microneedle arrays enhance the transport of compounds varying over a large range of molecular weight across human dermatomed skin." **J Control Release** 117, 2: 238–245.

Walters, Kenneth A., and Michael S. Roberts. (2002). "The Structure and Function of Skin." In **Dermatological and Transdermal Formulations**, 1–39. Edited by Kenneth A. Walters. New York: Marcel Dekker, Inc.

Wang Yiping et al. (2005). "Transdermal iontophoresis: combination strategies to improve transdermal iontophoretic drug delivery." **Eur J Pharm Biopharm** 60, 2: 179–191.

Wang, Ping M. et al. (2006). "Precise microinjection into skin using hollow microneedles." **J Invest Dermatol** 126, 5: 1080–1087.

Watkinson Adam C., and Keith R. Brain. (2002). "Basic Mathematical Principles in Skin Permeation." In **Dermatological and Transdermal Formulations**, 61–88. Edited by Kenneth A. Walters. New York: Marcel Dekker, Inc.

Wermeling, Daniel P. et al. (2008). "Microneedles permit transdermal delivery of a skin-impermeant medication to humans." **Proc Natl Acad Sci U S A** 105, 6: 2058–2063.

Williams, Adrian C. (2003). **Transdermal and topical drug delivery**. London: Pharmaceutical Press.

Williams, Adrian C., and Brian W. Barry. (2004). “Penetration enhancers.” **Adv Drug Deliv Rev** 56, 5: 603–618.

Wu Xueming, Hiroaki Todo, and Kenji Sugibayashi. (2006). “Effects of pretreatment of needle puncture and sandpaper abrasion on the in vitro skin permeation of fluorescein isothiocyanate (FITC)-dextran.” **Int J Pharm** 316, 1–2: 102–108.

Wu Xueming, Hiroaki Todo, and Kenji Sugibayashi. (2007). “Enhancement of skin permeation of high molecular compounds by a combination of microneedle pretreatment and iontophoresis.” **J Control Release** 118, 2: 189–195.

Xie Yu, Bai Xu, and Yunhua Gao. (2005). “Controlled transdermal delivery of model drug compounds by MEMS microneedle array.” **Nanomedicine** 1, 2: 184–190.

Yamashita Fumiyoshi and Mitsuru Hashida. (2003). “Mechanistic and empirical modeling of skin permeation of drugs.” **Adv Drug Deliv Rev** 55, 9: 1185–1199.

Yan Guang et al. (2010). “Evaluation needle length and density of microneedle arrays in the pretreatment of skin for transdermal drug delivery.” **Int J Pharm** 391, 1–2: 7–12.

Yan Keshu, Hiroaki Todo, and Kenji Sugibayashi. (2010) “Transdermal drug delivery by in-skin electroporation using a microneedle array.” **Int J Pharm** 397, 1–2: 77–83.

Yoshida Daisuke et al. (2007). “Dermatopharmacokinetics of salicylate following topical injection in rats: effect of osmotic pressure and injection volume on salicylate disposition.” **Int J Pharm** 337, 1–2: 142–147.

Yoshida Daisuke et al. (2008). “Effect of molecular weight on the dermatopharmacokinetics and systemic disposition of drugs after intracutaneous injection.” **Eur J Pharm Sci** 35, 1–2: 5–11.

APPENDIX

APPENDIX A

Standard curve for the *in vitro* skin release study

1. Determination of the amount of FD-4 released

Standard	:	FD-4
Method	:	Fluorescence spectrophotometry
Detector	:	The excitation wavelength at 495 nm
		The emission wavelength at 515 nm
Concentration (µg/mL)	:	0.05, 0.10, 0.25, 0.50, 1.00

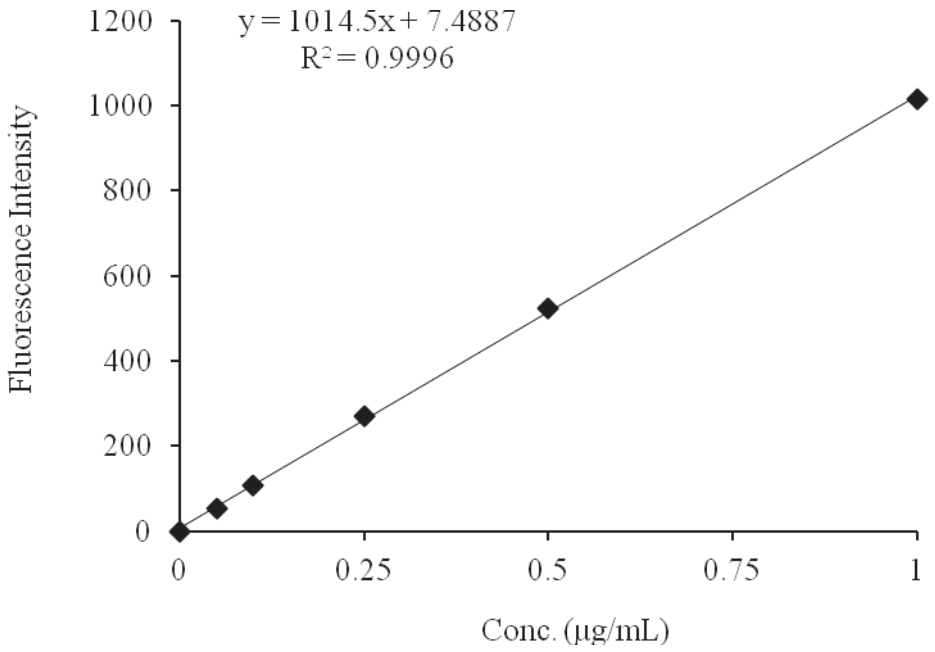

Figure 26 Standard curve of FD-4 for the *in vitro* skin release study.

2. Determination of the amount of FD-10 released

Standard	:	FD-10
Method	:	Fluorescence spectrophotometry
Detector	:	The excitation wavelength at 495 nm
		The emission wavelength at 515 nm
Concentration (µg/mL)	:	0.005, 0.010, 0.050, 0.100, 0.150

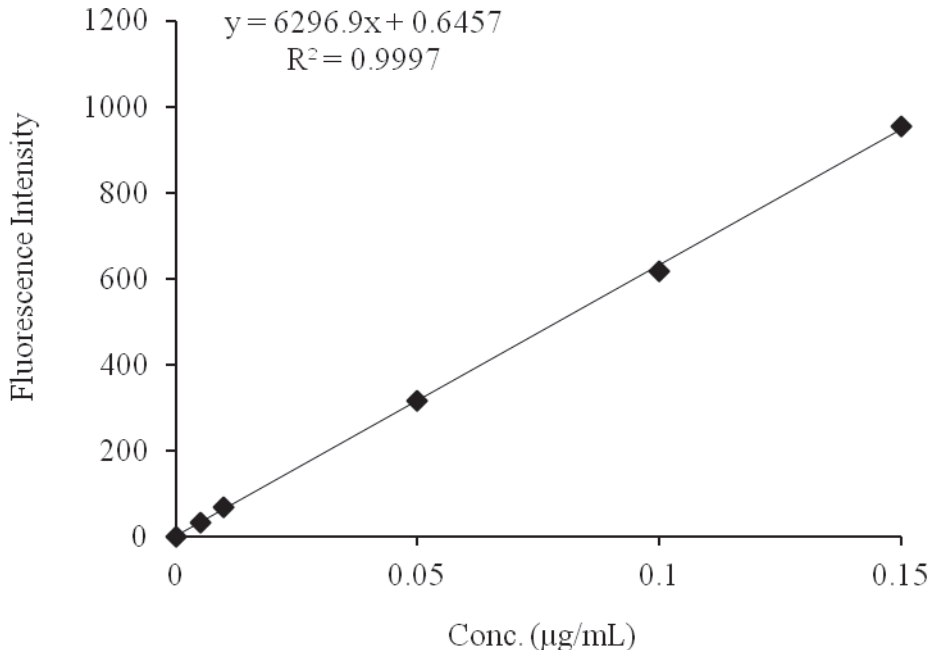

Figure 27 Standard curve of FD-10 for the *in vitro* skin release study.

3. Determination of the amount of FD-40 released

Standard	:	FD-40
Method	:	Fluorescence spectrophotometry
Detector	:	The excitation wavelength at 495 nm
		The emission wavelength at 515 nm
Concentration (µg/mL)	:	0.01, 0.05, 0.10, 0.25, 0.50

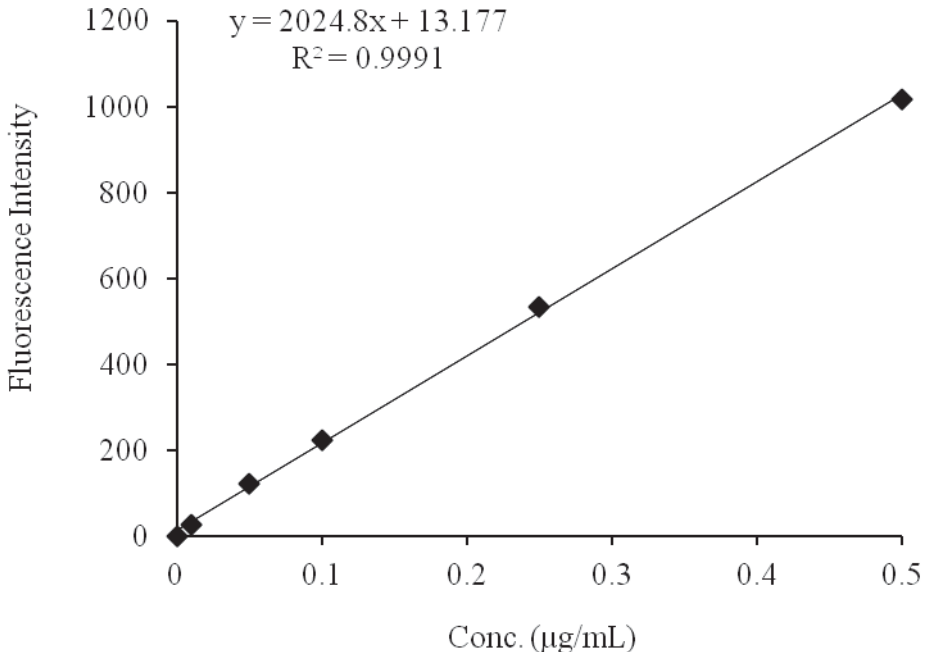

Figure 28 Standard curve of FD-40 for the *in vitro* skin release study.

4. Determination of the amount of calcein sodium (CAL) released

Standard	:	Calcein sodium
Method	:	Fluorescence spectrophotometry
Detector	:	The excitation wavelength at 490 nm
		The emission wavelength at 515 nm
Concentration (ng/mL)	:	0.1, 1.0, 5.0, 10.0, 25.0

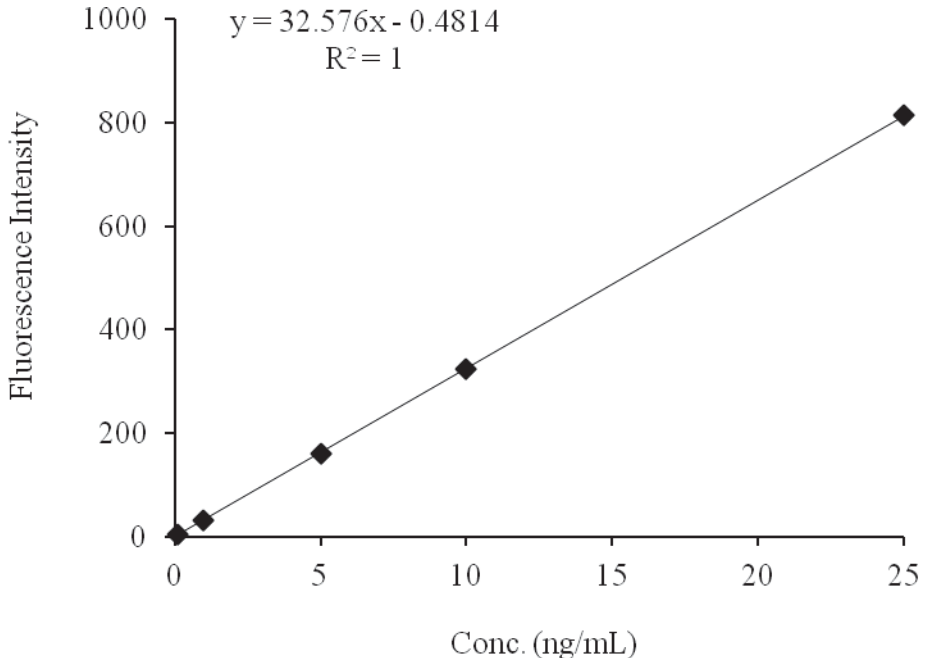

Figure 29 Standard curve of calcein sodium for the *in vitro* skin release study.

5. Determination of the amount of D_2O released

Standard	:	Deuterium oxide
Method	:	Fourier transform infrared spectroscopy
Detector	:	Wavenumbers 400–4600 cm^{-1} (Measurement the intensity of O–D stretching vibrational band at 2512 cm^{-1})
Concentration (mg/mL):		1, 5, 10, 25, 50

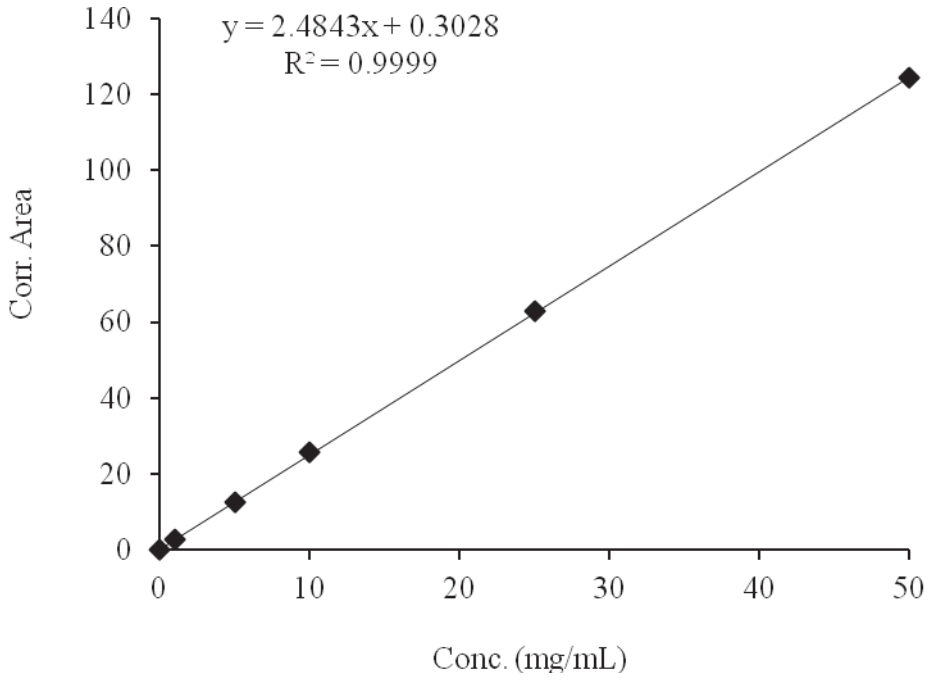

Figure 30 Standard curve of D_2O for the *in vitro* skin release study.

APPENDIX B

Release measurement

Table 11 Effect of injection volume on the release profile of FD-4 from skin after administration of 1 mM FD-4 solution by a hollow microneedle.

Time (h)	Cumulative amount of FD-4 released from skin (nmol/cm^2)							
	5 μL		10 μL		20 μL		Passive diffusion	
	Ave.	S.E.	Ave.	S.E.	Ave.	S.E.	Ave.	S.E.
0.0833	0.0037	0.0037	0.0257	0.0256	0.0174	0.0035	–	–
0.1667	0.0020	0.0020	0.0712	0.0447	0.0507	0.0052	–	–
0.25	0.0059	0.0039	0.1304	0.0675	0.0988	0.0061	–	–
0.3333	0.0166	0.0056	0.1881	0.0819	0.1566	0.0067	–	–
0.5	0.0527	0.0115	0.3141	0.1085	0.2965	0.0141	0.0066	0.0032
1	0.1779	0.0240	0.7073	0.1536	0.9202	0.1687	0.0064	0.0032
2	0.4920	0.0384	1.2132	0.1460	1.8751	0.1826	0.0086	0.0038
3	0.7552	0.0487	1.5487	0.1686	2.8664	0.1911	–	–
4	0.9599	0.0670	1.8852	0.1542	3.6619	0.2589	0.0169	0.0042
5	1.1161	0.0703	2.0201	0.1991	4.2460	0.2917	–	–
6	1.2605	0.0588	2.2818	0.1859	4.6968	0.3079	0.0236	0.0051
7	1.3497	0.0627	2.4367	0.1727	5.0849	0.3062	–	–
8	1.4575	0.0641	2.5717	0.1692	5.3518	0.2924	0.0314	0.0045

Table 12 Effect of number of injections on the release profile of FD-4 from skin after administration of 1 mM FD-4 solution by a hollow microneedle.

Time (h)	Cumulative amount of FD-4 released from skin (nmol/cm^2)					
	10 μL single injection		5 μL two injections		2.5 μL four injections	
	Ave.	S.E.	Ave.	S.E.	Ave.	S.E.
0.0833	0.0257	0.0256	0.0683	0.0286	0.0669	0.0669
0.1667	0.0712	0.0447	0.1229	0.0369	0.1123	0.1037
0.25	0.1304	0.0675	0.1893	0.0444	0.1647	0.1387
0.3333	0.1881	0.0819	0.2568	0.0498	0.2121	0.1644
0.5	0.3141	0.1085	0.4075	0.0593	0.3341	0.2330
1	0.7073	0.1536	0.7508	0.0463	0.6302	0.3301
2	1.2132	0.1460	1.3240	0.0771	1.1131	0.4120
3	1.5487	0.1686	1.9030	0.0718	1.5646	0.4737
4	1.8852	0.1542	2.2703	0.0499	1.8505	0.4669
5	2.0201	0.1991	2.5967	0.0597	2.0917	0.3874
6	2.2818	0.1859	2.8387	0.0650	2.2813	0.3784
7	2.4367	0.1727	3.0253	0.0630	2.4799	0.3976
8	2.5717	0.1692	3.1859	0.0695	2.6006	0.4063

Table 13 Effect of different concentrations on the release profile of FD-4 from skin after administration of various concentrations of 10 μL FD-4 solution by a hollow microneedle.

Time (h)	Cumulative amount of FD-4 released from skin (nmol/cm^2)							
	1 mM		2 mM		4 mM		10 mM	
	Ave.	S.E.	Ave.	S.E.	Ave.	S.E.	Ave.	S.E.
0.0833	0.0257	0.0256	0.0261	0.0200	0.0429	0.0357	0.1050	0.0595
0.1667	0.0712	0.0447	0.0949	0.0567	0.0590	0.0167	0.3375	0.1631
0.25	0.1304	0.0675	0.1861	0.1018	0.1253	0.0121	0.6475	0.2840
0.3333	0.1881	0.0819	0.2919	0.1393	0.2132	0.0059	1.0486	0.4374
0.5	0.3141	0.1085	0.5257	0.2217	0.4461	0.0309	1.9792	0.8200
1	0.7073	0.1536	1.1620	0.3307	1.2955	0.1116	5.2180	1.5708
2	1.2132	0.1460	2.1667	0.3848	3.5601	0.2810	11.6838	2.1951
3	1.5487	0.1686	3.1802	0.4835	5.2442	0.4680	17.5801	2.7965
4	1.8852	0.1542	3.8791	0.4869	6.9191	0.6714	23.3840	3.0954
5	2.0201	0.1991	4.4056	0.3725	8.2293	0.7178	26.8414	2.9831
6	2.2818	0.1859	4.8473	0.3594	8.8410	0.8333	30.1724	2.7701
7	2.4367	0.1727	5.1131	0.2984	9.5765	0.8413	31.9356	2.0733
8	2.5717	0.1692	5.4229	0.2792	10.2061	0.8992	33.4944	2.8460

Table 14 Effect of different concentrations on the release profile of FD-4 from skin after administration of various concentrations of 10 nmol FD-4 solution by a hollow microneedle.*

Time (h)	Cumulative amount of FD-4 released from skin (nmol/cm^2)							
	10 μL of 1 mM		5 μL of 2 mM		2.5 μL of 4 mM		1 μL of 10 mM	
	Ave.	S.E.	Ave.	S.E.	Ave.	S.E.	Ave.	S.E.
0.0833	0.0257	0.0256	0.0392	0.0204	0.0122	0.0027	0.0149	0.0034
0.1667	0.0712	0.0447	0.0628	0.0355	0.0375	0.0273	0.0190	0.0037
0.25	0.1304	0.0675	0.1050	0.0464	0.0410	0.0166	0.0271	0.0034
0.3333	0.1881	0.0819	0.1499	0.0590	0.0605	0.0161	0.0389	0.0027
0.5	0.3141	0.1085	0.2605	0.0930	0.1198	0.0174	0.0773	0.0032
1	0.7073	0.1536	0.5555	0.1717	0.3406	0.0294	0.2765	0.0201
2	1.2132	0.1460	1.0824	0.2475	0.8399	0.0669	0.7594	0.0405
3	1.5487	0.1686	1.5190	0.2312	1.3198	0.0898	1.3559	0.0672
4	1.8852	0.1542	1.8483	0.2532	1.7220	0.1138	1.8001	0.1234
5	2.0201	0.1991	2.0504	0.2984	2.0193	0.1190	2.2061	0.1937
6	2.2818	0.1859	2.2442	0.2878	2.3231	0.1613	2.5807	0.2005
7	2.4367	0.1727	2.4290	0.2762	2.4632	0.1536	2.8269	0.2304
8	2.5717	0.1692	2.6195	0.2121	2.6576	0.1735	3.0777	0.2737

*The total amount of FD-4 injected was adjusted to be equally of 10 nmol.

Table 15 Effect of different molecular sizes of the hydrophilic model compounds on the release profile from skin after administration by a hollow microneedle.

Time (h)	Cumulative amount of hydrophilic model compounds released from skin									
	FD-40		FD-10		FD-4		Calcein		D_2O	
	$nmol/cm^2$						$nmol/cm^2$		$\mu mol/cm^2$	
	Ave.	S.E.	Ave.	S.E.	Ave.	S.E.	Ave.	S.E.	Ave.	S.E.
0.0833	0.0007	0.0002	0.0085	0.0009	0.0257	0.0256	0.2652	0.0446	–	–
0.1667	0.0039	0.0005	0.0254	0.0042	0.0712	0.0447	0.4461	0.0807	–	–
0.25	0.0107	0.0013	0.0512	0.0081	0.1304	0.0675	0.6030	0.1076	283.86	19.88
0.3333	0.0206	0.0026	0.0889	0.0135	0.1881	0.0819	0.7249	0.1178	–	–
0.5	0.0501	0.0063	0.1695	0.0230	0.3141	0.1085	1.0859	0.1876	376.75	18.62
1	0.1743	0.0223	0.4283	0.0476	0.7073	0.1536	1.7078	0.2083	434.75	16.88
2	0.5094	0.0177	0.9391	0.0733	1.2132	0.1460	2.6481	0.2202	457.73	18.07
3	1.0105	0.2013	1.3144	0.0745	1.5487	0.1686	3.1593	0.2161	466.30	21.20
4	1.0324	0.0461	1.6108	0.0789	1.8852	0.1542	3.5566	0.2149	474.08	23.76
5	1.2656	0.0557	1.8400	0.0843	2.0201	0.1991	3.7130	0.2238	480.15	27.40
6	1.3935	0.0659	2.0900	0.1076	2.2818	0.1859	3.8387	0.2141	488.05	29.16
7	1.5170	0.0868	2.1946	0.1276	2.4367	0.1727	3.8953	0.2445	495.08	32.48
8	1.5916	0.0898	2.3637	0.1120	2.5717	0.1692	4.1077	0.1410	498.24	34.48

APPENDIX C

The percentage of drug release

Table 16 Effect of injection volume on the percentage of FD-4 released from skin after administration of 1 mM FD-4 solution by a hollow microneedle.

Time (h)	% Drug release					
	5 μL		10 μL		20 μL	
	Ave.	S.E.	Ave.	S.E.	Ave.	S.E.
0.0833	0.2	0.2	0.7	0.6	0.2	0.1
0.1667	0.1	0.1	1.8	1.1	0.7	0.1
0.25	0.3	0.2	3.3	1.7	1.3	0.1
0.3333	0.7	0.3	4.8	2.1	2.0	0.1
0.5	2.4	0.5	8.0	2.7	3.8	0.1
1	7.9	1.1	18.2	3.9	11.8	1.9
2	22.0	1.9	31.2	3.7	24.2	2.0
3	33.7	2.5	39.9	4.3	37.1	1.8
4	42.9	3.5	48.6	3.9	47.4	2.5
5	49.9	3.8	52.0	5.0	55.0	3.1
6	56.3	3.3	58.8	4.6	60.8	3.4
7	60.3	3.5	62.8	4.3	65.9	3.2
8	65.1	3.7	66.2	4.2	69.3	3.1

Table 17 Effect of number of injections on the percentage of FD-4 released from skin after administration of 1 mM FD-4 solution by a hollow microneedle.

Time (h)	% Drug release					
	10 μL single injection		5 μL two injections		2.5 μL four injections	
	Ave.	S.E.	Ave.	S.E.	Ave.	S.E.
0.0833	0.7	0.6	1.7	0.7	1.8	1.8
0.1667	1.8	1.1	3.0	0.9	2.9	2.7
0.25	3.3	1.7	4.6	1.1	4.3	3.6
0.3333	4.8	2.1	7.0	1.3	5.5	4.3
0.5	8.0	2.7	12.2	1.5	9.0	6.1
1	18.2	3.9	19.3	1.3	16.5	8.7
2	31.2	3.7	33.1	2.2	29.0	10.8
3	39.9	4.3	47.4	2.1	41.1	12.5
4	48.6	3.9	56.4	1.7	47.7	12.3
5	52.0	5.0	63.3	1.9	54.6	10.3
6	58.8	4.6	69.3	2.1	59.4	10.0
7	62.8	4.3	73.8	2.0	64.6	10.5
8	66.2	4.2	77.7	2.1	67.7	10.8

Table 18 Effect of different concentrations on the percentage of FD-4 released from skin after administration of various concentrations of 10 μL FD-4 solution by a hollow microneedle.

Time (h)	% Drug release							
	1 mM		2 mM		4 mM		10 mM	
	Ave.	S.E.	Ave.	S.E.	Ave.	S.E.	Ave.	S.E.
0.0833	0.7	0.6	0.3	0.3	0.3	0.2	0.2	0.1
0.1667	1.8	1.1	1.2	0.7	0.4	0.1	0.8	0.3
0.25	3.3	1.7	2.4	1.3	0.8	0.1	1.4	0.6
0.3333	4.8	2.1	3.7	1.7	1.3	0.0	2.3	0.9
0.5	8.0	2.7	6.7	2.8	2.8	0.1	4.4	1.7
1	18.2	3.9	14.9	4.1	8.0	0.4	11.8	3.0
2	31.2	3.7	27.9	4.7	22.1	1.1	26.6	3.9
3	39.9	4.3	40.9	5.8	32.5	2.1	40.1	4.7
4	48.6	3.9	50.0	5.8	42.9	3.1	53.6	5.1
5	52.0	5.0	56.8	4.3	51.1	3.0	61.5	4.4
6	58.8	4.6	62.5	4.0	54.8	3.8	69.3	4.0
7	62.8	4.3	66.0	3.2	59.4	3.6	73.5	2.9
8	66.2	4.2	70.0	3.0	63.3	3.9	76.9	3.9

Table 19 Effect of different concentrations on the percentage of FD-4 released from skin after administration of various concentrations of 10 nmol FD-4 solution by a hollow microneedle.*

Time (h)	% Drug release							
	10 µL of 1 mM		5 µL of 2 mM		2.5 µL of 4 mM		1 µL of 10 mM	
	Ave.	S.E.	Ave.	S.E.	Ave.	S.E.	Ave.	S.E.
0.0833	0.7	0.6	0.7	0.5	0.3	0.1	0.4	0.1
0.1667	1.8	1.1	1.2	0.8	1.0	0.7	0.5	0.1
0.25	3.3	1.7	2.0	1.1	1.1	0.5	0.7	0.1
0.3333	4.8	2.1	2.9	1.5	1.6	0.4	1.0	0.1
0.5	8.0	2.7	5.0	2.4	2.4	0.4	1.9	0.1
1	18.2	3.9	13.3	4.3	7.0	0.7	5.2	0.7
2	31.2	3.7	24.0	6.4	13.2	1.6	10.1	1.5
3	39.9	4.3	37.5	6.3	24.2	2.3	27.0	2.2
4	48.6	3.9	44.2	7.4	36.8	3.0	41.3	3.3
5	52.0	5.0	53.5	6.3	51.1	3.1	58.7	4.4
6	58.8	4.6	55.8	7.1	61.4	4.2	64.0	4.7
7	62.8	4.3	61.7	5.9	65.2	4.2	70.0	4.9
8	66.2	4.2	68.1	6.3	70.3	4.6	76.3	6.1

*The total amount of FD-4 injected was adjusted to be equally of 10 nmol.

Table 20 Effect of different molecular sizes of the hydrophilic model compounds on the percentage of drug released from skin after administration by a hollow microneedle.

Time (h)	% Drug release									
	FD-40		FD-10		FD-4		Calcein sodium		D_2O	
	Ave.	S.E.	Ave.	S.E.	Ave.	S.E.	Ave.	S.E.	Ave.	S.E.
0.0833	0.0	0.0	0.2	0.0	0.7	0.6	3.8	0.6	–	–
0.1667	0.1	0.0	0.7	0.1	1.8	1.1	6.9	0.5	–	–
0.25	0.3	0.0	1.4	0.2	3.3	1.7	9.6	0.9	57.6	4.1
0.3333	0.6	0.1	2.4	0.3	4.8	2.1	12.4	0.9	–	–
0.5	1.4	0.2	4.6	0.6	8.0	2.7	17.2	0.8	76.8	4.8
1	4.8	0.6	11.6	1.1	18.2	3.9	30.4	0.8	88.6	4.7
2	14.0	0.3	25.7	1.6	31.2	3.7	50.6	1.7	93.1	4.0
3	27.6	5.3	36.0	1.1	39.9	4.3	64.1	2.3	94.5	3.3
4	28.3	1.1	44.2	0.9	48.6	3.9	71.1	3.7	95.8	2.4
5	34.7	1.2	50.5	0.9	52.0	5.0	77.3	2.5	96.8	1.6
6	38.2	1.5	57.3	1.3	58.8	4.6	81.0	2.9	98.3	1.4
7	41.6	2.0	61.0	1.7	62.8	4.3	84.8	2.8	99.5	0.5
8	43.7	2.1	65.0	0.9	66.2	4.2	85.7	2.6	100.0	0.0

BIOGRAPHY

Name	Nanthida Wonglertnirant, Ms.
Date of Birth	December 20, 1983
Place of Birth	Bangkok, Thailand
Nationality/Religion	Thai/Buddhism
E-mail address	w.nanthida@gmail.com

Education

2007 (June) – 2012 (May)	Doctor of Philosophy, Ph.D. in Pharmaceutical Technology Silpakorn University, Thailand
2002 (June) – 2006 (Jan)	Bachelor of Pharmacy (1st Class Honours) Silpakorn University, Thailand

Awards

2009	The AFPS Nagai-Shukri Pre-doctoral Oral Presentation Award from Asian Federation for Pharmaceutical Sciences 2009, Fukuoka, Japan.
2009	The Nagai Foundation Travel Awards for Graduate Students and Post-doctoral Scholar from Asian Federation for Pharmaceutical Sciences 2009, Fukuoka, Japan.

Presentation

Poster

1. Nanthida Wonglertnirant, Sureewan Duangjit, Tanasait Ngawhirunpat, Mont Kumpugdee-Vollrath. (2010). Enhancement in Skin Permeation of Lipophilic and Hydrophilic Compounds by Surfactants. 7th World Meeting on Pharmaceutics, Biopharmaceutics and Pharmaceutical

Technology at the Mediterranean Conference Centre, Valletta, Malta. (March 8–11, 2010)

2. Nanthida Wonglertnirant, Hiroaki Todo, Praneet Opanasopit, Tanasait Ngawhirunpat and Kenji Sugibayashi. (2010). Hollow Microneedles as A Carrier for Enhancing Skin Penetration of Hydrophilic Compounds. The 1st Current Drug Development International Conference at Woraburi Resort & Spa Hotel, Phuket, Thailand. (May 6–8, 2010)

3. Nanthida Wonglertnirant, Supinya Tipwichai, Praneet Opanasopit, Theerasak Rojanarata, Suwannee Panomsuk and Tanasait Ngawhirunpat. (2011). Development of Acrylic Matrix Type Ketoprofen Patch. Chiang Mai International Conference on Biomaterials & Applications 2011 at the Empress Hotel, Chiang Mai, Thailand. (August 9–10, 2011)

Oral

1. Nanthida Wonglertnirant, Praneet Opanasopit, Theerasak Rojanarata, Tanasait Ngawhirunpat, Uracha Ruktanonchai and Warisada Sila-on. (2008). Development of Lipid Emulsion Formulations for Camptothecin. The 2nd Thailand Nanotechnology Conference 2008 at Phuket Graceland Resort & Spa Patong, Phuket, Thailand. (August 13–15, 2008)

2. Nanthida Wonglertnirant, Hiroaki Todo, Praneet Opanasopit, Tanasait Ngawhirunpat and Kenji Sugibayashi. (2009). Skin Delivery of High Molecular Weight Hydrophilic Compound Using Hollow Microneedles. Asian Federation for Pharmaceutical Sciences 2009 at Centennial Hall Kyushu University School of Medicine, Fukuoka, Japan. (October 15–18, 2009)

Scientific Publication

1. Tanasait Ngawhirunpat, Nanthida Wonglertnirant, Praneet Opanasopit, Uracha Ruktanonchai, Rangrong Yoksan, Kaewkarn Wasanasuk and Suwabun Chirachanchai. (2009). Incorporation methods for cholic acid chitosan-g-mPEG self-assembly micellar system containing camptothecin. Colloids and Surfaces B: Biointerfaces 74, 1: 253–259.

2. Hilal Bilek, Nanthida Wonglertnirant, Tanasait Ngawhirunpat, Praneet Opanasopit and Mont Kumpugdee-Vollrath. (2009). Effect of Terpenes on the Skin Permeation of Ketoprofen through Shed Snake Skin. Silpakorn U Science & Tech J. 3, 2: 33–41.

3. Nanthida Wonglertnirant, Hiroaki Todo, Praneet Opanasopit, Tanasait Ngawhirunpat and Kenji Sugibayashi. (2010). Macromolecular Delivery into Skin Using a Hollow Microneedle. Biol Pharm Bull. 33, 12: 1988–1993.

4. Nanthida Wonglertnirant, Tanasait Ngawhirunpat, Praneet Opanasopit, Hiroaki Todo and Kenji Sugibayashi. (2011). A Hollow Microneedle Carrier for Enhancing Skin Penetration of Large Molecular Compounds. Advanced Materials Research 194–196, 549–553.

5. Maleenart Petchsangsai, Nanthida Wonglertnirant, Theerasak Rojanarata, Praneet Opanasopit and Tanasait Ngawhirunpat. (2011). Application of Hollow Microneedle for Transdermal Delivery of Bovine Serum Albumin-Fluorescein Isothiocyanate Conjugate. Advanced Materials Research 338, 365–368.

6. Nanthida Wonglertnirant, Tanasait Ngawhirunpat and Mont Kumpugdee-Vollrath. (2012). Evaluation of the Mechanism of Skin Enhancing Surfactants on the Biomembrane of Shed Snake Skin. Biol Pharm Bull. 35, 4: 523–532.

7. Nanthida Wonglertnirant, Supinya Tipwichai, Praneet Opanasopit, Theerasak Rojanarata, Suwannee Panomsuk and Tanasait Ngawhirunpat. Development of Acrylic Matrix Type Ketoprofen Patch. Advanced Materials Research, in press.

Article Publication

1. Nanthida Wonglertnirant and Tanasait Ngawhirunpat (September–October, 2009). Skin metabolism: Effect on transdermal administration, Study, and Factors affecting study. PHARMATIME 7, 79: 43–48.

2. Nanthida Wonglertnirant, Sureewan Duangjit, and Tanasait Ngawhirunpat (November–December, 2009). Microneedle and its application in pharmaceutical sciences. PHARMATIME 7, 80: 41–45.